AD680960

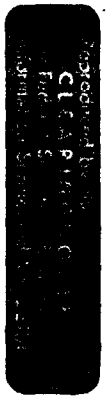

DISCLAIMER NOTICE

THIS DOCUMENT IS BEST QUALITY PRACTICABLE. THE COPY FURNISHED TO DTIC CONTAINED A SIGNIFICANT NUMBER OF PAGES WHICH DO NOT REPRODUCE LEGIBLY.

Technical Summary Report No. 2

Dec. 9, 1966 to Nov. 8, 1967

EQUATIONS OF STATE IN SOLIDS

by

G. E. Duvall, G. R. Fowles,
M. H. Miles, and C. T. Tung

Contract No.
DA-04-200-AMC-1702(X)

WSU SDL 68-01
February, 1968

Research sponsored by the U.S. Army
Ballistics Research Laboratory
Aberdeen Proving Ground, Maryland

ABSTRACT

An equation of state suitable for calculating the compression of a melting solid is described. Some elementary ideas about melting are reviewed and some standard relations between P and T in the melting region are described. The equation of state and melting law are combined in a program for calculating the Hugoniot through the mixed phase region. Results are described for lead, which melts at a shock pressure of about 400 kilobars with a Kennedy equation and 700 kilobars for a Simon equation.

The Eyring theory for equation of state of liquids is examined for argon, and Hugoniot curves are calculated. Calculations agree with the most dense case of van Thiel and Alder to 13 kilobars, then depart dramatically from measured values.

The theory of plastic wave propagation in two-dimensions is discussed and calculations of allowed directions are described. These will ultimately be of use in discussing the reflection of obliquely incident waves in an elastic-plastic medium.

Some of the basic physical mechanisms in solid-solid phase transitions are reviewed and the applicability of thermodynamics to such transitions is brought into question. An elementary model for a non-equilibrium transition in iron is suggested and p-v calculations are made for several values of the parameters. It is evident that no conclusions about the time dependence of the α-ε transition can be drawn from second state shock measurements, although it may be possible to infer useful information about metastable states.

TABLE OF CONTENTS

LIST OF TABLES

LIST OF ILLUSTRATIONS

PART A: SHOCK PROPAGATION AND MELTING. G. E. Duvall.

List of Illustrations.--Continued

PART B: ACOUSTIC WAVES FOLLOWING STRONG SHOCK WAVES. G. R. Fowles.

PART C: PHASE TRANSITIONS UNDER DYNAMIC CONDITIONS. M. H. Miles.

INTRODUCTION

This project, since its inception, has been concerned with problems of equations of state, constitutive relations, phase transitions, and wave propagation. These are large problems, not to be wrapped up and put aside in one-year packages by the part-time efforts of one man, or of several men. Instead, once having got started they stick in the mind and bits and pieces of new understanding or new accomplishments come along, sometimes in unexpected directions. When it comes time to put these together in a summary report at the end of a year, their unity is not always apparent; it is not always clear that they are parts of a whole which isn't very easy to subdivide. So it is with the present report; so it is presented in three distinct parts as it was worked out by three different men working on the problems and their assistants.

Part A deals quite directly and clearly with the stated objectives of the contract; it comprises a relatively straightforward and tedious calculation of the equilibrium shock Hugoniot of a melting solid. In the process of doing this calculation the author has experienced some revealing insights into the features of a <u>total</u> equation of state, and a side excursion into the theory of equations of state of liquids has shown that the Eyring Significant Structure Theory may be amenable to modifications which

would lead to a total equation of state, when coupled with suitable data.

Part B is a beginning, an introduction to the quite complex subject of propagation of multiple waves in anelastic, yielding materials. It shows even at this beginning stage that the mechanics is more complicated than we believed when we thought only of plane waves following parallel plane waves. In its present stage it begins to provide a foundation for understanding wave structures in more realistic solid models than have been heretofore commonly used. It may even eventually provide for better interpretation of experiments and designs for experiments.

Part C is something quite different--a summarizing of physical ideas about the causes of phase transitions and the mechanics of their occurrence. The metallurgist has long been aware that equilibrium thermodynamics plays only a minor role in solid-solid phase transitions. The thermodynamicist and the physicist are just beginning to learn this. This summary suggests an elementary model for martensitic phase transition. A calculation for iron shows that the quasi-stable p-v relation in the mixed phase can be varied almost at will by varying the assumed metallurgical parameters.

PART A

SHOCK PROPAGATION AND MELTING

G. E. Duvall

I. Melting Phase Boundaries in the P-V Plane

In Fig. 1, let OCFGBJ be the coexistence region for solid and liquid; φ_1 is the solid phase and φ_2 is liquid. Suppose ABCD to be the Hugoniot. We wish to determine first the phase boundaries GBJ and FCO in terms of known quantities.

The transition is first order, and at equilibrium the Clausius-Clapeyron equation obtains:

$$dP/dT = \Delta S/\Delta V = \Delta H/T\Delta V = f(P) \tag{1.1}$$

$$\Delta V = V_2(P,T) - V_1(P,T) \tag{1.2}$$

The rate of change of entropy with temperature on the phase boundary JBG is

$$dS_1/dT = (C_{p1}/T) - (\partial V/\partial T)_{p1}(dP/dT)$$

$$= C_{p1}(dP/dT)\left[(dT/TdP) - (1/C_{p1})(\partial V/\partial T)_{p1}\right] \tag{1.3}$$

where subscript "p1" denotes a quantity evaluated at constant pressure, in phase 1, on the phase boundary GBJ.

We assume that $C_{p1} > 0$ and $(\partial V/\partial T)_{p1} > 0$. Then if $dP/dT < 0$ in the mixed phase region, R, it follows that $dS_1/dT > 0$.

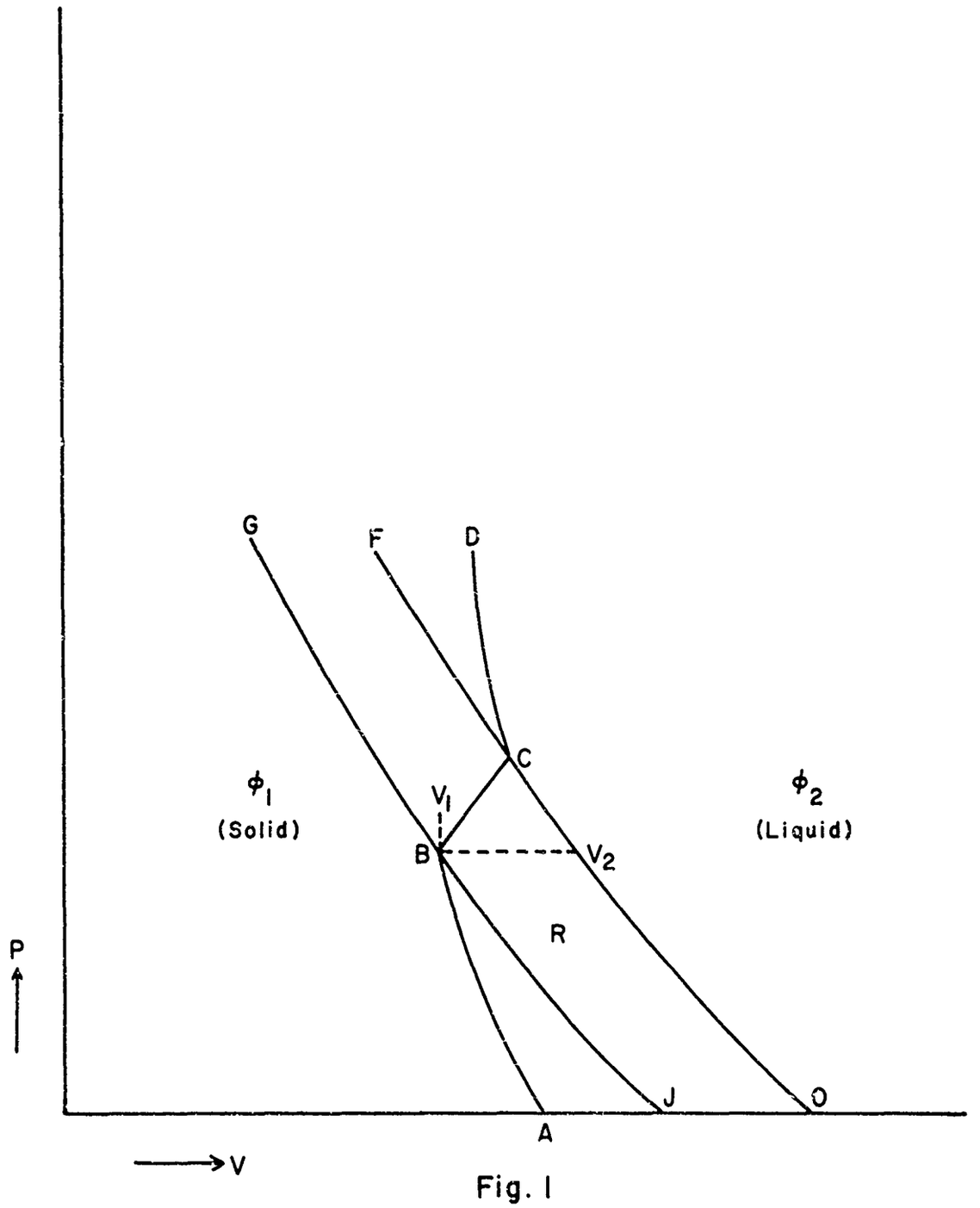

Fig. I

Melting Phase Boundaries

If $dP/dT > 0$, the sign of dS_l/dT depends upon the magnitude of dP/dT:

$$dT/dP > T(\partial V/\partial T)_{pl}/C_{pl}$$

$$dS_l/dT > 0$$

$$dT/dP < T(\partial V/\partial T)_{pl}/C_{pl}$$

$$dS_l/dT < 0$$

We may summarize these relations as in Table I, defining three distinct types of phase transitions.

Table I

Classification of Phase Transitions

$$\Delta V = V_\ell - V_s = V_2 - V_1 > 0$$

Type of Transition	dS_l/dT	dP/dT	ΔS
I	> 0	< 0	< 0
II	< 0	> 0	> 0
III	> 0	> 0	> 0

In terms of observables at the melting point, the defining conditions are

$$dP/dT < 0 \qquad \text{Type I}$$

$$dP/dT > 0; \quad \Delta V_m/\Delta H_m < (\partial V/\partial T)_{pl}/C_{pl} \qquad \text{Type II}$$

$$dP/dT > 0; \quad \Delta V_m/\Delta H_m > (\partial V/\partial T)_{pl}/C_{pl} \qquad \text{Type III}$$

where $\Delta V_m = V_{liq} - V_{sol}$ = volume expansion on melting

ΔH_m = latent heat of melting.

In this way melting transitions for which $\Delta V > 0$ are divided into three exhaustive categories.* The Metals Reference Handbook shows that Type III prevails among the metals (Table II). Of these three categories, II and III may be considered normal, i.e., S increases on melting.

The relative slopes of isotherm, adiabat, and phase boundary may be found as follows:

In the solid phase,

$$(\partial V/\partial P)_{S1} = (\partial V/\partial P)_{T1} + (\partial V/\partial T)_{P1} (\partial T/\partial P)_{S1} \tag{1.4}$$

Also, the slope of the phase boundary may be written as

$$dV_1/dP = (\partial V/\partial P)_{T1} + (\partial V/\partial T)_{P1} (dT/dP) \tag{1.5}$$

For transitions of Type III:

$$(\partial T/\partial P)_{S1} = T(\partial V/\partial T)_{P1}/C_{P1} < dT/dP \tag{1.6}$$

if C_{p1} and $(\partial V/\partial T)_p$ are both positive.

Substitution of this inequality into Eq. (1.5) and comparing with Eq. (1.4) yields the result

$$dV_1/dP > (\partial V/\partial P)_{S1} \tag{1.7}$$

Adiabats in the solid phase exit from the coexistence region with negative slope and increasing pressure.

---

*A closely related treatment has recently appeared in the literature. See Ref. 1. However, the author assigns lead to Type II instead of Type III as a result of numerical error.

Table II

Classification of Melting Transitions for Metals[1]

Element	$\Delta V_m/V_s$	ΔH_m cal/gm.	$C_p(s)$ cal/gm^oK	$\frac{1}{V}(\frac{\partial V}{\partial T})_p \times 10^6$ $^oC^{-1}$	$\frac{1}{V_s}\frac{\Delta V_m}{\Delta H_m} \times 10^5$	$\frac{1}{C_p}\cdot\frac{1}{V_s}(\frac{\partial V}{\partial T})_p \times 10^5$	Type
Ag	.038	25.306	.054	57.3	150.1	106.1	III
Al	.065	92.661	.219	78	70.1	35.6	III
Cu	.042	48.946	.0922	51.0	85.8	55.3	III
Fe	.030	64.996	.109	36.3	46.1	33.0	III
Mg	.0412	85.526	.248	78.0	48.1	31.5	III
Pb	.035	5.472	.031	87.0	642	280.6	III
Sn	.028	14.237	.054	69	196.6	128	III
Zn	.047	26.308	.094	84	178.6	89.5	III

[1]Handbook values of these constants vary considerably. Variations do not appear to be large enough to change Type.

ΔV_m = volume change due to melting

ΔH_m = latent heat of fusion

$C_p(s)$ = specific heat of solid at constant pressure

$(\partial V/\partial T)_p/V$ = thermal expansion coefficient of solid.

The three types of transition can also be characterized in terms of the relative slopes of isotherms, adiabats and the cylinder defining the mixed phase region in P-V-T space. First construct the P-V-T surface for the solid, extending it to arbitrary T in a metastable state. Suppose the mixed phase cylinder to be degenerate, i.e., a plane, in order to simplify the description. The plane always lies parallel to the V-axis. When it is also perpendicular to the T-axis, its intersection with the P-V-T surface of the solid, i.e. the phase boundary, coincides with an isotherm of the solid. This is the case $dT/dP = 0$.

If the plane inclines toward smaller T as P increases, $dT/dP < 0$ and the transition is of Type I. If it inclines toward larger T, it describes first Type II in which the phase boundary splits the isotherms and adiabats and then Type III in which both isotherms and adiabats issue from the phase boundary with increasing P. These three cases are illustrated in Figs. 2 and 3.

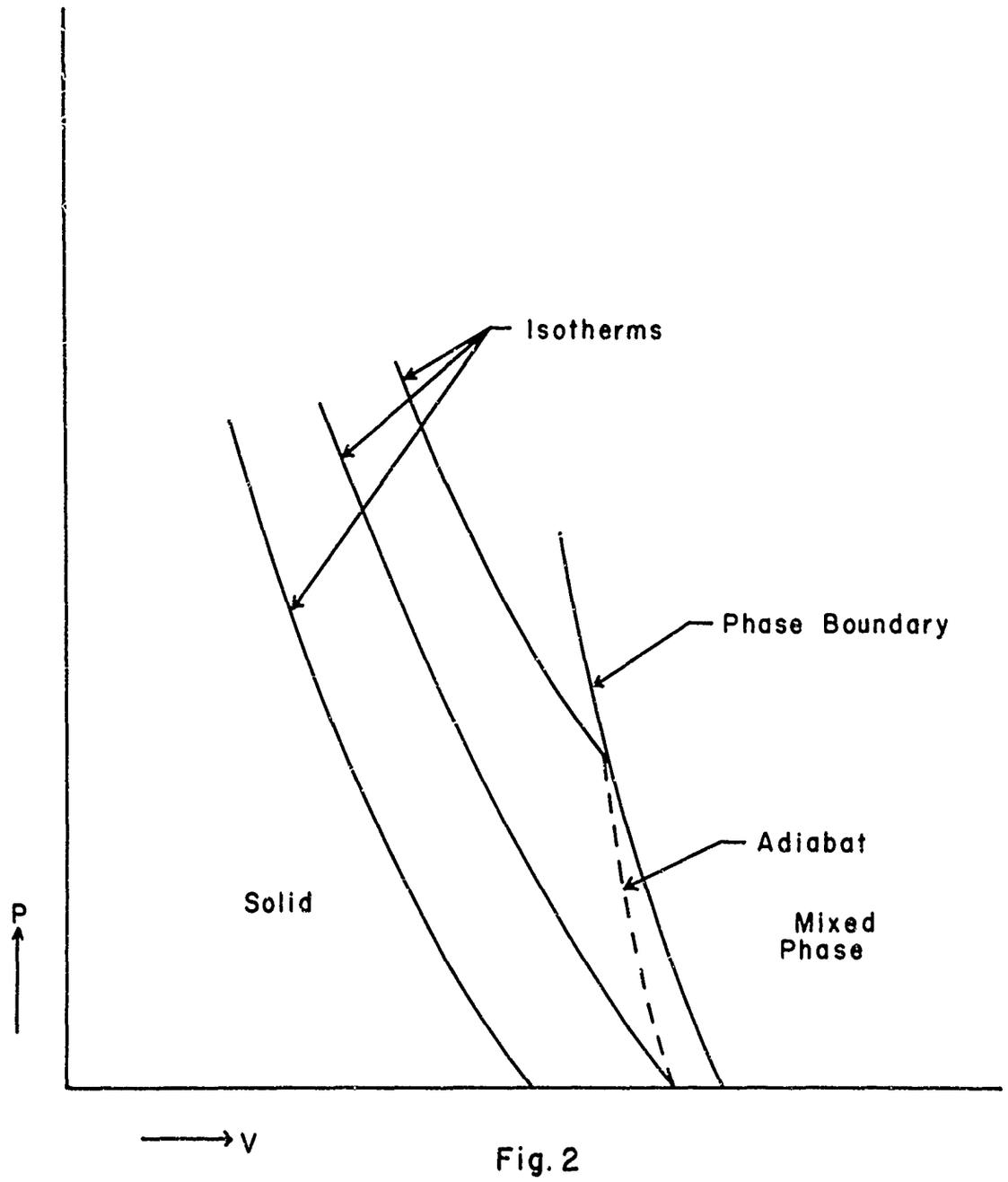

Fig. 2

Phase Boundary for Type II Melting

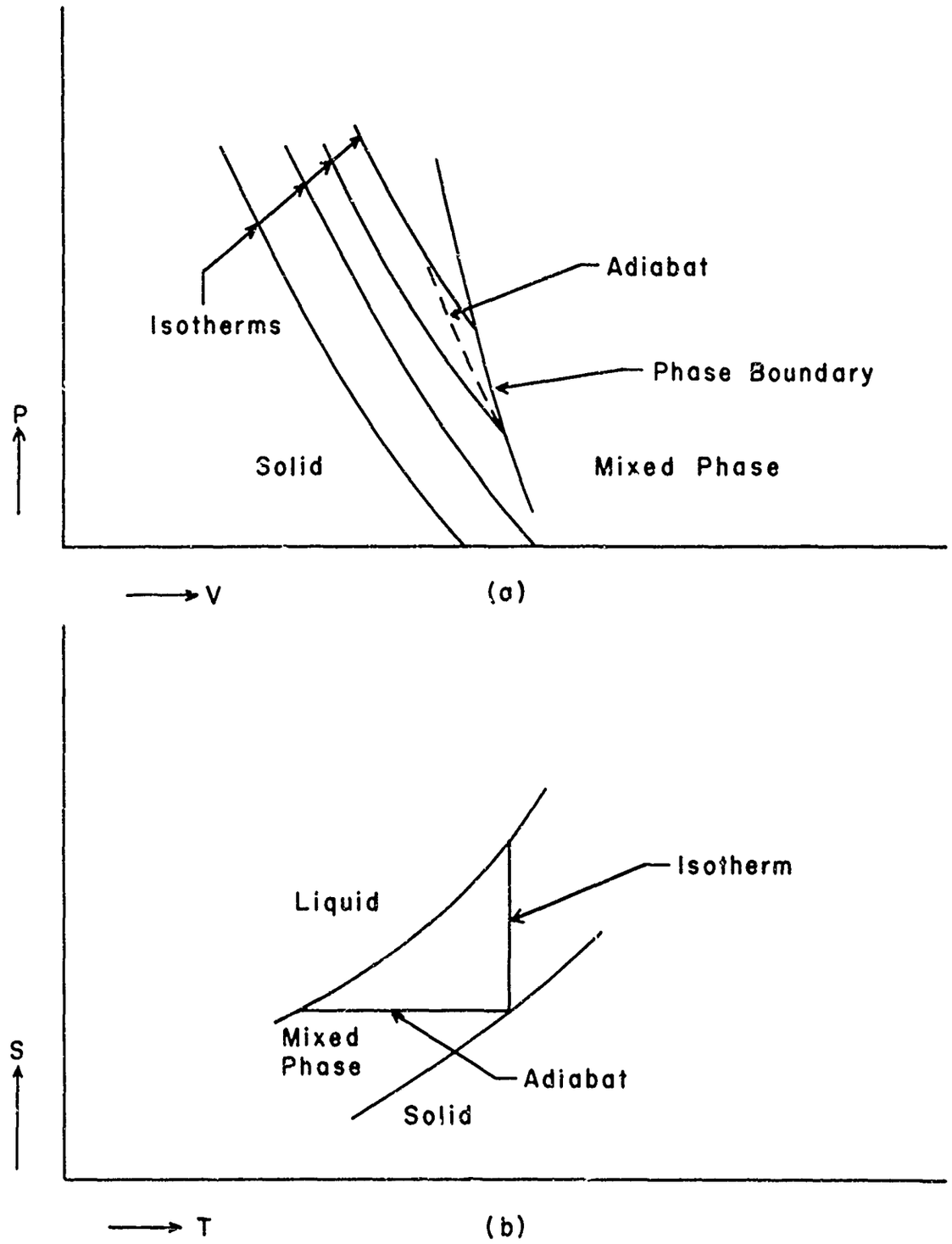

Fig. 3

Phase Boundary for Type III Melting

(a) P-V Plane
(b) S-T Plane

II. Adiabats in the Mixed Phase Region

Adiabats in the mixed phase region are shown in the P-V plane in Fig. 4. The entropy at point C is:

$$S_C = S_A + \int_A^B (dS_1/dP)dP + x\Delta S \tag{2.1}$$

where

$$x = (V-V_1)/(V_2-V_1) = \text{fraction of mass in phase 2 at point C} \tag{2.2}$$

$$\Delta S = S(B') - S(B) \tag{2.3}$$

$$V = V(C), \quad V_2 = V(B'), \quad V_1 = V(B)$$

Differentiating Eq. (2.1) yields

$$(dS_1/dP) + (\Delta S/\Delta V)\left((\partial V/\partial P)_{SM} - (dV_1/dP)\right) + (V-V_1)\, d(\Delta S/\Delta V)/dP = 0 \tag{2.4}$$

where $(\partial V/\partial P)_{SM}$ = adiabatic derivative in the mixed phase region, R. Neglecting the last term in Eq. (2.4) yields an expression for the adiabat

$$(\partial V/\partial P)_{SM} = (dV_1/dP) - (dS_1/dP)(dT/dP)$$

$$= (\partial V/\partial P)_{T1} + 2\,(\partial V/\partial T)_{P1}(dT/dP) - C_{p1}(dT/dP)^2/T \tag{2.5}$$

The discontinuity in the slope of the adiabat is

$$(\partial V/\partial P)_{S1} - (\partial V/\partial P)_{SM1} = \left[(T/C_{p1})^{\frac{1}{2}}\,(\partial V_1/\partial T)_P - (C_{p1}/T)^{\frac{1}{2}}\,(dT/dP)\right]^2 > 0\ ; \tag{2.6}$$

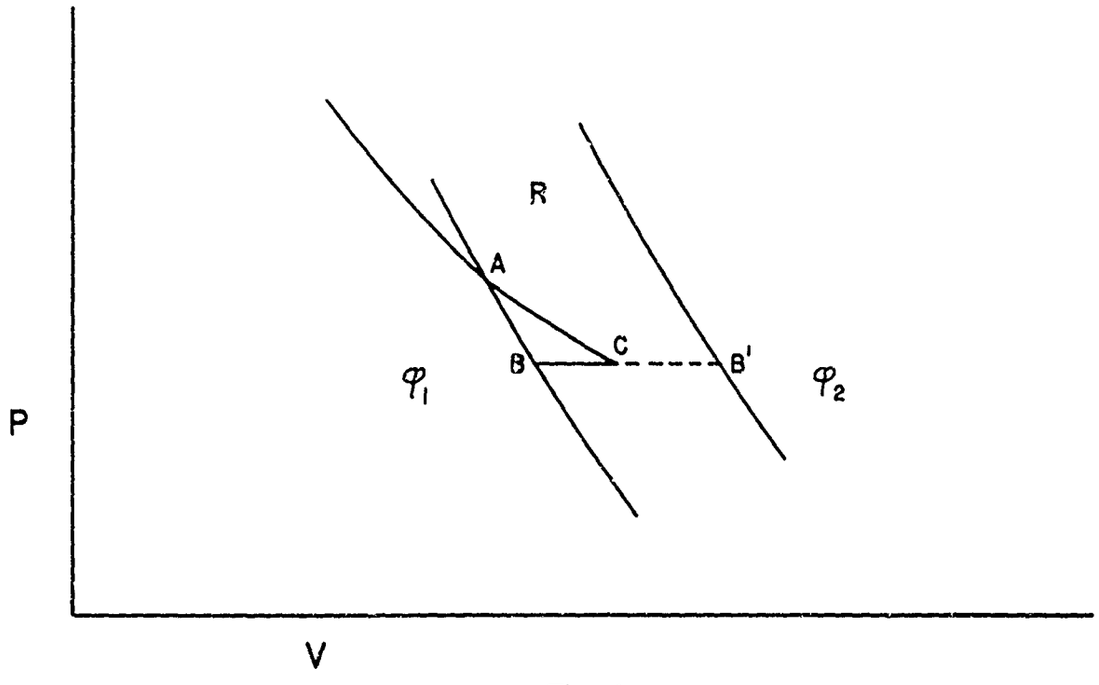

Fig. 4

ADIABAT IN MIXED PHASE REGION

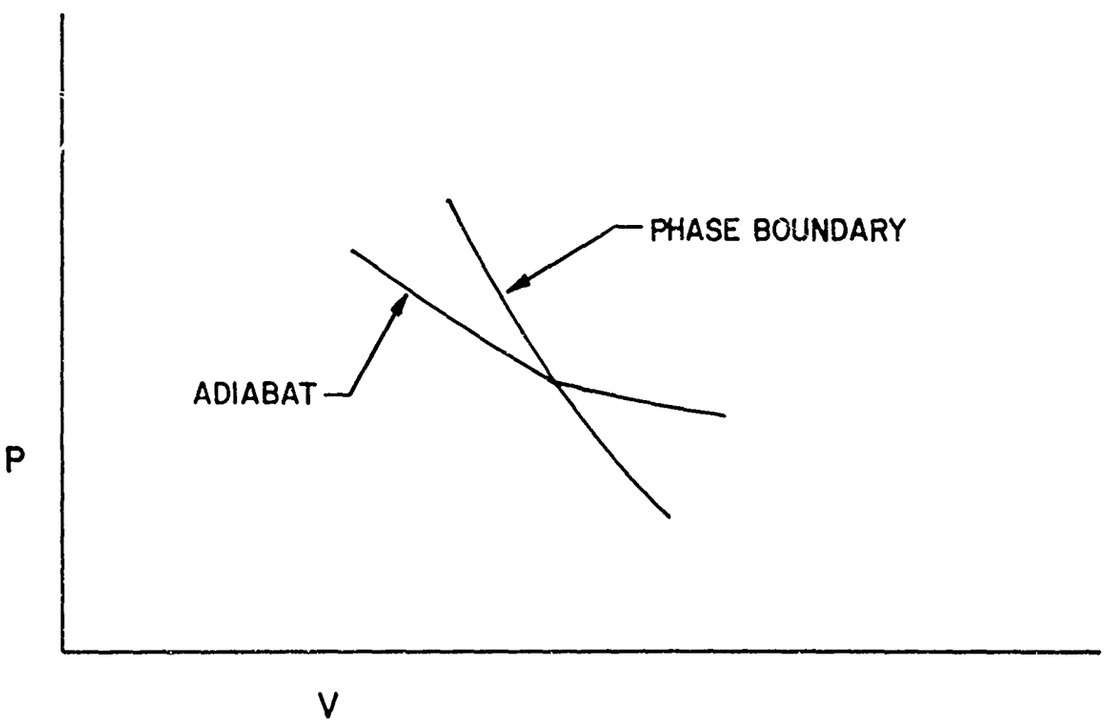

Fig.5

DISCONTINUITY IN ADIABAT AT PHASE BOUNDARY FOR TYPE III TRANSITION

i.e., the adiabat is always discontinuous at the phase boundary and the sign of the discontinuity is such that

$$| \partial P/\partial V |_{S1} > | \partial P/\partial V |_{SM1} . \qquad (2.7)$$

III. Construction of the Hugoniot

We suppose the material to be shocked from a point in the solid state to a final state which may lie in the solid, in the mixed phase region, or in the liquid state. It is not known in advance whether the final state is reached through single or multiple shocks, consequently it is most appropriate to construct the Hugoniot incrementally, examining at each step to determine whether or not a new shock is initiated.

A. Solid Phase Hugoniot

The differential equation of the Hugoniot curve for an equation of state of the form of Eq. (4.1) in a single phase is (1)*

$$dP/dV = \left[(\partial P/\partial V)_S + (\Gamma/2V)(P - P_o)\right]/\left[1 - (\Gamma/2V)(V_{o2} - V)\right] \qquad (3.1)$$

where (P_o, V_{o2}) is the initial state and Γ is the Grüneisen ratio. We now consider whether or not a single, stable shock to pressure P_1 will also be stable to $P_1 + \delta P$. Since a single shock from P_o to P is assumed to be stable, the Rayleigh line connecting (P_o, V_o) with (P_1, V_1) intersects the Hugoniot curve only at those two points;

---

*Numbers in parentheses reference to references on pp. 39-40.

then

$$- dP/dV)_{RH,P_1^-} \geq (P_1-P_o)/(V_{o2}-V_1) \qquad (3.2)$$

Here P_1^- denotes the slope on the lower side of the point P_1, V_1 if the Hugoniot is discontinuous there. If the point $P_1 + \delta P_1$ is also to be attained through a single shock, Condition (3.2) must hold on the upper side of P_1, denoted by P_1^+ :

$$- dP/dV)_{RH,P_1^+} \geq (P_1-P_o)/(V_{o2}-V_1) \qquad (3.3)$$

Substitution of Eq. (3.1) into (3.3) yields the condition for stability:

$$\left[a_1^2/(U_1-u_1)^2 - \Gamma_1(V_{o2}-V_1)/2V_1\right] / \left[1 - (\Gamma_1/2V_1)(V_{o2}-V_1)\right] \geq 1 \qquad (3.4)$$

where

$$a_1^2 = -V_1^2 \, (\partial P/\partial V)_{S,P_1^+}$$

$$(U_1-u_1)^2 = V_1^2 \, (P_1-P_o)/(V_{o2}-V_1) \quad .$$

If $\Gamma(V_{o2}-V_1)/2V_1 < 1$ the stability condition further reduces to

$$a_1^2/(U-u_1)^2)_{P1^+} \geq 1 \quad . \qquad (3.5)$$

B. Mixed Phase Hugoniot

In Fig. 6, the region ABCD denotes the part of the mixed phase region through which the Hugoniot passes. F is the intersection of the solid phase Hugoniot with the boundary between

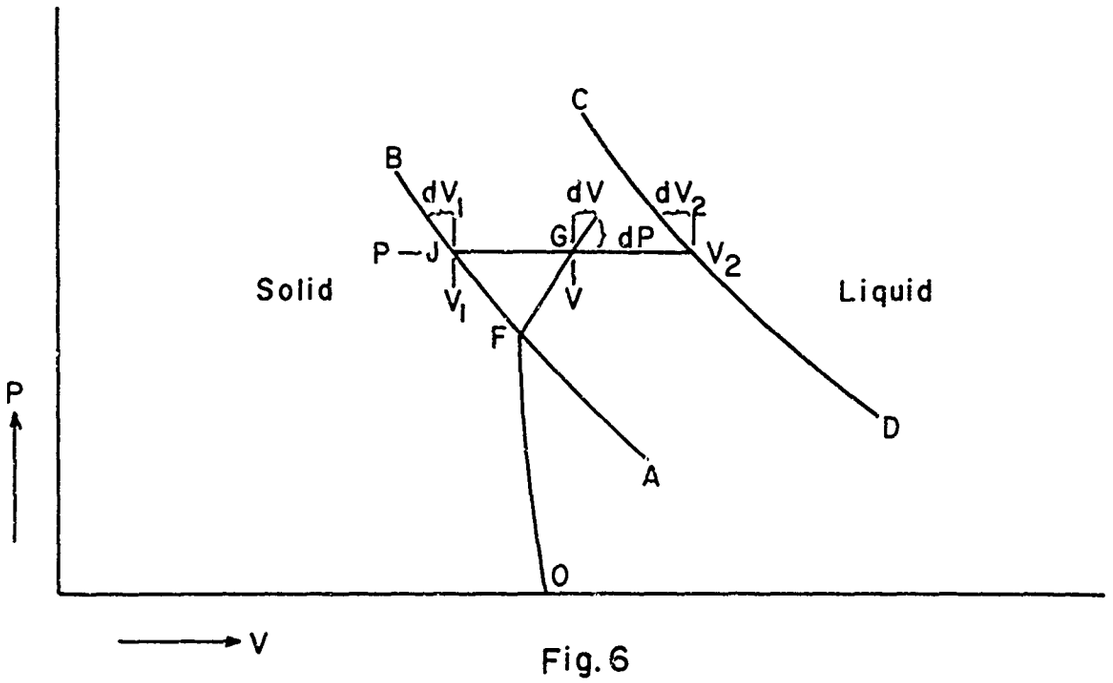

Fig. 6

Hugoniot in the Mixed Phase Region

solid and mixed phase. G is a point on the mixed-phase equilibrium Hugoniot. The enthalpy difference between G and F can be written

$$H_G - H_F = \int_F^J (dH/dP)dP + \Delta H(V-V_1)/(V_2-V_1) \tag{3.6}$$

where dH/dP is the variation of enthalpy along the phase boundary and $\Delta H(P,T)$ is the enthalpy difference between liquid and solid at pressure P, temperature T:

$$\Delta H = T(V_2-V_1)\, dP/dT = H_2 - H_1 . \tag{3.7}$$

The Clausius-Clapeyron equation has been used to obtain this result. Substitution of Eq. (3.7) into (3.6) yields the result

$$H_G - H_F = H_J - H_F + T(V-V_1)dP/dT . \tag{3.8}$$

From the Rankine-Hugoniot relation we have, for a single shock from 0 to G:

$$H_G - H_{o2} = (P-P_o)(V_{o2}+V)/2 \tag{3.9}$$

Combining Eqs. (3.8) and (3.9) yields the result:

$$(P-P_o)(V_{o2}+V)/2 = H_J + T(V-V_1)(dP/dT) - H_{o2} \tag{3.10}$$

Differentiate Eq. (3.10) to obtain:

$$dP/dV = \left((TdP/dT) - (P-P_o)/2\right)/(A' + B') \tag{3.11}$$

$$A' = (V_{o2}-V)/2 - T(V-V_1)(dT/dP)(d^2P/dT^2) \tag{3.12}$$

$$B' = V_1 - dH_1/dP + T\, dV_1/dT \tag{3.13}$$

$$V_1 - dH_1/dP = T(\partial V_1/\partial T)_P - C_{p1}\, dT/dP \tag{3.14}$$

where subscript "1" denotes quantities evaluated in the solid phase at the phase boundary. Two further relations are required:

$$TdV_1/dT = T(\partial V_1/\partial T)_P + T(\partial V_1/\partial P)_T(dP/dT) \tag{3.15}$$

$$C_{p1} = C_{V1} + T(\partial P_1/\partial T)_V\, (\partial V_1/\partial T)_P \tag{3.16}$$

Substitution of Eqs. (3.14)-(3.16) into (3.13) yields:

$$B' = 2T(\partial V_1/\partial T)_P - C_{V1}\, dT/dP - T(\partial P_1/\partial T)_V\, (\partial V_1/\partial T)_P\, (dT/dP) \tag{3.17}$$

Combining this with Eq. (3.12) yields

$$A' + B' = B - A$$

where

$$B = 2T(\partial V_1/\partial T)_P + T(\partial V_1/\partial P)_T\, (dP/dT) + (V_{o2}-V)/2 \tag{3.18}$$

$$A = \left(C_{V1} + T(\partial P_1/\partial T)_V\, (\partial V/\partial T)_P + T(V-V_1)(d^2P/dT^2)\right)(dT/dP) \tag{3.19}$$

Then

$$dP/dV = ((P-P_o)/2 - TdP/dT)/(A-B) \tag{3.20}$$

Equation (3.20) is equivalent to one given by V. D. Urlin and A. A. Ivanov in Ref. 2.

C. Liquid Phase

At the boundary between mixed phase and liquid phase a test must be made according to Eq. (3.3) to determine whether or not a single shock into the liquid phase is stable. If it is, the integration is continued to higher values of P, using

the generalized form of Eq. (3.1):

$$dP/dV = \left((\partial P/\partial V)_S + (P-P_o)(\partial P/\partial T)_V/2C_V\right) / \left(1 - (V_{o2}-V)(\partial P/\partial T)_V/2C_V\right) . \quad (3.21)$$

IV. Equations of State

A. Solid Phase

Calculation of the Hugoniot curve through the solid and mixed phases can be accomplished using only the equation of state of the solid. Since both the Hugoniot and the phase boundary must be calculated in the P-V plane, the equation of state must be complete and internally consistent. For simplicity we choose a Mie-Grüneisen equation with Debye variations of thermal energy. As we shall see, this produces some disagreement with measurements, but for the present we ignore these for the sake of theoretical consistency. The Mie-Grüneisen equation is

$$P(V,E) = P_K(V) + (\Gamma/V)\left(E(V,T) - E_K(V)\right) \quad (4.1)$$

where $P_K(V)$ and $E_K(V)$ are pressure and internal energy on the 0^oK isotherm, and Γ is the Grüneisen parameter:

$$\Gamma(V) = (V/C_V)(\partial P/\partial T)_V \quad (4.2)$$

where C_V is specific heat at constant volume. Following Rice, McQueen and Walsh (13) we write:

$$P_K(V) = P_K(\mu) = b_1\mu + b_2\mu^2 + b_3\mu^3 + P_o \quad (4.3)$$

$$\Gamma(V) = a_o + a_1\mu + a_2\mu^2 + a_3\mu^3 \qquad (4.4)$$

$\mu = (V_o/V) - 1 = (\rho/\rho_o) - 1$

V_o = specific volume at $P = P_o$, $T = 0^oK$

The difference $E - E_K \equiv Eth$ is the thermal energy:

$$Eth = 3RT\, D(\theta/T) \qquad (4.5)$$

where θ is the Debye temperature, R is the gas constant divided by the molecular weight, and $D(\theta/T)$ is the Debye function:

$$D(\theta/T) = \left(3/(\theta/T)^3\right)\int_o^{\theta/T} (x^3/(\exp(x) - 1))dx\,. \qquad (4.6)$$

For small values of θ/T, D can be expanded in series:

$$D \simeq 1 - .375\,(\theta/T) + .05\,(\theta/T)^2 \qquad (4.7)$$

This is accurate to .3% for $\theta/\tau < .3$.

The Debye temperature is related to the Grüneisen parameter by the equation

$$d\ell n\theta/d\ell nV = -\Gamma\,. \qquad (4.8)$$

Using Eq. (4.4) for Γ, this integrates to

$$\theta = \theta_o \exp\Big((a_o - a_1 + a_2 - a_3)\,\ell n(\mu+1) + (a_1 - a_2 + a_3)\mu + (a_2 - a_3)\,\mu^2/2 + a_3\mu^3/3\Big) \qquad (4.9)$$

The specific heat is defined as

$$C_V = (\partial E_{th}/\partial T)_V \tag{4.10}$$

$$= 3R\left(4D - 3(\theta/T)/(\exp(\theta/T) - 1)\right) \tag{4.11}$$

$$\simeq 3R\left(1 - .05(\theta/T)^2\right) . \tag{4.12}$$

In calculating the Hugoniot, we shall need some thermodynamic coefficients which can be calculated from the above equations:

$$d(\Gamma/V)/dV = - (V_o/V^3)(a_1+2a_2\mu + 3a_3\mu^2) - \Gamma/V^2 \tag{4.13}$$

$$(\partial E_{th}/\partial V)_T = 3R\, D'\, d\theta/dV \tag{4.14}$$

$$\simeq - 3R\Gamma\theta\left(-.375 + .1(\theta/T)\right)/V \tag{4.15}$$

$$D' = dD/d(\theta/T) \tag{4.16}$$

$$dP_K/dV = (-V_o/V^2)(b_1 + 2b_2\mu + 3b_3\mu^2) \tag{4.17}$$

$$(\partial P/\partial V)_T = dP_K/dV + E_{th}\, d(\Gamma/V)/dV + (\Gamma/V)(\partial E_{th}/\partial V)_T \tag{4.18}$$

$$(\partial V/\partial T)_P = - \Gamma C_V (\partial V/\partial P)_T/V \tag{4.19}$$

$$(\partial P/\partial V)_S = (\partial P/\partial V)_T - \Gamma^2\, C_V T/V^2 \tag{4.20}$$

B. Liquid Phase

One of the most promising theories of the liquid state for computational purposes is Henry Eyring's Significant Structure Theory (Ref. 9). The essence of the theory is that a liquid consists of a solid containing holes of atomic dimensions, and

that the holes behave like the molecules of an ideal gas. In order to test it at high pressures, isotherms, adiabats and Hugoniot curves for argon have been calculated from it and the last compared with measured values reported in the literature (Ref. 12). The two agree remarkably well at low pressures, but the theory fails to properly account for the energy of cold compression and the computation fails at higher pressures (> 12 Kbars for the highest initial density). These computations are reported in Appendix B.

Various authors have used simplified versions to describe liquids at high pressures. In the present application the theory is used in its simplest form:

$$P(V_\ell,T) = P_K(V_s) + (\Gamma_s/V_s)\, E_{ths}(V_s) + n_h kT/V_\ell \qquad (4.21)$$

$$E_\ell = E_s + E_h \qquad (4.22)$$

$$E_h = (3/2) n_h kT \qquad (4.23)$$

$$n_h = N(V_\ell - V_s)/MV_s \qquad (4.24)$$

where subscripts "s," "h," "ℓ," denote solid, holes, and liquid respectively; N is Avogadro's number, M is molecular weight and k is Boltzmann's constant. Substituting Eq. (4.24) into (4.21) yields

$$P(V_\ell,T) = P_k(V_s) + (\Gamma_s/V_s)\, E_{ths}(V_s) + RT(V_\ell - V_s)/MV_\ell V_s \qquad (4.25)$$

Equation (4.25) does not contain an interaction term between holes and molecules, though that is important in Eyring's theory.

However it may be less important at high pressure than proper treatment of the solid compression.

The above equations are supplemented by an expression for ΔV_m , the change of volume on melting at constant pressure:

$$\Delta V_m = \Delta H(dT/dP)/T_m = V_\ell - V_s \qquad (4.26)$$

With these equations the Hugoniot can be continued into the liquid region.

V. Melting Equations

Attempts to predict melting parameters from atomic theories have been many and varied. The earliest one normally noted is that of Lindemann in 1910 (Ref. 4). Assuming an Einstein model of a solid with single vibration frequency f, suppose that the amplitude of vibration increases with temperature, and that when the amplitude reaches a critical fraction of the interatomic distance, melting occurs. Equating the energy of vibration to the thermal energy of the crystal leads to an equation of the form

$$3R\ T_m = C\ f^2\ V_M^{2/3}\ M \qquad (5.1)$$

where T_m = melting temperature, V_M = molar volume at T_m, M is molecular weight, and C is a constant. By writing $4\pi^2 f^2 = k/m$, where m is atomic mass, and setting the energy of an oscillator equal to $k(r - r_o)^2/2$, where $r - r_o$ is the

deviation of interatomic distance from equilibrium, we obtain

$$e = k(r - r_o)^2/2$$

$$k = d^2e/dr^2 .$$

Identify the oscillator energy, e, with the molar energy, $\mathcal{E}_k$, of cold compression by the relation

$$\mathcal{E}_k = 3Ne = \mathcal{E}_k(\dot{V}) .$$

Then Eq. (5.1) can be converted to the following relation:

$$RT = 3M\alpha^2V^2(d^2E_k/dV^2)/2 \qquad (5.2)$$

$$= A\ V^2\ d^2\ E_k/dV^2 \qquad (5.3)$$

where V = specific volume as in Section 4, E_k = specific internal energy, α = fraction of interatomic distance at which melting occurs, and M is molecular weight. Eq. (5.3) is the form given by Urlin and Ivanov in Reference 2. They also propose an alternative melting law in the form

$$L\ V_m/T_m\ \Delta V_m = Ra \qquad (5.4)$$

where L = latent heat of fusion, V_m = specific volume at which melting occurs, T_m = melting temperature, ΔV_m is volume change on melting, and Ra is a constant. This is a modification of the Lindemann formula which can be seen as follows:

$$d^2E_k/dV^2 \equiv (-dPk/dV)_{p=o}$$

$$= b_1/V_o$$

where the last expression is obtained from Eq. (4.17). Substituting this into Eq. (5.3) yields

$$RT = AV^2 b_1/V_o$$

Differentiate with respect to P to obtain

$$RdT/dP = 2AV(dV/dP)b_1/V_o$$

or

$$dP/dT = L/T\Delta V_m$$

$$= RV_o(dP/dV)/2Ab_1V \ , \tag{5.5}$$

which is of the form Eq. (5.4) with dP/dV assumed constant.

One of the most commonly used forms for the melting curve is Simon's equation (Ref. 5):

$$P - P_m + a = a(T/T_m)^C \tag{5.6}$$

where P_m and T_m represent one point on the melting curve and C and a are constants determined from the relations

$$aC = T_m(dP/dT)_{Tm} \tag{5.7}$$

and

$$a = (dE_k/dV)_{T=0,P=0} \tag{5.8}$$

according to Simon. Later work by Salter, using the Mie-Grüneisen equation of state, identifies C as

$$C = (6\Gamma_s+1)/(6\Gamma_s-2) \tag{5.9}$$

where Γ_s is the Grüneisen parameter of Eq. (4.4).

A melting relation recently proposed by G. C. Kennedy (Ref 6) relates volume on the melting curve to temperature:

$$T_m = T_m^o(1 + C_k \Delta V/V_o) \tag{5.10}$$

where T_m^o is melting temperature at volume V_o and $\Delta V = (V_o - V_m)$. Ross and Alder (Ref. 7) have criticized this as being of lower validity than Lindemann's law and of giving too low values of T_m at high compressions. Gilvarry (Ref. 8) suggests that it is the first term in the expansion of the formula

$$T_m/T_m^o = (V_o/V_m)^{2(\Gamma_o - 1/3)} \tag{5.11}$$

where Γ_o is the Grüneisen parameter at V_o.

At present it appears very much as if there is as much justification for picking one rule as another, in the absence of experimental data. In the calculations to be reported later we use the Simon equation and the Kennedy equation.

VI. Calculation of the Hugoniot

The computing process is illustrated in Fig. 7. Volume and temperature are assumed to be known on the phase boundary and on the Hugoniot at pressure P. P is increased to $P + \Delta P$ and new values of temperature are calculated from Eqs. (5.6) and (4.5). This allows calculation of the coefficients dV/dP from Eqs. (1.5) and (3.1). Subscripts 1 and 2 refer to values on the solid-mixed phase boundary and the Hugoniot, respectively. Values of V_1 and V_2 are then determined from the relations

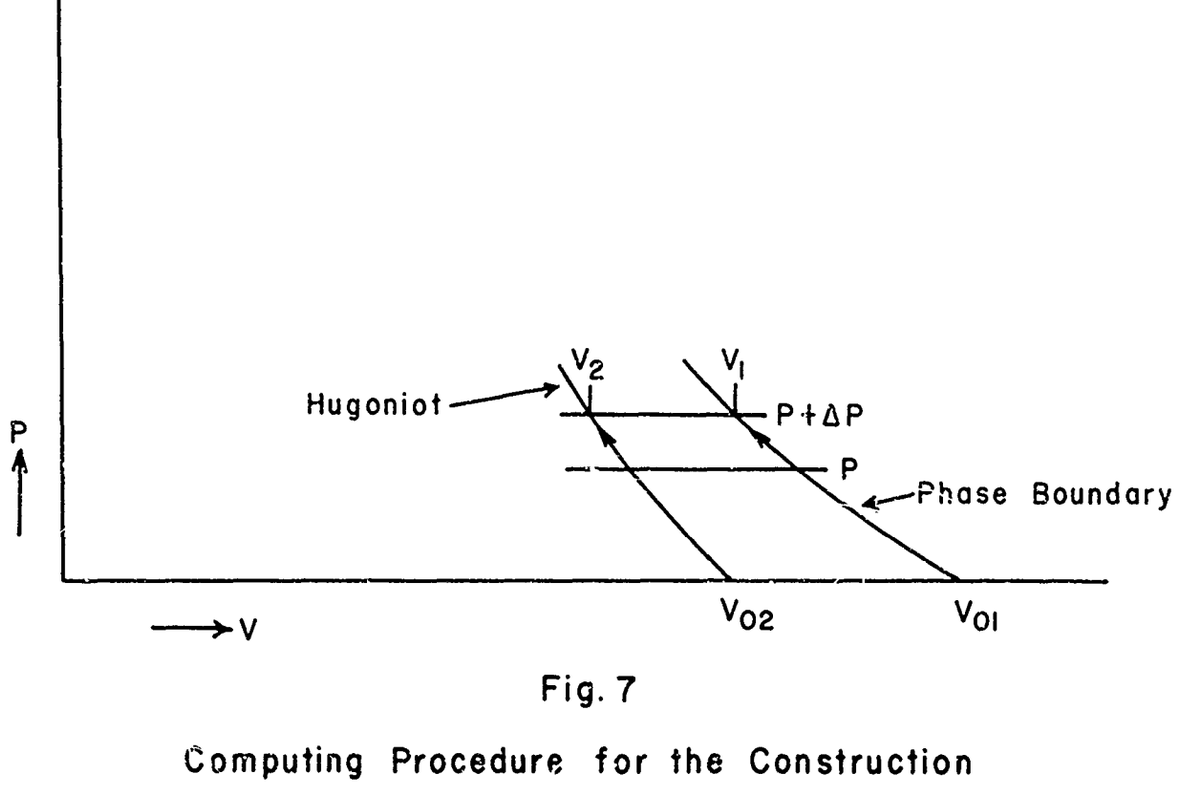

Fig. 7

Computing Procedure for the Construction of the Equilibrium Hugoniot

$$V_1(P + \Delta P) = V_1(P) + (.5)\left((dV_1/dP)_{P+\Delta P} + (dV_1/dP)_P\right)\Delta P \qquad (6.1)$$

$$V_2(P + \Delta P) = V_2(P) + .5\left((dV_2/dP)_{P+\Delta P} + (dV_2/dP)_P\right)\Delta P \qquad (6.2)$$

The equations are iterated until $V_1(P + \Delta P)$ and $V_2(P + \Delta P)$ do not change, then the process is repeated.

After each set of values (V_1, V_2) has been calculated, a test is made to determine whether or not an intersection between $V_1(P)$ and $V_2(P)$ has occured. If it has, the Hugoniot Eq. (3.1) is replaced by Eq. (3.20) for the mixed phase and the process continues, testing at each step to see if the Hugoniot has entered the liquid phase. When it does, Eq. (3.21) is used again with the equations of Section IVB for the equation of state.

A flow chart for the computing program is shown in Fig. 8; definition of symbols and a program listing are given in Appendix A.

The output of the program is illustrated in Figs. 9-13 and in Table 3 for lead. Fig. 9 shows the total Hugoniot to one megabar pressure using the Simon Equation. It enters the mixed phase region from the solid at about .645 megabars and leaves at about .675. Inspection of the curve shows that a single shock will be stable at all pressures (elastic waves are ignored). This is verified by the slopes given in Table 3. The narrow mixed phase region and the small kink it produces in the Hugoniot curve suggest also that melting will have a small effect on wave propagation, even if it occurs in shock.

This remains to be verified by incorporation of the model into a one-D wave program.

Table III

Slopes of Hugoniots and Rayleigh Lines at Melting Phase Boundaries

P, Megabars	$\lvert dP/dV \rvert_{Hugoniot}$ Megabar g/cc			$\lvert (P-P_o)/(V_o-V) \rvert$ Megabar cc/g	
	Solid	Mixed Phase	Liquid	Solid Boundary	Liquid Boundary
.645*	67.4	107.2	...	21.9	...
.675*	...	114.1	52.6	...	22.7
.392†	39.0	37.2	...	16.0	...
.428†	...	39.4	42.4	...	16.8

*Simon Equation (5.6) †Kennedy Equation (5.10)

Figure 10 shows the Hugoniot in the region of mixed phase in more detail, again for the Simon Equation.

Figure 11 shows temperatures on the melting curve and on the Hugoniot for the Simon Equation. In region A, where the Hugoniot is passing through the mixed phase, the two curves should coincide. That they do not reflects imperfections in the equation of state.

Flaws in the equation of state are revealed when measured specific volume of the solid at melting, V_m , is found to disagree with that calculated from the equation

$$V_{o1} = V_{o2} + \int_{T_{o2}}^{T_{o1}} (\partial V/\partial T)_{P=P_o} dT \quad , \tag{6.1}$$

where T_{o2} is room temperature; V_{o2} is specific volume at room temperature and pressure P_o; T_{o1} is melting temperature at P_o; and V_{o1} is specific volume at P_o, T_{o1}. For this reason a procedure for calculating V_{o1} is incorporated in the program (Appendix A). Even with this correction, a slight difference between T1N and T2N occurs, as shown in Fig. 11. The difficulty probably arises from a minor inconsistency between the equations for Γ and P_k.

Parameters and material constants used in the calculations for lead are listed in Appendix A.

Figures 12, 13 and 14 display the results when the Simon Equation is replaced by the Kennedy Equation. The temperature and pressure at which the Hugoniot enter the melting region are about half the values obtained with the Simon Equation. These tremendous differences represent the state of our ignorance about the melting process at high pressures, and unless detection of melting in shock is possible, that state of affairs is very likely to persist.

Fig. 8.--Flow Chart for Calculation of Hugoniot when Melting Occurs

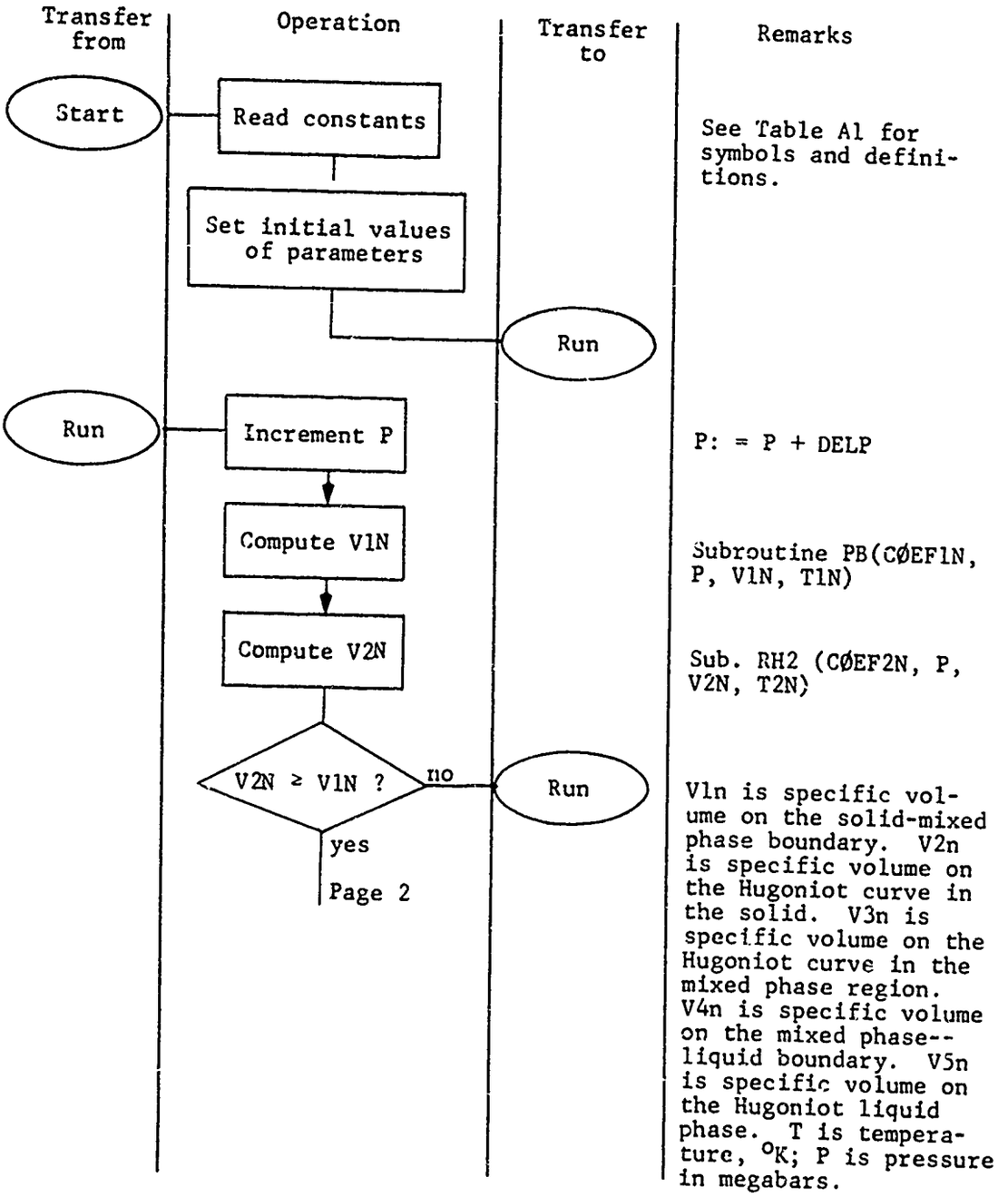

Fig. 8.--Continued

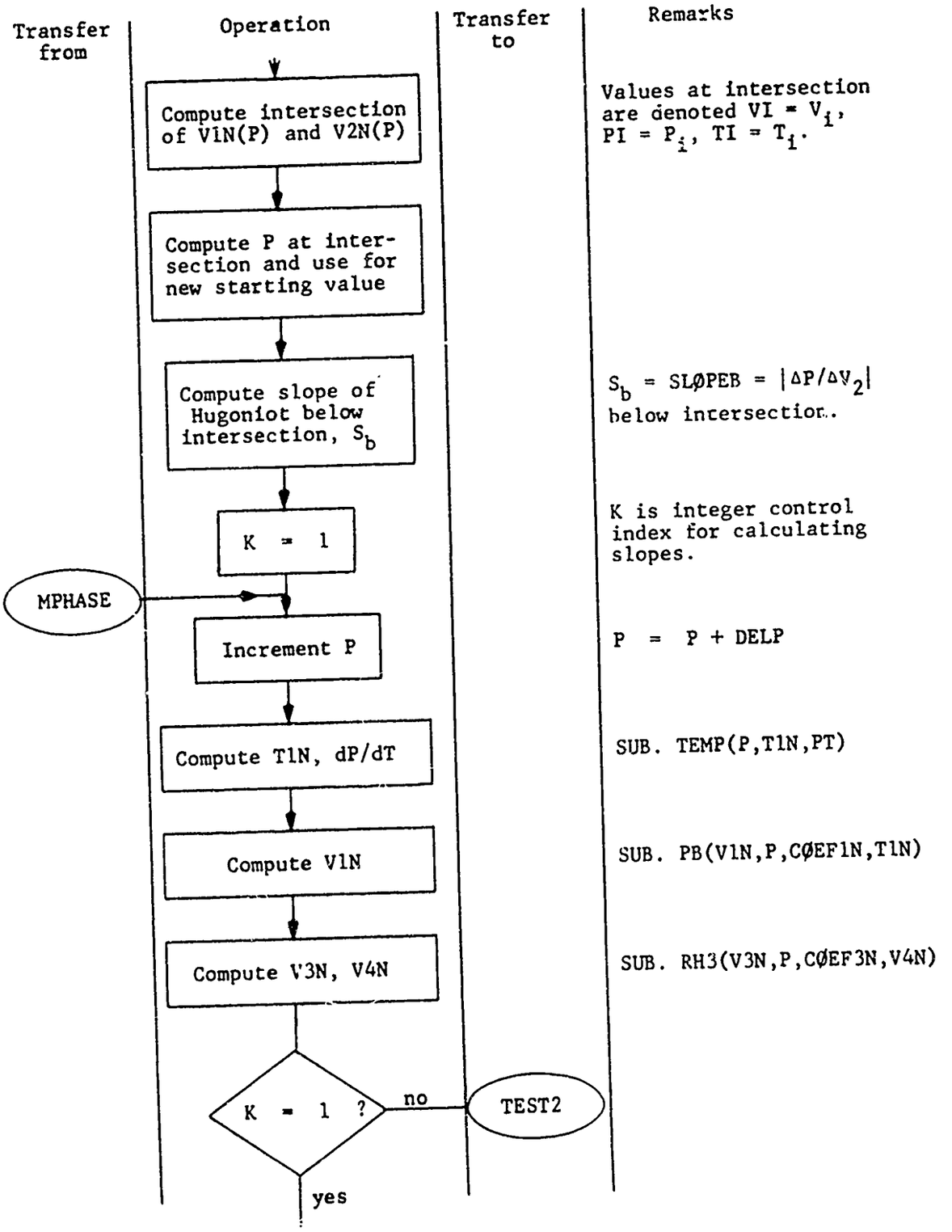

Fig. 8.--Continued

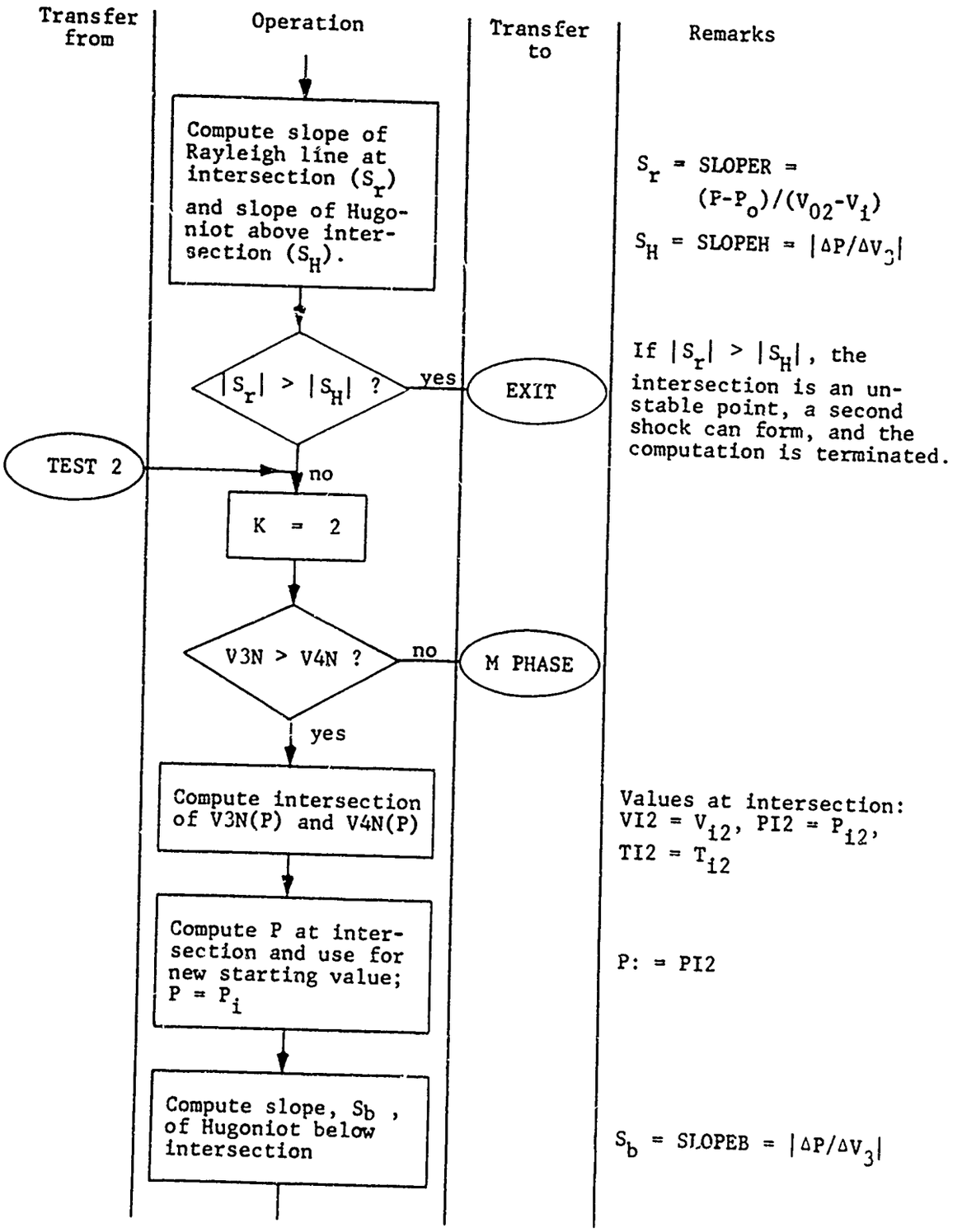

Fig. 8.--Continued

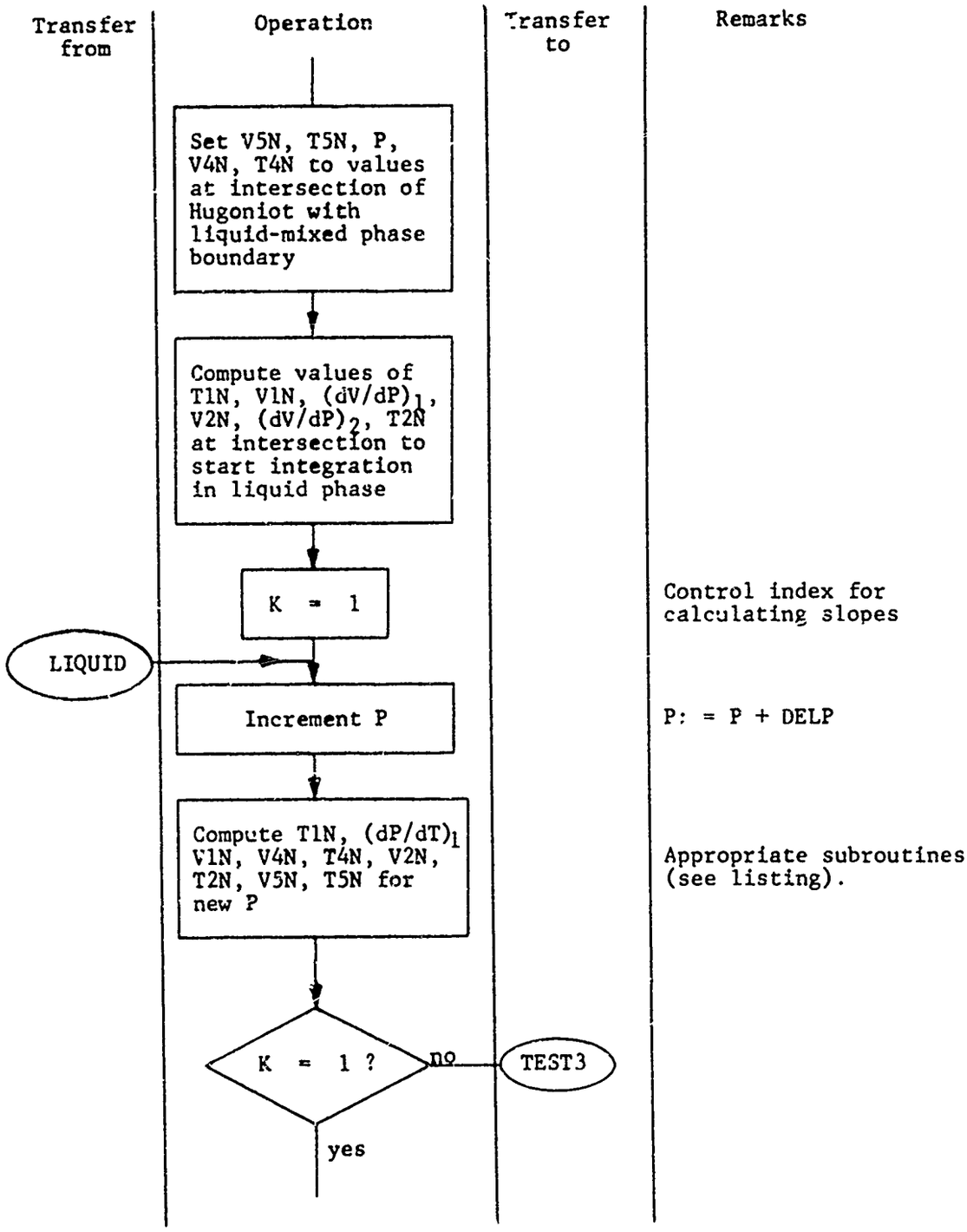

Fig. 8.--Continued

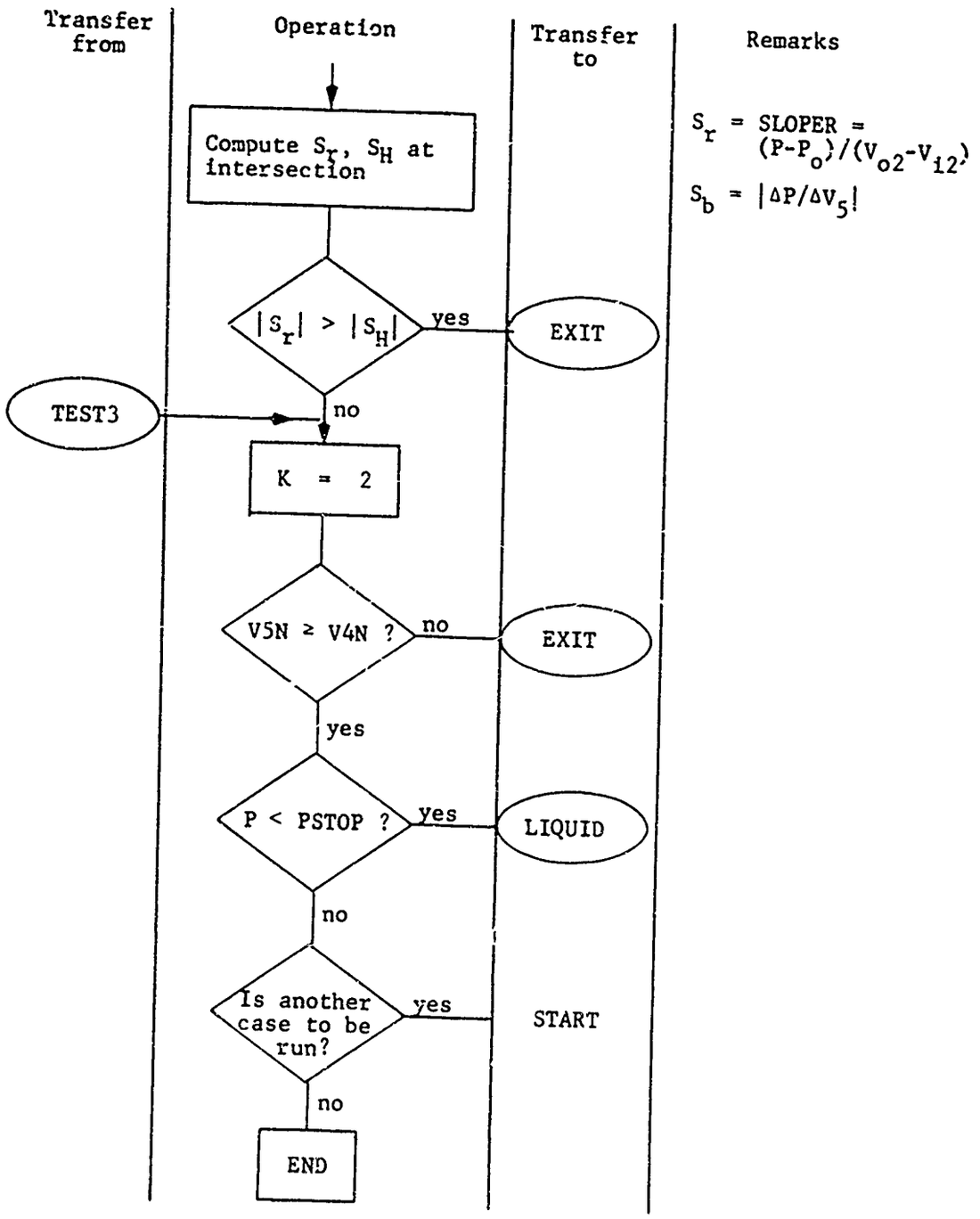

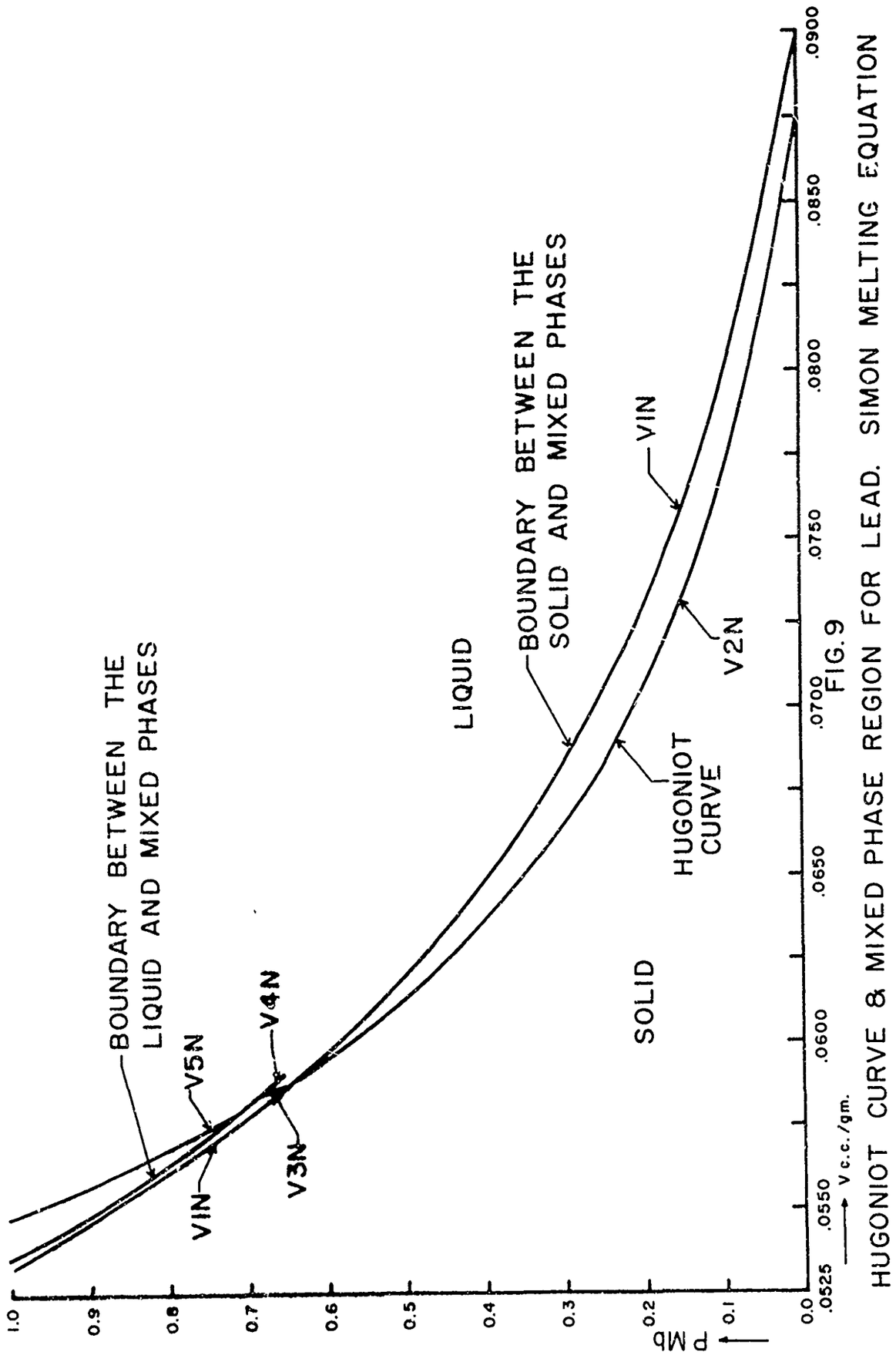

FIG. 9

HUGONIOT CURVE & MIXED PHASE REGION FOR LEAD. SIMON MELTING EQUATION

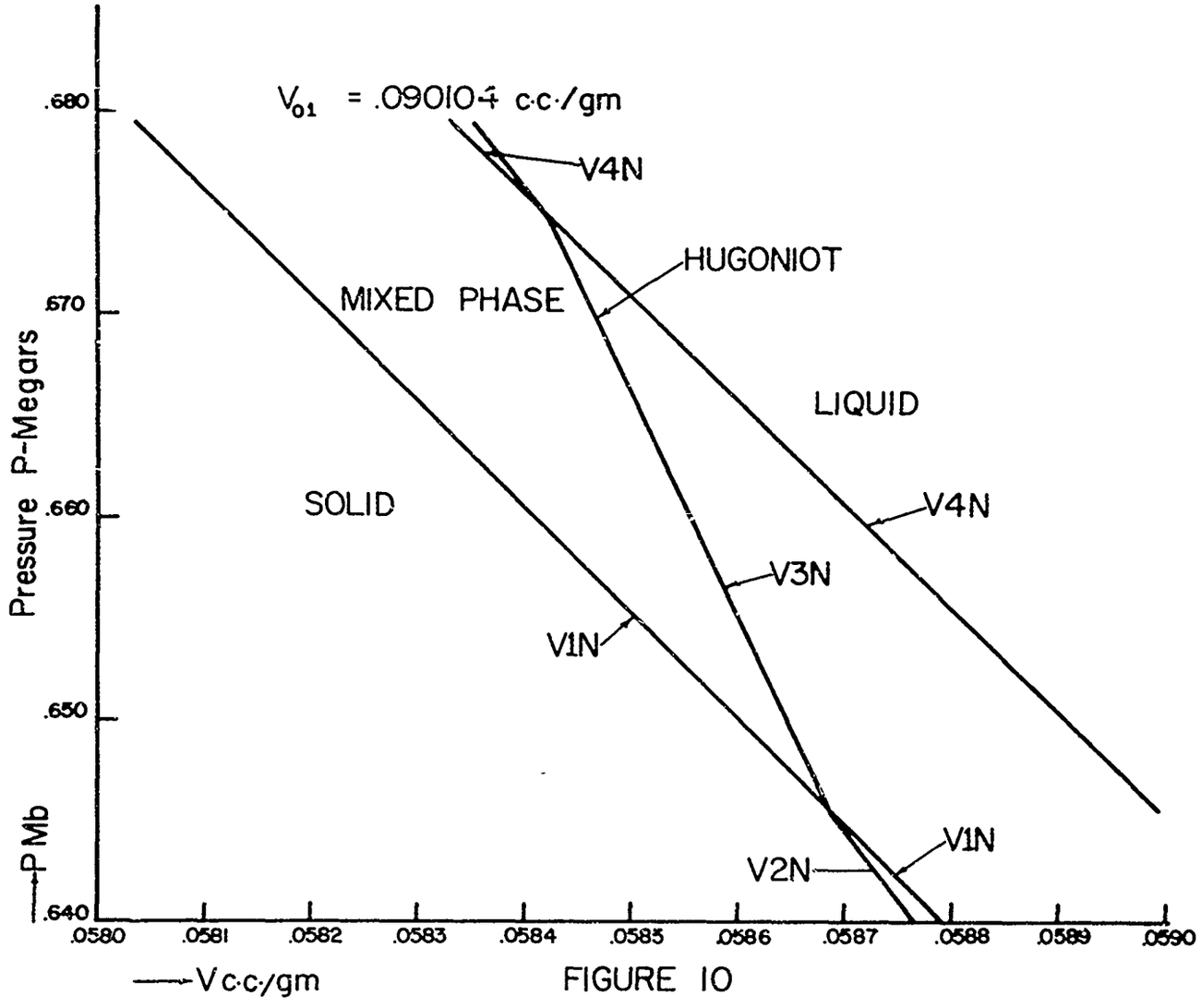

FIGURE 10

HUGONIOT CURVE FOR LEAD IN THE MIXED PHASE REGION. SIMON MELTING EQUATION

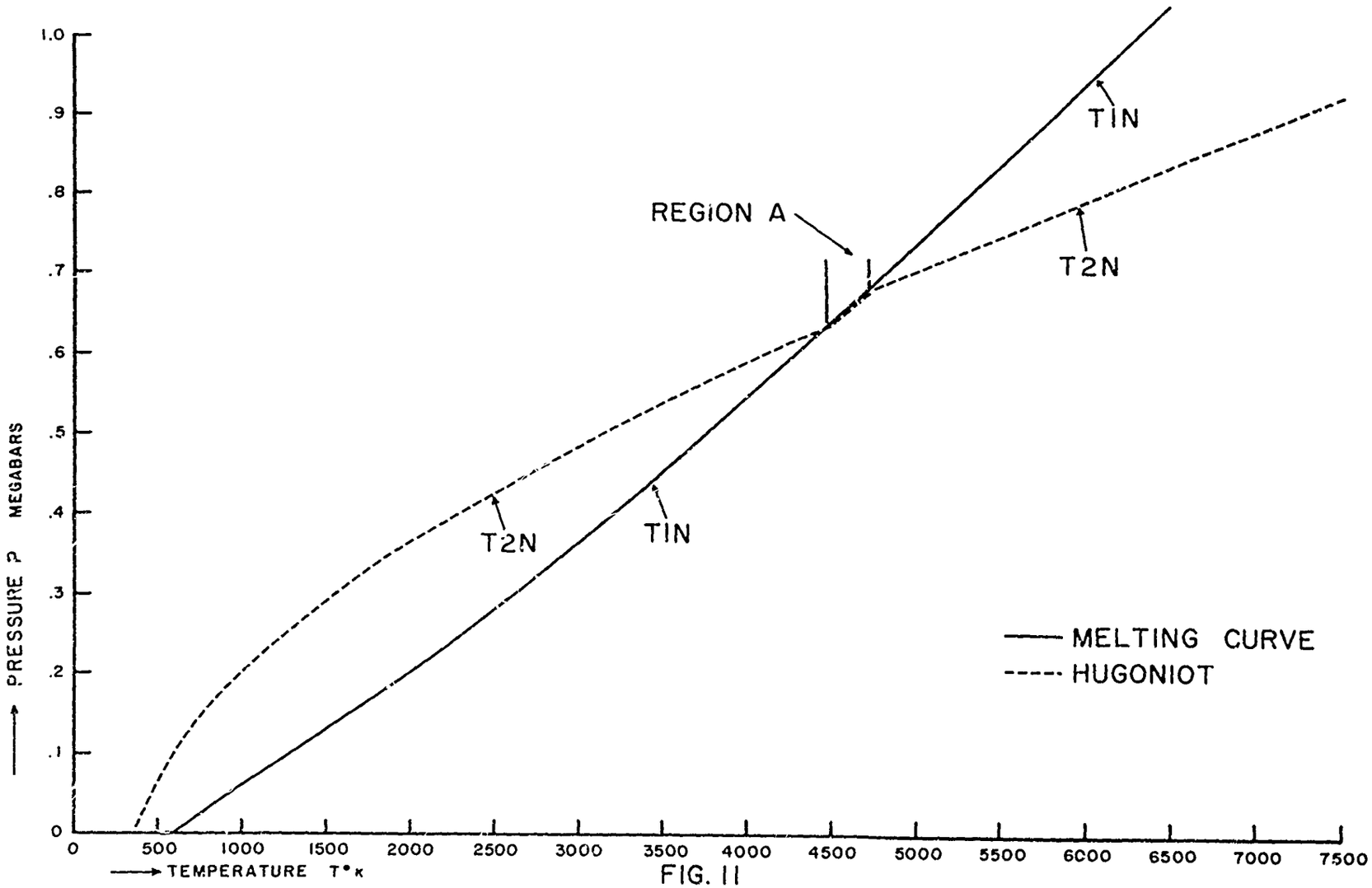

FIG. 11

TEMPERATURE IN LEAD. SIMON EQUATION

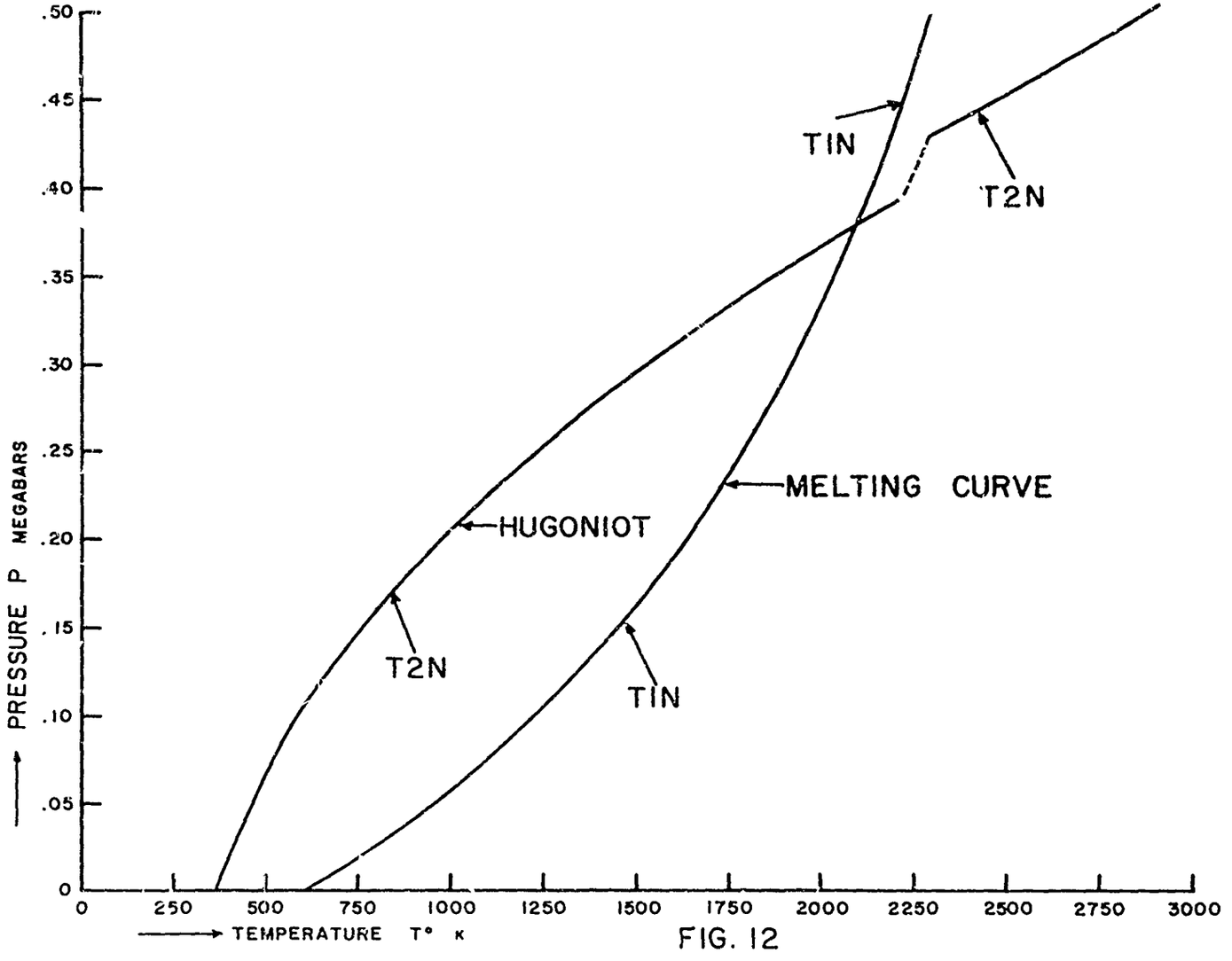

FIG. 12

TEMPERATURE IN LEAD. KENNEDY EQUATION

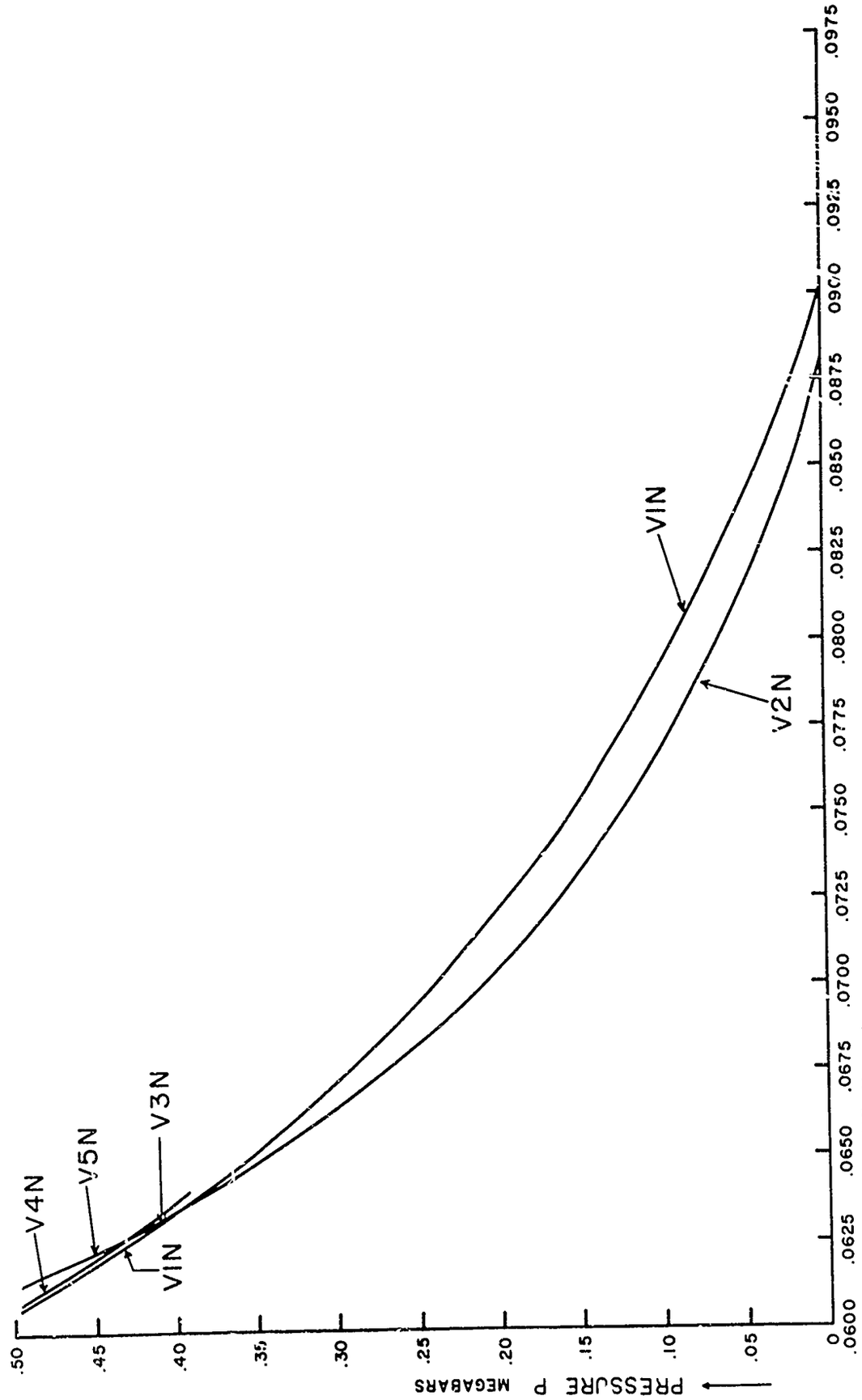

FIG. 13

HUGONIOT AND MELTING PHASE BOUNDARIES FOR LEAD. KENNEDY EQUATION

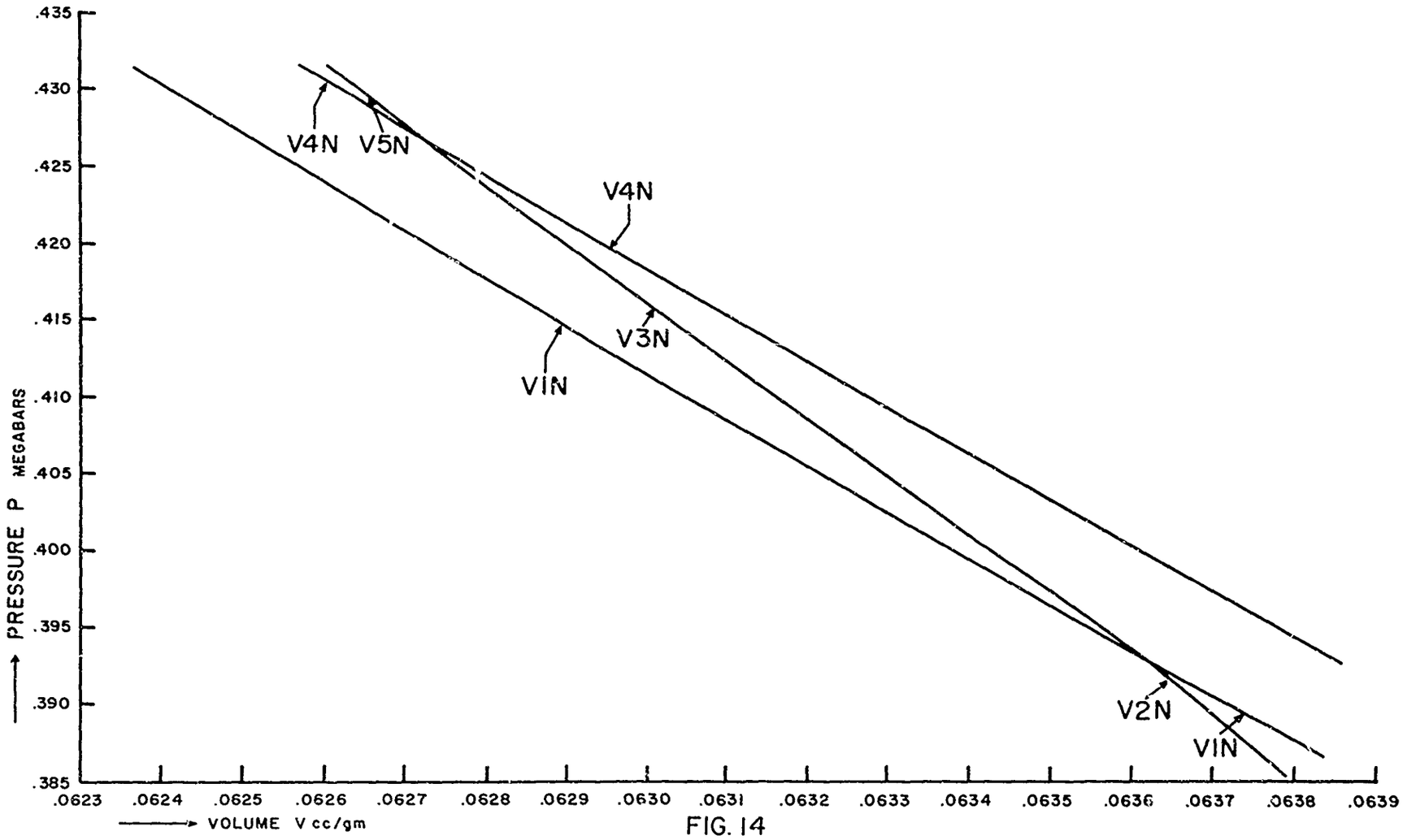

FIG. 14

HUGONIOT CURVE FOR LEAD IN THE MIXED PHASE REGION. KENNEDY EQUATION

REFERENCES

1. G. E. Duvall and Y. Horie, "Shock Induced Phase Transitions," Proceedings of 4th Symposium (International) on Detonation, NOL, October, 1965. U.S. Government Printing Office, 1967.
2. V. D. Urlin and A. A. Ivanov, "Melting Under Shock Compression," Sov. Phys. Doklady 8, 4, 380 (October, 1963).
3. R. G. McQueen and S. P. Marsh, "Equation of State for Nineteen Metallic Elements from Shock-Wave Measurements to Two Megabars," J. Appl. Phys. 31, 7, 1253-1269 (July, 1960).
4. A. R. Ubbelohde, Melting and Crystal Structure, Oxford Press, 1965. Chapter 3.
5. R. S. Bradley, "First and Second Order Phase Changes in One-Component Systems," Ch. 5.iii of High Pressure Physics and Chemistry, Academic Press, 1963, Vol. I; R. S. Bradley, Ed.
6. Edgar A. Kraut and G. C. Kennedy, "New Melting Law at High Pressures," Phys. Rev. Letters 16, 608 (4 April 66).
7. M. Ross and B. J. Alder, Phys. Rev. Letters 16, 1077 (13 June 66).
8. J. J. Gilvarry, Phys. Rev. Letters 16, 1089 (13 June 66).
9. H. Eyring and R. P. Marchi, J. Chem. Educ. 40, 562 (November, 1963).
10. R. Gasnier, "Équation d'État Semi-empirique des Métaux," Proceedings of Symposium on High Dynamic Pressure, " IUTAM, 11-15 September, 1967, Paris.

11. Kormer, Funtikov, Urlin, Kolesnikova, "Dynamic Compression of Porous Metals," Sov. Physics, JETP 15, 3 (1962).

12. M. Van Thiel and B. Alder, J. Chem. Phys. 44, 1056 (1966).

13. M. H. Rice, R. G. McQueen, J. M. Walsh, "Compression of Solids by Strong Shock Waves," Solid State Physics, Vol. 6, 1958. Seitz and Turnbull, Eds. (Academic Press.)

APPENDIX A

PROGRAM FOR COMPUTING THE HUGONIOT OF A MELTING SOLID

Program Name: MELT

Language: FØRTRAN IV

Constants

Report symbol	Equation	Program symbol	Remarks
P_o	3.1, 5.6	PØ	atmospheric pressure, megabars
ρ_o	4.4a	RHØØ	density at P_o, T = 0^oK
		RHØ2	density at P_o, T = TØ2 (room temperature)
3R	4.5	R3	R = gas constant, Mb cc/g^o
V_{o1}	A1	VØ1	specific volume of solid at melting temperature and P = P_o
T_{o1}	A1	TØ1	melting temperature at P = P_o
a_o, a_1, a_2, a_3	4.4	AØ,A1,A2,A3	
b_1, b_2, b_3	4.3	B1,B2,B3	
θ_o	4.9	TDØ	
V_o	4.4a	VØ	
ΔP	7.1	DELP	
a,c	5.6	A,C	
V_{o2}	3.1	VØ2	sp. vol. on Hugon. at P = P_o

Report symbol	Equation	Program symbol	Remarks
		TØ2	temperature at PØ,VØ2
		PSTØP	pressure at which computation stops
		ICØNT	integer allowing several data sets to be used in one run
dT	A1	DELT	increment in temperature used to calculate VØ1 from VØ2,TØ1,TØ2

Parameters in MAIN

A final letter "N" on a parameter symbol indicates a value at pressure P + ΔP, an "Ø" indicates a value at P; e.g., V1N = V1 at P + ΔP, V1Ø = V1 at P.

Report symbol	Equation	Program symbol	Remarks
		ALG,ALIN	Program computed constants used in evaluating TD
		ASQ,ACUBE	
V_1	1.5	V1N,V1Ø	specific volume on solid-mixed phase boundary
T	1.6, 5.6	T1N,T1Ø	melting temperature
V	3.1	V2N,V2Ø	specific volume on solid phase Hugoniot
T	4.5-4.20	T2N,T2Ø	temperature on solid phase Hugoniot
V	3.18,3.19	V3N,V3Ø	specific volume on mixed phase Hugoniot
T	3.20	T3N,T3Ø	temperature on mixed phase Hugoniot
V_2	1.2	V4N,V4Ø	specific volume on liquid-mixed phase boundary

Report symbol	Equation	Program symbol	Remarks
		T4N,T4Ø	same as T1N,T1Ø
V_{ℓ}	4.25	V5N,V5Ø	specific volume on liquid phase Hugoniot
T	4.25	T5N,T5Ø	temperature on liquid phase Hugoniot
dV_1/dP	1.5	CØEF1	slope of phase boundary
dV/dP	3.2	CØEF2	slope of solid phase Hugoniot
V	A1	VX	value of V at $P = P_o$, $T = TX$ $(T\emptyset 2 \leq TX \leq T\emptyset 1)^o$ used to calculate VØ1 from VØ2,TØ1,TØ2
T	A1	TX	temperature. $T\emptyset 2 \leq TX \leq T\emptyset 1$ used in the calculation of VØ1.
		TXT	TXT = TX-DELT
		VXT	value of VX at TXT
		MU,TD1,X,D,DP G1,Q1,W,ET,M1, ETT,R1,S1	same as in subroutine PB
		JC	integer used to control what part of a subroutine is to be used in a particular calculation
		K	controlling integer used in main, similar to JC in operation
-dP/dV	3.1	SLOPEB	dP/dV for the Hugoniot just inside the one phase
-dP/dV	3.20,3.21	SLOPEH	dP/dV for the Hugoniot just inside the next phase
$(P_1-P_o)/(V_o-V_1)$	3.3	SLOPER	slope of the Rayleigh line from the foot of the Hugoniot to its intersection with the phase boundary

Report symbol	Equation	Program symbol	Remarks
dV/dP	3.20	CØEF3	slope of mixed phase Hugoniot
dV/dP	3.21	CØEF5	slope of liquid phase Hugoniot
		VI	sp. vol, pressure and temperature at intersection of $V_1(P)$ and $V_2(P)$
		PI	
		TI	
		VI2	sp. vol., pressure and temperature at intersection of $V_3(P)$ and $V_4(P)$
		PI2	
		TI2	
dP/dT	1.1	PT	Clausius-Clapeyron coefficient
ΔV	1.1, 1.2	DELV	sp. vol. change on melting
ΔH	1.1	LATHT	latent heat of melting

Parameters in SUBRØUTINE PB(CØEF1N,P,V1N,T1N)

Report symbol	Equation	Program symbol	Remarks
		V1NN	temporary value of V1N used to test convergence of iteration
μ	4.4a	MU	
θ	4.9	TD1	
T	5.6	T1	
		X	θ/T
dT/dP		CC	reciprocal of Clausius-Clapeyron coefficient
D	4.7	D	Debye function
D'	4.16	DP	

Report symbol	Equation	Program symbol	Remarks
Γ	4.4	G1	
C_v	4.12	CV1	
$d(\Gamma/V)/dV$	4.13	Q1	
dP_k/dV	4.17	W	
E_{th}	4.5	ET	
$(\partial P/\partial V)_T$	4.18	M1	
C_v	4.10-4.12	ETT	
$(\partial E_{th}/\partial V)_T$	4.15	ETV1	
$(\partial V/\partial P)_T$	...	R1	
$(\partial V/\partial T)_P$	4.19	S1	
dV_1/dP	1.5	CØ1	same as CØEF1N
		CØ1Ø	same as CØEF1Ø

Parameters in SUBRØUTINE RH2(V,P,CØEF2N,T2N)

Report symbol	Equation	Program symbol	Remarks
V		V2NN	temporary value of V2N used to test convergence of iteration
μ	4.49	MU	
V	3.1	V	same as V2N
Γ	4.4	G2	
θ	4.9	TD2	
P_k	4.3	PKØ	
D	4.7	D	
C_v	4.12	CV	
E_{th}	4.5	ETH	
dP_k/dV	4.17	DPK	

Report symbol	Equation	Program symbol	Remarks
$d(\Gamma/V)/dV$	4.13	Q2	
$(\partial E_{th}/\partial V)_T$	4.15	ETV2	
$(\partial P/\partial V)_T$	4.18	M2	
$(\partial P/\partial V)_S$	4.20	MS2	
dV/dP	3.2	CØEF2N	
θ/T	4.5	X	
D'	4.16	DX	

Parameters in SUBRØUTINE RH3(CØEF3N,P,V3N,V4N)

Report symbol	Equation	Program symbol	Remarks
		V3NN	temporary value of V3N used to test convergence of iteration
		T1	temperature at P + ΔP, transferred from SUB-RØUTINE PB
		V1	V1N at P + ΔP transferred from Sub. PB
d^2P/dT^2	3.19	PTT	
A	3.19	Y1	
$.5(P-P_o)-TdP/dT$	3.20	ANUM1	
A-B	3.20	DEN1	
		CØEF3N	same as in MAIN
		V4N	" " " "
		CØEF3Ø	" " " "

Parameters in SUBROUTINE TEMP1(P)

Report symbol	Equation	Program symbol	Remarks
dP/dT	5.6	PT	
d^2P/dT^2	5.6	PTT	
T	5.6	T	T = T1N of the main program

Values of constants used for lead:

ρ_o = 11.616 ; 3R = 0.1202506 x 10^{-5}

; T_{o1} = 601 ^oK

V_{o2} = 0.08818340 ; T_{o2} = 293^oK

a_o = 2.7091 ; a_1 = -2.5282

a_2 = 1.413 ; a_3 = 0.0

b_1 = 0.54168 ; b_2 = 0.749041 ; b_3 = 0.605839

θ_o = 96.3

γ = 0.06257 c = 1.20436

Constants independent of material:

P_o = 1.034 x 10^{-6} megabars

ΔP = .005 megabars

PSTØP = 1 megabar

Computation of V_{o1}

The equation of state used for the solid in Section IVA is self-consistent but not entirely consistent with all available measured data. In particular if V_{o1} is taken to be the handbook value, $T_1 \neq T_2$ at the intersection of $V_1(P)$ and $V_2(P)$. To

remedy this, V_{o1} was calculated from the equation

$$V_{o1} = V_{o2} + \int_{T_{o2}}^{T_{o1}} (\partial V/\partial T)_{P=P_o} \, dT \qquad (A1)$$

where T_{o2} is the value at the foot of the Hugoniot and T_{o1} is the handbook value for melting at $P = P_o$. Handbook and calculated values of V_{o1} are:

V_{o1} = .091148 cc/g (metal reference hbk)

V_{o1} = .090352 cc/g (Eq. (A1))

Program listing

The program listing follows on separate pages.

```
//LISTJOBS JOB  (0000,CC,5,10),MACHRCOM,MSGLEVEL=1
//JOBLIB DD UNIT=2311,VOLUME=SER=DLIB02,DISP=OLD,DSNAME=SYS1.UTIL.TY
//STEP EXEC PGM=LISTCRD
//SYSLST DD SYSOUT=A,DCB=(LRECL=80,BLKSIZE=80,RECFM=F)
//SYS004 DD UNIT=SYSDA,VOLUME=SER=SCR001,DSNAME=LISTER,                X
//             SPACE=(CYL,(5,1)),DCB=(RECFM=FBS,BLKSIZE=80,LRECL=80)
//SYSRDR DD *
IEF236I ALLOC. FOR LISTJOBS STEP
IEF237I JOBLIB   ON 293
IEF237I SYS004   ON 290
IEF237I SYSRDR   ON 00C
```

```
C     THIS PROGRAM INTEGRATES THE EQUILIBRIUM HUGONICT P-V CURVE
C   OF A SOLID IN INITIAL STATE TO2,PO2(=PC),VO2 ASSUMING A SINGLE SHOCK
C   FROM PO TO THE FINAL PRESSURE P. IT SIMULTANEOUSLY CALCULATES
C   THE MELTING CURVE AND AT EACH STEP TESTS TO SEE WHETHER MELTING OCCURS.
C   IF IT DOES, THE SLOPE OF THE HUGONIOT IN THE MIXED PHASE IS COMPARED
C   WITH THE SLOPE OF THE RAYLEIGH LINE TO SEE WHETHER OR NOT A SINGLE
C   SHOCK IS STILL STABLE. IF NOT, THE COMPUTATION IS TERMINATED;
C   IF IT IS, THE COMPUTATION IS CONTINUED THROUGH THE MIXED PHASE REGION
C   AND TESTS FOR INTERSECTION WITH THE BOUNDARY BETWEEN THE MIXED PHASE
C   AND THE LIQUID PHASE ARE MADE. IF THE INTERSECTION OCCURS THE STABILITY TEST
C   IS REPEATED AND THE COMPUTATION IS STOPPED IF INSTABILITY IS INDICATED;
C   OTHERWISE IT CONTINUES IN THE LIQUID PHASE. IF THE CURVE RE-ENTERS
C   THE MIXED PHASE, THE COMPUTATION IS STOPPED; OTHERWISE IT CONTINUES
C   UNTIL P=PSTOP.
C
C     TO RUN THE PROGRAM, PREPARE DATA ACCORDING TO THE  FORMAT IN
C   STATEMENT NUMBERS 100 AND 101(MAIN);
C   PO=INITIAL PRESSURE=1.034E-06
C   RHOO=DENSITY AT PO,ZERO DEGREES KELVIN
C   RHO2=DENSITY AT THE FOOT OF THE HUGONIOT
C   MOLWT=MOLECULAR WEIGHT OF THE MATERIAL IN GRAMS
C   TO2=TEMPERATURE AT THE FOOT OF THE HUGONIOT
C   TOO=DEBYE TEMPERATURE AT VO=1/RHOO
C   AO,A1,A2,A3 ARE THE COEFFICIENTS IN THE EQUATION FOR GRUNEISEN'S PARAMETER, G
C   WHERE G=AO+MU*(A1+MU*(A2+MU*A3)) AND MU=VO/V-1.
C   B1,B2,B3 ARE THE COEFFICIENTS IN THE EQUATION FOR PRESSURE ON THE
C   ZERO DEGREE ISOTHERM:
C   PK=MU*(B1+MU*(B2+MU*B3))
C   DELP IS THE INCREMENT IN P USED FOR THE INTEGRATION.
C   ICONT IS AN INTEGER WHICH ENABLES THE USER TO INPUT AS MANY DATA SETS
C   AS DESIRED IN ONE RUN OF THE PROGRAM.
C   ICONT=1 OR 2 FOR A COMPLETE OR PARTIAL NEW SET OF DATA (RESP.) TO BE READ IN.
C   IN THE LAST DATA SET ICONT=AN INTEGER OTHER THAN 1 OR 2 FOR THE
C   PROGRAM TO TERMINATE AFTER THE LAST EXECUTION.
C
C     VO1, THE SPECIFIC VOLUME OF THE SOLID AT TO1,PC IS CALCULATED
C   IN THE PROGRAM SO THAT TEMPERATURE ON THE MELTING CURVE IS COMPATIBLE
C   WITH THAT ON THE HUGONIOT.
C
      COMMON AO,A1,A2,A3,B1,B2,B3,ALG,ALIN,ASQ,ACUBE,VO,PO,DELP,R3,V1C,
     +V2O,VO2,T02,TOO,TO1,T2O,JC,PTT
      COMMON /WRT1/ P,V1N,T1N,COEF1N,V2N,T2N,COEF2N
      COMMON/CO1PB1/TO1,G1,CV1,Q1,M,ET,M1,ETT,ETV1,R1,S1,PT,MU1,X1,D1,
     +DP,TT,VV
      COMMON/CO2RH2/G2,TO2,CV,ETH,DPK,Q2,ETV2,M2,MS2,MU2,X2,D2
      COMMON/PRESOK/PKO
      REAL LATHT,MU1,MU2,M1,M2,MS2,MU,MOLWT
      WRITE (6,10)
   10 FORMAT ('1'/' ',8X,'P',19X,'V1',19X,'T1',18X,'V2',18X,'T2')
  103 READ(5,100) PO,RHOO,RHO2,MOLWT,TO1,TO2,TOO
  100 FORMAT(E20.7,6F10.6)
  104 READ(5,101) AO,A1,A2,A3,B1,B2,B3,DELP,PSTOP,ICONT
  101 FORMAT(7F10.6/2F10.6,I2)
      VO=1./RHOO
      VO2=1./RHO2
```

```
      R3=(5.955*4.1*E-5)/MOLWT
      ALG=AC-A1+A2-A3
      ALIN=A1-A2+A3
      ASQ=(A2-A3)/2.
      ACUBE=A3/3.
      DELT=0.5
      VX=VO2
      TX=TO2
   98 MC=VC/VX-1.
      TC1=TC(MU)
      X=TO1/TX
      D=1.-X*(0.375-0.05*X)
      DP=-0.375+0.1*X
      G1=G(MU)
      G1=G(VX,VC)
      W=-(VC*(B1+MU*(2.*B2+3.*B3*MU)))/(VX**2)
      ET=R3*D*TX
      V1=W+ET*Q1-R3*TO1*((G1/VX)**2)*DP
      ETT=R3*(1.-0.05*(X**2))
      R1=1./V1
      S1=-R1*G1*ETT/VX
      VXT=VX
      TXT=TX
      VX=VX+S1*DELT
      TX=TX+DELT
      IF(TX.LE.TC1) GO TO 98
      VO1=VX+(VX-VXT)*(TO1-TX)/DELT
      WRITE (6,2) PO,RHOO,R3,VO1,TO1,AO,A1,A2,A3,B1,B2,B3,TDO,DELP,TO2
    2 FORMAT ('0',E20.7,'=PO',E20.7,'=RHOO',E20.7,'=R3',E20.7,'=VO1'//
     +E20.7,'=TO1',E20.7,'=AO',E20.7,'=A1',E20.7,'=A2'//
     +E20.7,'=A3',E20.7,'=B1',E20.7,'=B2',E20.7,'=B3'//
     +E20.7,'=TDO',E20.7,'=DELP',E20.7,'=TO2')
      WRITE(6,3) ALG,ALIN,ASQ,ACUBE,VO,VO2
    3 FORMAT (' ',E20.7,'=ALG',E20.7,'=ALIN',E20.7,'=ASQ'/E20.7,'=ACUBE'
     +,E20.7,'=VO',E20.7,'=VO2')
      V2N=VO2
      T1N=TC1
      T2N = TO2
      P=PC
      CALL TEMP1(P)
      COEF2N=-VO1/B1
      JC=1
      V1N=VC1
      CALL TEMP(P,T1N,PT)
      CALL PR(V1N,PC,COEF1N,T1N)
      CALL PR2(V2N,PC,COEF2N,T2N)
      JC=2
      WRITE(6,2447)P,T1N,PT,V1N,MU1,TO1,X1,D1,DP,G1,CV1,Q1,ET,V1,ETT,
     1 ETV1,B1,S1, COEF1N
      WRITE(6,2448) P,T2N,V2N,MU2,TO2,X2,D2,DPK,G2,CV,Q2,ETH,V2,ET2V2,
     1 MS2,COEF2N,PKO
    4 V1C=V1N
      V2C=V2N
      T1C=T1N
      T2C=T2N
```

```
    5 P=P+DELP
      CALL TEMP(P,T1N,PT)
      CALL PB(V1N,P,COEF1N,T1N)
      CALL RH2(V2N,P,COEF2N,T2N)
      WRITE(6,2447)P,T1N,PT,V1N,MU1,TD1,X1,D1,DP,G1,CV1,Q1,ET,M1,ETT,
     1 ETV1,R1,S1, COEF1N
      WRITE(6,2448) P,T2N,V2N,MU2,TD2,X2,D2,DPK,G2,CV,Q2,ETH,M2,ET2V2,
     1 PS2,COEF2N,PKO
C
C               TEST FOR INTERSECTION WITH PHASE BOUNDARY
C
      IF (V2N .LT. V1N ) GO TO 4
C
C               FIND INTERSECTION OF R-H AND PHASE BOUNDARY
C
      VI=(V2N*V1O-V1N*V2O)/(V2N-V2O-V1N+V1O)
      PI=P+DELP*(VI-V1N)/(V1N-V1O)
      TI=T1N+(T1N-T1O)*(VI-V1N)/(V1N-V1O)
      WRITE (6,16) PI,TI,VI
   16 FORMAT ('0',E20.7,'=PI',E20.7,'=TI',E20.7,'=VI')
      SLOPE8=DELP/(V2O-V2N)
      WRITE(6,102)
  102 FORMAT('C'///' ',20X,'CONTINUE IN MIXED PHASE'///)
C
C               CONTINUE IN MIXED PHASE
C
      P=PI
      V1N=VI
      V3N=VI
      T1N=TI
      JC=1
      CALL TEMP(P,T1N,PT)
      CALL PB(V1N,P,COEF1N,T1N)
      CALL RH3(V3N,P,COEF3N,V4N)
      WRITE(6,2447)P,T1N,PT,V1N,MU1,TD1,X1,D1,DP,G1,CV1,Q1,ET,M1,ETT,
     1 ETV1,R1,S1, COEF1N
      WRITE (6,17)  P,T1N,V1N,COEF1N,COEF3N,V4N
   17 FORMAT (F20.7,'=P',E20.7,'=T1N',E20.7,'=V1N'/E20.7,'=COEF1N',F20.7
     +,'=COEF3N',E20.7,'=V4N')
      K=1
      JC=2
   11 V1O=V1N
      V3O=V3N
      V4O=V4N
      T1O=T1N
      P=P+DELP
      CALL TEMP(P,T1N,PT)
      CALL PB(V1N,P,COEF1N,T1N)
      CALL RH3(V3N,P,COEF3N,V4N)
      WRITE(6,2447)P,T1N,PT,V1N,MU1,TD1,X1,D1,DP,G1,CV1,Q1,ET,M1,ETT,
     1 ETV1,R1,S1, COEF1N
      WRITE (6,18) P,V1N,V3N,V4N,T1N
   18 FORMAT (E20.7,'=P',F20.7,'=V1N',E20.7,'=V3N'/E20.7,'=V4N',E20.7,'=
     +T1N')
      IF(K.NE.1) GO TO 55
```

```
      SLOPEH=DELP/(V1-V3N)
      SLOPER=(P1-P0)/(VC2-V1)
C
C   SLOPER IS THE SLOPE OF RAYLEIGH LINE FROM THE FOOT OF THE HUGONIOT
C   TO ITS INTERSECTION WITH THE PHASE BOUNDARY
C   SLOPEH IS DP/DV FOR THE HUGONIOT JUST INSIDE THE MIXED PHASE REGION
C   SLOPER IS DP/DV FOR THE HUGONIOT IN THE SOLID
C   JUST OUTSIDE THE MIXED PHASE REGION
C
      WRITE(6,51) SLOPEH,SLOPER,SLOPEB
   51 FORMAT('0',E15.7,'=SLOPEH',5X,E15.7,'=SLOPER',5X,E15.7,'=SLOPEB'/)
      IF(SLOPEH.GE.SLOPER) GO TO 55
      RETURN
   55 K=2
      IF (V3N .LT. V4N) GO TO 11
      VI2 = (V40*V3N - V30*V4N)/(V3N - V3C - V4N + V40)
      PI2 = P + DELP*(VI2 - V4N)/(V4N - V40)
      TI2 = T1N + (T1N - T1C)*(VI2 - V4N)/(V4N - V4C)
      WRITE (6,19) PI2,VI2,TI2
   19 FORMAT (E20.7,'=PI2',E20.7,'=VI2',E20.7,'=TI2')
      WRITE(6,106)
  106 FORMAT('0'///' ',20X,'CONTINUE IN LIQUID PHASE'///)
      SLOPEB=DELP/(V3C-V3N)
      V5N=VI2
      T5N=TI2
      P=PI2
      T4N=TI2
      T1N=T4N
      V4N=VI2
      T2N=T5N
      JC=1
      CALL TEMP(P,T1N,PT)
      DELV=LATHT(T1N,P)/(T1N*PT)
      V1N=V4N-DELV
      CALL PB(V1N,P,COEF1N,T1N)
      V2N=V5N-DELV
      CALL RH2(V2N,P,COEF2N,T2N)
      WRITE(6,602)DELV
  602 FORMAT(' ',E14.6,'=DELV')
      WRITE(6,2447)P,T1N,PT,V1N,MU1,TD1,X1,D1,DP,G1,CV1,Q1,ET,M1,ETT,
     1 ETV1,R1,S1, COEF1N
      WRITE(6,2448) P,T2N,V2N,MU2,TD2,X2,D2,DPK,G2,CV,Q2,ETH,M2,ET2V2,
     1 MS2,COEF2N,PKO
      K=1
      JC=2
   25 T2C=T2N
      T1C=T1N
      V1C=V1N
      V2C=V2N
      P=P+DELP
      CALL TEMP(P,T1N,PT)
      CALL PB(V1N,P,COEF1N,T1N)
      DELV=LATHT(T1N,P)/(T1N*PT)
      V4N=V1N+DELV
      T4N=T1N
```

```
      CALL RH2(V2N,P,COEF2N,T2N)
      V5N=V2N+CELV
      T5N=T2N
      IF(K.NE.1) GO TO 70
      SLOPEP=(P12-P0)/(V02-V12)
      SLOPER=DELP/(V12-V5N)
      WRITE(6,51) SLOPEP,SLOPER,SLOPEB
      IF(SLOPEP.GE.SLOPER) GO TO 70
      RETURN
   70 K=2
      WRITE(6,2447)P,T1N,PT,V1N,MU1,TD1,X1,D1,DPK,G1,CV1,Q1,ET,M1,ETT,
     1 ETV1,R1,S1, COEF1N
      WRITE(6,2448) P,T2N,V2N,MU2,TD2,X2,D2,DPK,G2,CV,Q2,ETH,M2,ET2V2,
     1 MS2,COEF2N,PKO
 2447 FORMAT('0',E15.7,'=P',5X,E15.7,'=T1N',5X,E15.7,'=PT',5X,E15.7,'=V
     11N',5X,E15.7,'=MU1'/' ',E15.7,'=TD1',5X,E15.7,'=X1',5X,E15.7,'=D1'
     2,5X,E15.7,'=DP',5X,E15.7,'=G1'/' ',E15.7,'=CV1',5X,E15.7,'=Q1',5X,
     3E15.7,'=ET',5X,E15.7,'=M1',5X,E15.7,'=ETT'/' ',E15.7,'=ETV1',5X,E1
     45.7,'=R1',5X,E15.7,'=S1',5X,E15.7,'=COEF1N')
 2448 FORMAT('0',E15.7,'=P',5X,E15.7,'=T2N',5X,E15.7,'=V2N',5X,E15.7,'=M
     1U2',5X,E15.7,'=TD2'/' ',E15.7,'=X2',5X,E15.7,'=D2',5X,E15.7,'=DPK'
     2,5X,E15.7,'=G2',5X,E15.7,'=CV'/' ',E15.7,'=Q2',5X,E15.7,'=ETH',5X,
     3E15.7,'=M2',5X,E15.7,'=ET2V2',5X,E15.7,'=MS2'/' ',E15.7,'=COEF2N',
     45X,E15.7,'=PK')
      WRITE(6,600)P,V1N,V4N,V2N,V5N,T4N,T5N
  600 FORMAT(' ',7E15.6)
      IF(V5N.GE.V4N) GO TO 72
      RETURN
   72 CONTINUE
      IF(P.LT.PSTOP)GO TO 25
      IF(ICONT.EQ.1) GO TO 103
      IF(ICONT.EQ.2) GO TO 104
      RETURN
      END
      SUBROUTINE TEMP1(P)
      COMMON A0,A1,A2,A3,B1,B2,B3,ALG,ALIN,ASQ,ACUBE,V0,P0,DELP,R3,V10,
     +V20,V02,T02,TDC,TC1,T20,JC,PTT
C  A AND C ARE THE CONSTANTS IN THE SIMON EQUATION OF MELTING:
      A=0.06257
      C=1.20436
      WRITE(6,1)A,C
    1 FORMAT(' ',E15.7,'=A',5X,E15.7,'=C')
      RETURN
      ENTRY TEMP(P,T,PT)
      IF(JC.NE.1) GO TO 2
      PT=A*C*(T**(C-1.))/(TC1**C)
      PTT=C*(C-1.)*(P-P0+A)/(T**2)
      RETURN
    2 CONTINUE
      T=TC1*(((P-P0+A)/A)**(1./C))
      PT=A*C*(T**(C-1.))/(TC1**C)
      PTT=C*(C-1.)*(P-P0+A)/(T**2)
      RETURN
      END
      SUBROUTINE PB(V1,P,CO1,T1)
```

```
      COMMON AC,A1,A2,A3,B1,B2,B3,ALG,ALIN,ASQ,ACUBE,VC,PO,DELP,R3,V1C,
     +V2O,VC2,TG2,TDC,TC1,T2O,JC,PTT
      COMMON/CG1PB1/TD1,G1,CV1,Q1,W,ET,M1,ETT,ETV1,P1,S1,PT,MU1,X1,D1,
     +DP,TT,VV
      REAL MU,M1,MU4,MU1
      IF(JC.EQ.1) CO1=0.
      CC1O=CC1
      DO 8 J=1,10
      IF(JC.EQ.1) GO TO 10
      V1NN=V1
      V1=V1C+0.5*(CO1O+CO1)*DELP
      IF(ABS((V1-V1NN)/V1).GE.4.E-5) GO TO 10
      RETURN
   10 MU=(VC/V1)-1.
      TC1=TC(MU)
      X=TC1/T1
      CC=1./PT
      D=1.-X*(0.375-0.05*X)
      DP=-0.375+0.1*X
      G1=G(MU)
      CV1=R3*(4.*G-3.*X/(EXP(X)-1.))
      Q1=Q(V1,VC)
      W=B1+MU*(2.*B2+3.*B3*MU)
      W=-VC*W/(V1**2)
      ET=R3*C*T1
      M1=W+ET*Q1-R3*TC1*((G1/V1)**2)*DP
      ETT=  R3*(1.-0.05*(X**2))
      ETV1=R3*DP*(1-G1*TD1)/V1)
      R1=1./M1
      S1=-R1*G1*ETT/V1
      CC1=R1+S1*CC
      TT=T1
      VV=V1
      MU1=MU
      X1=X
      D1=D
      IF(JC.EQ.1) GO TO 12
    8 CONTINUE
      WRITE(6,600) V1,V1NN
  600 FORMAT('0','SUBR.PB,ITERATION FAILED',2E20.7)
      CALL EXIT
   12 CONTINUE
      RETURN
      END
      SUBROUTINE RH2(V,P,COEF2N,T2N)
      COMMON AC,A1,A2,A3,B1,B2,B3,ALG,ALIN,ASQ,ACUBE,VC,PO,DELP,R3,V1C,
     +V2O,VC2,TG2,TDC,TC1,T2C,JC,PTT
      COMMON/CG2RH2/G2,TD2,CV,ETH,DPK,Q2,ETV2,M2,MS2,MU2,X2,D2
      COMMON/PRESOK/PKO
      REAL MU,M2,MS2,MU2
      IF(JC.EQ.1) COEF2N=0.
      CCEF2C=CCEF2N
      DO 8 J=1,10
      IF(JC.EQ.1) GO TO 10
      V2NN=V
```

```
      V=V2C+0.5*(COEF2N+COEF2O)*DELP
      IF(ABS((V-V2NN)/V).GE.4.E-5) GO TO 10
      RETURN
   10 MU=VO/V-1.
      G2=G(MU)
      TC2=TC(MU)
      PKC=PK(MU)
      ETH=((P-PKO)*V)/G2
      X=((ETH/(R3*TO2)+.375)-SQRT((ETH/(R3*TO2)+.375)**2-0.2))/0.1
      T2N=TC2/X
      D=1.-0.375*X+0.05*X**2
      DDDX=-0.375+0.1*X
      ETV2=R3*G2*TO2*(+0.375-.1*X)/V
      CV=R3*(1.-0.05*(X**2))
      DPK=B1+MU*(2.*B2+MU*3.*B3)
      DPK=-DPK*VC/(V**2)
      Q2=Q(V,VC)
      M2=CPK+ETH*Q2+G2*ETV2/V
      MS2=M2-CV*T2N*((G2/V)**2)
      COEF2N=(1.-G2*(V02-V)/(2.*V))/(MS2+G2*(P-PO)/(2.*V))
      MU2=MU
      X2=X
      C2= C
      IF(JC.EQ.1) GO TO 12
    8 CONTINUE
      WRITE(6,600)V,V2NN
  600 FORMAT('0','SUBP.RH2,ITERATION FAILED',2E20.7)
      CALL EXIT
   12 CONTINUE
      RETURN
      END
      SUBROUTINE RH3(V3N,P,COEF3N,V4N)
      COMMON AC,A1,A2,A3,B1,B2,B3,ALG,ALIN,ASQ,ACUBE,VC,PO,DELP,R3,V10,
     +V20,VO2,TO2,TOO,TC1,T20,JC,PTT
      COMMON/CC1PB1/TC1,G1,CV1,Q1,W,ET,M1,ETT,ETV1,R1,S1,PT,MU1,X1,D1,
     +DP,TT,VV
      REAL MU,LATHT,M1,MU1
      IF(JC.EQ.1) COEF3N=0.
      COEF3O=COEF3N
      V3O=V3N
      DO 8 J=1,10
      IF(JC.EQ.1) GO TO 10
    1 V3NN=V3N
      V3N=V3O + .5*(COEF3O + COEF3N)*DELP
      IF(ABS((V3N-V3NN)/V3N).GE.4.E-5) GO TO 10
      RETURN
   10 T1=TT
      V1=VV
      Y1=(CV1*(1.+G1*T1*S1/V1)+T1*(V3N-V1)*PTT)/PT
      DEN1=Y1-2.*T1*S1-T1*R1*PT-(VO2-V3N)/2.
      ANUM1=.5*(P-PO)-T1*PT
      COEF3N=DEN1/ANUM1
      V4N=V1+LATHT(T1,P)/(T1*PT)
      IF(JC.EQ.1) GO TO 12
    8 CONTINUE
```

```
      WRITE(6,600)V3N,V3NN
  600 FORMAT ('0',*R-3; ITER. FAILED',2E20.7)
      CALL EXIT
   12 CONTINUE
      RETURN
      END
      FUNCTION G(MU)
      COMMON AO,A1,A2,A3,B1,B2,P3,ALG,ALIN,ASQ,ACUBE,VO,PO,DELP,R3,V1O,
     +V2O,VO2,TO2,TOO,TO1,T2O,JC,PTT
      REAL MU
      G=AO+MU*(A1+MU*(A2+MU*A3))
      RETURN
      END
      FUNCTION TO(MU)
      COMMON AO,A1,A2,A3,B1,B2,B3,ALG,ALIN,ASQ,ACUBE,VO,PO,DELP,R3,V1O,
     +V2O,VO2,TO2,TOO,TO1,T2O,JC,PTT
      REAL MU
      TO=TOO*EXP(ALG*ALOG(ML+1.)+MU*(ALIN+MU*(ASQ+ML*ACUBE)))
      RETURN
      END
      FUNCTION Q(V,VX)
      COMMON AO,A1,A2,A3,B1,B2,P3,ALG,ALIN,ASQ,ACUBE,VO,PO,DELP,R3,V1O,
     +V2O,VO2,TO2,TOO,TO1,T2O,JC,PTT
      REAL MU
      MU=(VO/V)-1.
      Q=-(VO/(V**3))*(A1+MU*(2.*A2+3.*A3*MU))-G(MU)/(V**2)
      RETURN
      END
      FUNCTION PK(MU)
      COMMON AO,A1,A2,A3,B1,B2,B3,ALG,ALIN,ASQ,ACUBE,VO,PO,DELP,R3,V1O,
     +V2O,VO2,TO2,TOO,TO1,T2O,JC,PTT
      REAL MU
      PK=MU*(B1+MU*(B2+MU*B3))
      RETURN
      END
      REAL FUNCTION LATHT (T,P)
      LATHT = 6.26*4.18E-5
      RETURN
      END
/*
//GO.SYSIN DD *
          1.034E-04     11.416     11.340      207.0      600.0      293.0       96.3
    2.7091   -2.9292      1.413        0.0     .54168    .749041    .605839
     0.005        1.0 3
/*
/*
```

```
IEF285I   SYS1.UTILITY                                    KEPT
IEF285I   VOL SER NOS= CLIBC2.
IEF285I   SYSOUT                                          SYSOUT
IEF285I   VOL SER NOS=
IEF285I   LISTER                                          DELETED
IEF285I   VOL SER NOS= SCROC1.
```

APPENDIX B

HUGONIOT CURVE OF LIQUID ARGON OBTAINED BY USING THE SIGNIFICANT STRUCTURE MODEL OF LIQUIDS

C. T. Tung

I. Introduction

The significant structure theory of liquids has been developed by Eyring and co-workers. According to the theory, a liquid is considered as having three significant structures; solid-like, gas-like, and degenerate. These three structures contribute essentially to the thermodynamic properties of the bulk system. On the basis of these considerations, the partition function, f, for a monatomic liquid such as argon can be expressed as[1]*:

$$f = (a_1 a_3/a_2^3)^{N V_s/V} \left(a_4^3(V-V_s)\right)^{N(V-V_s)/V} / (N(V-V_s)/V)! \qquad (1)$$

where:

$$a_1 = \exp(E_s/RT)$$

$$a_2 = 1 - \exp(-\theta/T)$$

$$a_3 = 1 + \eta_h \exp(-\epsilon/RT)$$

$$a_4 = (2\pi MKT)^{\frac{1}{2}}/h$$

---

*Superscripts refer to literature at end of Appendix F.

The first set of brackets stands for the solid-like portion of the partition function, for which the Einstein oscillator model is used. The quantity $(1 + n_h \exp(-\epsilon/RT)$ is the geometrical degeneracy factor; the remaining portion is the gas-like part. Using Sterling's approximation, $y! \approx (y/e)^y$, Eq. (1) can be rewritten in more compact form,

$$f = (a_1 a_3 / a_2^3)^{NV_s/V} (a_4^3 eV/N)^{N(V-V_s)/V} \qquad (2)$$

In Eq. (2), the number of neighboring positions, n_h, is equal to $n(V-V_s)/V_s$, and the energy needed to occupy a vacant site, ϵ, is equal to $aE_s V_s/(V-V_s)$. Both n and a are proportionality factors, E_s is the energy of sublimation.

At high pressures and temperatures a few corrections are necessary. Hence, Einstein partition function in Eq. (2) should be replaced by[1]:

$$a_1\left(((1-g)/a_2) + g a_4 V_f^{1/3}\right)^3$$

where $g = \exp(-\ell\theta/T)$, ℓ is the vibrational quantum number and V_f is the molar free volume in the solid. V_f may be represented by:

$$V_f = \left((V_s/N)^{2/3} - (b/4N)^{1/3}\right)^3$$

where b is the van der Waals constant and b/4N is the net molecular volume. With these corrections, the partition function for a monatomic liquid at high pressures and

temperatures should be written as:

$$f = \left(a_1((1-g)/a_2) + ga_5((V_s/N)^{1/3} - (b/4N)^{1/3})\right)^3 \qquad (3)$$

where:

$$a_5 = 1 + b_2b_3$$
$$b_2 = \eta(V-V_s)/V_s$$
$$b_3 = \exp(-b_4)$$
$$b_4 = aE_sV_s/RT(V-V_s) \ .$$

In addition to the corrections mentioned above, the pressure effect on V_s must also be considered. For moderately high pressures, Eyring suggests the linear correction:

$$V_s' = V_s(1-\beta p) \qquad (4)$$

In order to extend calculations to higher pressures we replace (4) by:

$$V_s' = V_s \exp(-\beta p) \ , \qquad (5)$$

which reduces to Eq. (4) for small pressures and also has positive curvature, which is necessary for shock stability. Hence, β is solid compressibility and p is excess pressure above a standard pressure.[2]

Knowing the total partition function as a function of T and V , we are able to calculate thermodynamic equations of state from:

$$A = -kT \ln f \tag{6}$$

$$P = -(\partial A/\partial V)_T = kT(\partial \ln f/\partial V)_T \tag{7}$$

$$E = -T^2(\partial(A/T)/\partial T)_V = kT^2(\partial \ln f/\partial T)_V \tag{8}$$

$$S = -(\partial A/\partial T)_V = k \ln f + kT(\partial \ln f/\partial T)_V \tag{9}$$

where A, P, E, and S are the Helmholtz free energy, pressure, internal energy, and entropy.

II. Calculation of the Hugoniot Curve for Liquid Argon

As mentioned, the partition function, f, is a function of temperature and molar volume. Obviously, to calculate pressure, internal energy, and entropy from Eq. (6) to Eq. (9) is straightforward, but tedious. The results are:

$$P = RT\left(L+B+C+((V-V_s)/V^2) - (3V_s/V^2)\ln(a_2F)\right) \tag{10}$$

$$E = RT^2(D+J) \tag{11}$$

$$S = (E/T) + RTJ + (RV_s/V)\left((E_s/RT) + \ln (a_5/a_2{}^3)\right) \tag{12}$$

where:

$$L = -(V_s/V^2)\left((E_s/RT) + \ln(a_5/a_2{}^3)\right)$$

$$B = (b_3\eta/gV)(1 + b_4)$$

$$C = (V_s/V^2)\left(H + \ln(T^{3/2}V)\right)$$

$$D = (V_s/V)\left((-E_s/RT^2) + (3\theta\exp(-\theta/T)/T^2a_2) + (b_3\eta aE_s/a_5RT^2)\right) + 3(V-V_s)/2TV$$

$$F = \left((1-g)/a_2\right) + \left(v_s^{1/3} - (b/4)^{1/3}\right)a_4 g/N^{1/3}$$

$$G = \theta\left(-\ell g + 1 - a_2 + (\ell-1)\, g\,(1-a_2)\right)/(Ta_2)^2 + gT^{1/2}\left((\ell\theta/T^2) + (1/2T)\right) a_4\left(V_s^{1/3} - (b/4)^{1/3}\right) / N^{1/3}$$

$$H = \ell n(a_4^{\,3}\, e/N)$$

$$J = (3V_s/V)\left((G/F) - \theta(1-a_2)/T^2 a_2\right)$$

and the parametric values for liquid argon are[3,4]

n (proportionality factor) = 10.7

a (proportionality factor) = 0.0052

E_s (sublimation energy) = 1888.6 cal/mole

b (van der Waals constant) = 32.2 cc/mole

ℓ (vibrational quantum number) = 5

V_s (molar volume of solid at 1 atm) = 24.98 cc/mole

θ (Einstein characteristic temperature) = 60.0 (^oK)

m (atomic weight) = 39.944 gm/mole

N (Avogadro number) = $6.024 \times 10^{23}(\text{mole})^{-1}$

h (Planck constant) = 6.6252×10^{-27} erg-sec

$\beta = 2.5 \times 10^{-5}/\text{atm}$ = compressibility of solid argon below 10^4 atm.

k (Boltzmann constant) = 1.380×10^{-16} erg/deg

R = 1.986 cal/mol ^oK

In order to find the Hugoniot curve the Rankine-Hugoniot jump condition:

$$E - E_o = \tfrac{1}{2}(P + P_o)(V_o - V) \qquad (13)$$

is required to be satisfied. The problem of finding the Hugoniot

curve is equivalent to eliminating both T and E among Eqs. (10), (11), and (13) so that P can be expressed in terms of V only. The relation between P and V represents the Hugoniot curve. In principle the Hugoniot curve can be obtained no matter how complicated Eqs. (10) and (11) may be. But in practice we accomplish this by numerical methods.

The calculation procedure is schematically as follows:

1. Assign a value for V (less than initial volume V_o).
2. Guess a value for T (higher than initial temperature T_o).
3. Substitute both T and V in Eq. (10) and calculate the value of P.
4. Substitute the calculated P into Eq. (5); using the new V_s (V_s'), P is recalculated from Eq. (10). This process is repeated until consistency is obtained.
5. Use present T, V, and V_s to calculate E from Eq. (11).
6. Substitute P, V, and E in Eq. (13) which can be written in the form,

   $$H(P,V,E) = E - E_o - \tfrac{1}{2}(P + P_o)(V_o - V)$$

   If $H(P,V,E) \approx 0$, P is the right value which corresponds to the assigned V. If $H(P,V,E) \approx 0$, knowing H is positive or negative, T can be appropriately adjusted, and then follow with step (3). This loop is repeated until $H(P,V,E) \approx 0$ is satisfied.

From this double iterative method the relation between P and V under the jump condition, Eq. (13), can be satisfied. This relation presents the Hugoniot curve. Furthermore, using a similar method, with Eq. (13) replaced by Eq. (12), the

adiabatic curve can also be obtained. Details of this double iterative method are shown in the computer program listing at the end of this appendix.

III. Discussion of Results

Each isotherm in a P-V diagram shows both the existence of a maximum pressure and a discontinuity at $V = V_s$ (See Fig. 1). This is due to using the Einstein oscillator model for the solid partition function. In the Einsten model the binding energy is assumed to be volume-independent.

The Hugoniot and adiabatic P-V curves can exist and have been calculated only in the region well to the right of the maximum-pressure curve of Fig. 15 where $(\partial p/\partial V)_T < 0$. Both are shown in Fig. 16 relative to the isotherms. In Fig. $\bar{U}$ the calculated curves are compared with measurements reported by van Thiel and Alder. The agreement is remarkably close and suggests that minor modifications of the Eyring theory may make it valid at even higher pressures.

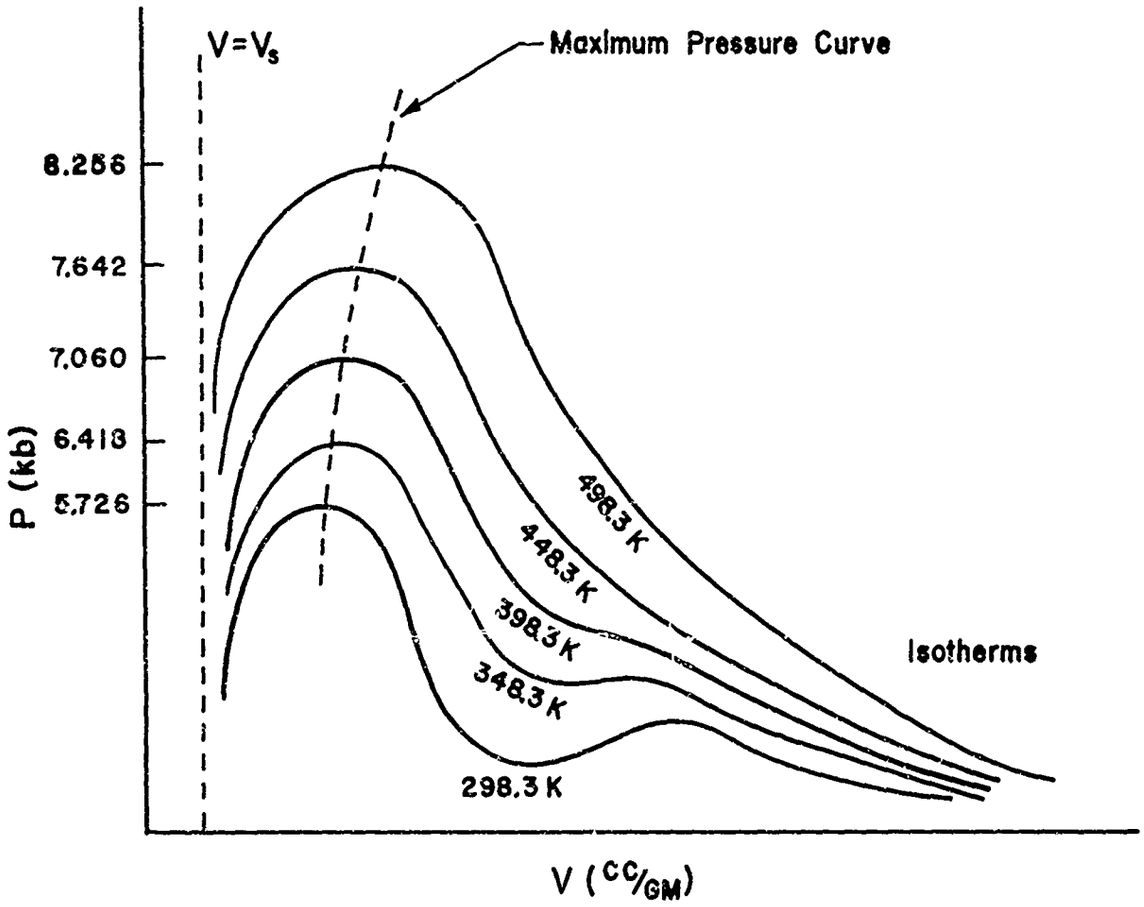

Fig. 15

ISOTHERMS IN P-V DIAGRAM

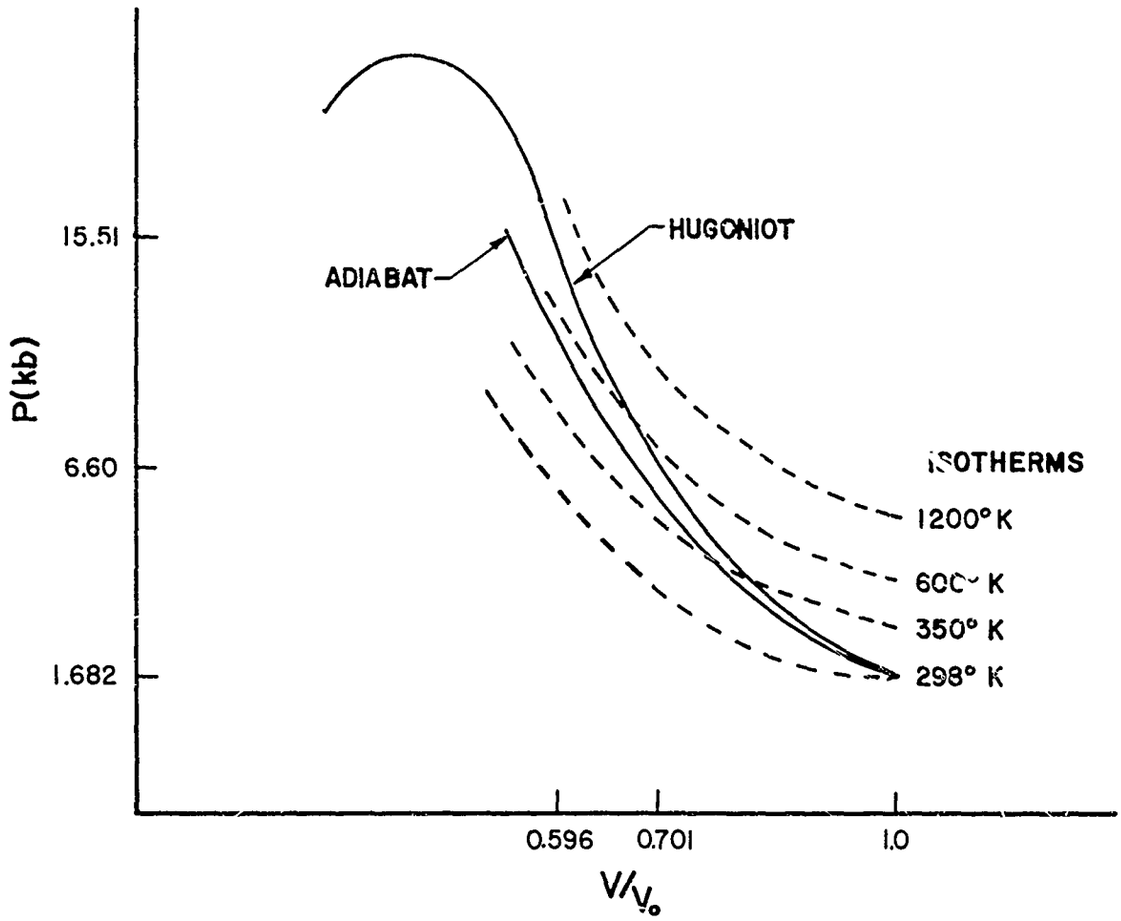

Fig. 16
HUGONIOT CURVE, ADIABAT, AND ISOTHERMS
IN P-V DIAGRAM

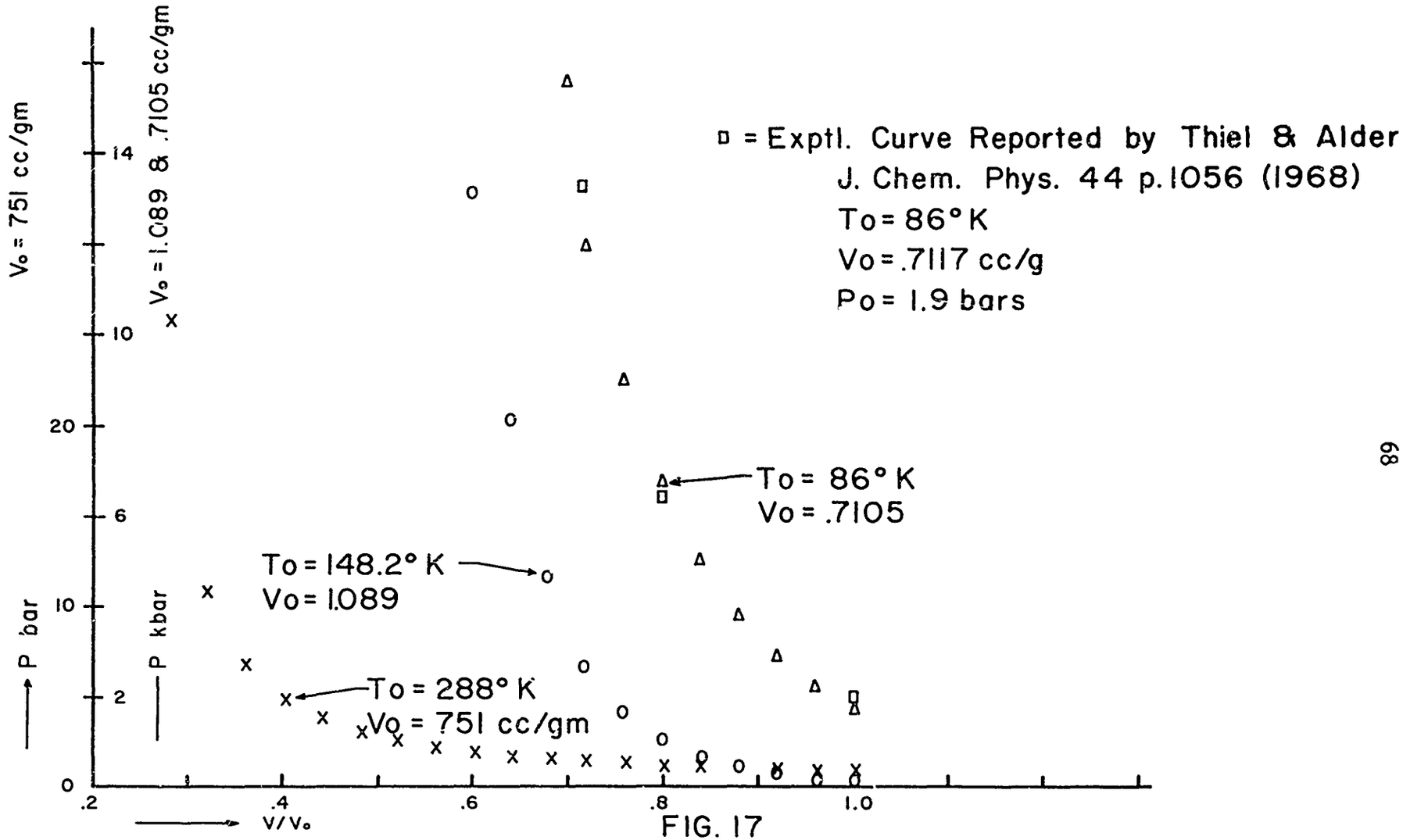

FIG. 17

COMPARISON OF CALCULATED AND MEASURED HUGONIOT CURVES FOR ARGON

REFERENCES

1. Henry Eyring and R. P. Marchi, J. Chem. Educ. 40, 562 (November, 1963).
2. T. S. Ree, T. Ree, and Henry Eyring, Proc. Natl. Acad. Sci. 48, 4, 501-517 (April, 1962).
3. T. S. Ree, T. Ree, Henry Eyring, and Richard Perkins, J. Phys. Chem. 69, 3322 (1965).
4. Henry Eyring and Taikyue Ree, Proc. Natl. Acad. Sci. 47, 4, 526-537 (April, 1961).
5. R. N. Keeler and Dieter R. Tuerpe, American Physics Society Meeting, Stanford, California, Dec. 28-30, 1966.

```
IV G LEVEL 0, MOD 0             MAIN              DATE = 67264          14/50/12

      C     HUGONIOT CURVE FOR LIQUID ARGON
            COMMON/DATAM/M
            COMMON/ESOES/ESO
            COMMON/APLOT/AP(101,101)
            COMMON/CTVSET/T1,T1T,EXPT,DOWN,EXPST
            COMMON/VSET/V,UVOO
            COMMON/CIOSET/A,ES,VS,SN,SS,CK,EEO,PPO,VO,TO,CKK ,VSC
            COMMON/BOC/BLANK,DOT,C(13)
      C     READ CHARACTERS (FOR PLOTTING CURVES)
            READ(5,100)BLANK,DOT,(C(K),K=1,13)
        100 FORMAT(15A1)
      C     GIVE PARAMETRIC VALUES FOR LIQUID ARGON
            A=0.0052
            ES=1888.6
            ESO=ES
            VS=24.98
            SN=10.7
            SS=60.0
            CKK=10.0*(8.0*3.141*8.37)**1.5/((6.625**3.0)*(6.02**4.0))
            CK=ALOG(CKK)+1.0
            VSO=VS
            M=0
      C     READ BOTH INITIAL VOLUME AND INITIAL TEMPERATURE
        500 READ(5,300)V,T
        300 FORMAT(2F10.0)
      C     IF DATA CARDS ARE USED UP,STOP
            IF(V.LE.0.0)  GO  TO  112
            M=M+1
            WRITE(6,70)M
         70 FORMAT('0',' DATA  ',I1)
      C     SET 'BLANK' IN TWO DIMENTIONAL SPACE(100*100)
            DO   210  K=1,100
             DO  210 N=2,101
            AP(K,N)=BLANK
        210 CONTINUE
      C     SET UP COORDINATES BY 'DOT'
            DO 211 K=1,101
            AP(K,1)=DOT
        211 CONTINUE
            DO  212  N=1,101
            AP(101,N)=DOT
        212 CONTINUE
            TO=T
            VO=V
      C     CALCULATE THE ISOTHERMS
            CALL  PLOT1(V,T)
      C     CALCULATE AN ADIABATIC CURVE THROUGH INITIAL STATE
            CALL   ADIAB(V,T)
```

```
IV G LEVEL 0, MOD 0            MAIN              DATE = 67264          14/50/12

      C     CALCULATE THE HUGONIOT CURVE
            CALL  SHOCK(V,T)
      C     PLOT THE HUGONIOT CURVE,THE ADIABATIC CURVE,AND THE ISOTHERMS
            WRITE(6,302)  ((AP(I,J),J=1,101),I=1,101)
        302 FORMAT(' ',10X,101A1)
            VV=VC/39.944
      C     WRITE THE INITIAL STATE UNDER THE HORIZONTAL AXIS
            WRITE(6,900)TO,VV
        900 FORMAT('0',30X,'(INITIAL STATE T=',F7.2,'(K) V=',F10.5,
           1'(CC/GM) )')
      C     GO TO READ NEXT DATA
            GO TO  500
        112 CONTINUE
            RETURN
            END
```

```
G LEVEL 0, MOD 0            MAIN              DATE = 67264          14/50/12

C            SUB    SHOCK
C      FIND HUGONIOT CURVE
       SUBROUTINE  SHOCK(V,T)
       COMMON/BCC/BLANK,DOT,C(13)
       COMMON/YSET/Y,UVOO
       COMMON/C10SET/A,ES,VS,SN,SS,CK,EEO,PPO,VO,TO,CKK ,VSO
       VV=V/39.944
       WRITE(6,450)T,VV
  450  FORMAT('0',2X,'HUGONIOT  CURVE',' (INITIAL STATE T=',F7.2,
     1'(K)  V=',F10.5,'(CC/GM) )')
       WRITE(6,201)
  201  FORMAT('0',16X,'V(CC/GM)',13X,'T(K)',15X,'P(BAR)',12X,
     1'E(CAL/GM)',13X,'S(CAL/GM-K)',10X,'V/VO')
       VIN=V
       TIN=T
C      ASSIGN A CHARACTER FOR HUGONIOT CURVE
       Y=C(11)
C      CALCULATE THE INITIAL VALUES(P. AND E.)
       CALL WRITE1(V,T)
       PPO=P(V,T)
       EEO=E(V,T)
C      ASSIGN A VALUE FOR V AND FIND THE CORRESPONDED P
  511  V=V-VO/25.0
       T=TO
       TL=T
C      START ON THE DOUBLE ITERATIVE CALCULATIONS
       IF(F(V,T).GE.0.0)        GO   TO   591
       SFTL=-1.0
       GO   TO   592
  591  SFTL=1.0
  592  TU=TL+300.0
       T=TU
       IF(F(V,T).GE.0.0)      GO    TO    593
       SFTU=-1.0
       GO   TO    594
  593  SFTU=1.0
  594  IF(SFTL*SFTU.LT.0.0)    GO  TO   595
       TL=TU
        SFTL=SFTU
       IF(TU.GT.10000.0)  GO  TO  611
       GO   TO   592
  595  TM=(TL+TU)/2.0
C      UPPER BOUND AND LOWER BOUND HAVE BEEN FOUND
       T=TM
       IF(F(V,T).GE.0.0)      GO    TO    596
       SFTM=-1.0
       GO    TO      696
  596  SFTM=1.0
```

```
V G LEVEL 0, MOD 0              SHOCK              DATE = 67264          14/50/12

      696 IF(SFTM.EQ.SFTU)      GO    TO     796
          TL=TM
          GO   TO    597
      796 TU=TM
      597 IF((TU-TL).GT.5.0)    GO   TO   595
          T=(TU+TL)/2.0
    C     THE SOLUTION OF T IS FOUND
    C     USE PRESENT T AND V TO CALCULATE P
          CALL   WRITE1(V,T)
          IF(V.LT.V0/10.0)        GO   TO   611
          GO  TO   511
      611 CONTINUE
          V=VIN
          T=TIN
          RETURN
          END
```

```
/ G LEVEL 0, MOD 0            MAIN              DATE = 67264          14/50/12

      C
      C     FIND AN ADIABATIC CURVE THROUGH INITIAL STATE
      C     (THE METHOD IS SIMILAR TO THAT FOR FINDING HUGONIOT)
            SUBROUTINE    ADIAB(V,T)
            COMMON/BCC/BLANK,DOT,C(13)
            COMMON/C10SET/A,ES,VS,SN,SS,CK,EEO,PPC,VO,TO,CKK ,VSO
            COMMON/YSET/Y,UVOO
            WRITE(6,450)
        450 FORMAT('C',2X,'ADIABATIC  CURVE')
            WRITE(6,201)
        201 FORMAT('C',10X,'V(CC/GM)',13X,'T(K)',15X,'P(BAR)',12X,
           1'E(CAL/GM)',13X,'S(CAL/GM-K)',10X,'V/VO')
            VIN=V
            TIN=T
            Y=C(12)
            CALL   WRITE1(V,T)
            SSO=S(V,T)
        511 V=V-VO/20.0
            T=TO
            TL=T
      C     GET THE RIGHT V
            NEWVS=P(V,T)
            IF(S(V,T).GE.SSO)  GO  TO                        591
            SFTL=-1.0
            GO   TO  592
        591 SFTL=1.0
        592 TU=TL+100.0
            T=TU
            NEWVS=P(V,T)
            IF(S(V,T).GE.SSO)  GO  TO                    593
            SFTU=-1.0
            GO   TO    594
        593 SFTU=1.0
        594 IF(SFTL*SFTU.LT.0.0)    GO  TO   595
            TL=TU
             SFTL=SFTU
            IF(TU.GT.100C0.0)  GO  TO  611
            GO   TO  592
        595 TM=(TL+TU)/2.0
            T=TM
            NEWVS=P(V,T)
            IF(S(V,T).GE.SSO)  GO  TO                    596
            SFTM=-1.0
            GO    TO     696
        596 SFTM=1.0
        696 IF(SFTM.EQ.SFTU)     GO    TO     796
            TL=TM
            GO   TO    597
```

```
 G LEVEL 0, MOD 0              ADIAB              DATE = 67264          14/50/12

      796 TU=TM
      597 IF((TU-TL).GT.5.0)       GO  TO    595
          T=(TU+TL)/2.0
          CALL    WRITE1(V,T)
          IF(V.LT.V0/10.0)         GO   TO   611
          GO  TO   511
      611 CONTINUE
          V=VIN
          T=TIN
          RETURN
          END
```

```
IV G LEVEL 0, MOD 0          MAIN          DATE = 67264          14/50/12

      C
      C     HUGONIOT JUMP CONDITION
            FUNCTION    F(V,T)
            COMMON/CIOSET/A,ES,VS,SN,SS,CK,EEO,PPO,VO,TO,CKK ,VSC
            F=VC-V-(2.0/(P(V,T)+PPO))*(E(V,T)-EEO)
            RETURN
            END
```

```
V G LEVEL 0, MOD 0              MAIN              DATE = 67264          14/50/12

      C
      C       ENTROPY FUNCTION
              FUNCTION  S(V,T)
              COMMON/CLOSET/A,ES,VS,SN,SS,CK,EEO,PPC,VC,TO,CKK ,VSO
              COMMON/CTVSET/T1,T1T,EXPT,DOWN,EXPST
              COMMON/E1F1/E1,F1,F12
              XL=5.0
              B=32.2
               S=(2.0*VS/V)*(ES/(2.0*T)-3.0*ALOG(1.0-EXPST)+ALOG(DOWN))+
             1(2.0*(V-VS)/V)*(CK+1.5*ALOG(T)+ALOG(V))+E(V,T)/T
              S1=E1/T+(6.0*VS/V)*ALOG(F1*(1.0-EXPST))
              S=S+S1
               RETURN
              END
```

```
/ G LEVEL 0, MOD 0            MAIN              DATE = 67264          14/50/12

      C
      C       INTERNAL ENERGY FUNCTION
              FUNCTION  E(V,T)
              COMMON/CLOSET/A,ES,VS,SN,SS,CK,EEO,PPO,VO,TO,CKK ,VSC
              COMMON/CTVSET/TL,TLT,EXPT,DOWN,EXPST
              COMMON/E1F1/E1,F1,F12
              XL=5.0
              B=32.2
              EEVT=(VS/V)*(-ES/(2.0*T*T)+3.0*SS*EXPST/(T*T*(1.0-EXPST))+
             1SN*A*ES*EXPT/(2.0*T*T*DOWN))+1.5*(V-VS)/(T*V)
              E=2.0*T*T*EEVT
              F21=(SS/(T*T))*(-XL*EXPST**XL+EXPST+(XL-1.0)*EXPST**(XL+1.0))
             1/((1.0-EXPST)**2.0)
              F2=F21+F12*(XL*SS/T+0.5)/T
              E1=(6.0*VS*T*T/V)*(F2/F1-(SS*EXPST)/(T*T*(1.0-EXPST)))
              E=E+E1
               RETURN
              END
```

```
V G LEVEL 0, MOD 0            MAIN              DATE = 67264          14/50/12

      C     SUB   TVSET
      C      A SET OF VARIABLES IN TERMS OF V AND T
             SUBROUTINE    TVSET(V,T)
             COMMON/CLOSET/A,ES,VS,SN,SS,CK,EEO,PPC,VO,TC,CKK ,VSG
             COMMON/CTVSET/T1,T1T,EXPT,DOWN,EXPST
             T1=A*ES*VS/(2.0*(V-VS))
             T1T=T1/T
             EXPT=EXP(-T1T)
             DOWN=1.0+SN*(V-VS)*EXPT/VS
             EXPST=EXP(-SS/T)
             RETURN
             END
```

```
V G LEVEL 0, MOD 0            MAIN              DATE = 67264          14/50/12

      C
      C     PRESSURE FUNCTION
            FUNCTION  P(V,T)
            COMMON/ESGES/ESO
            COMMON/CLOSET/A,ES,VS,SN,SS,CK,EEO,PPO,VO,TO,CKK ,VSO
            COMMON/CTVSET/T1,T1T,EXPT,DOWN,EXPST
            COMMON/E1F1/E1,F1,F12
            XL=5.0
            BO=32.2
            BETA=2.5/2421.0
            M=0
            N=0
            POLD=0.0
            VS=VSO
            IF(V.LE.VS)   GO    TO   99
            ES=ESO
      C     OBTAIN THE RIGHT VALUES FOR THOSE VARIABLES IN'COMMON CTVSET'
            CALL   TVSET(V,T)
        100 AA=-(VS/(V*V))*(ES/(2.0*T)-3.0*ALOG(1.0-EXPST)+ALOG(DOWN))
            BB=(SN/V)*(1.0+T1T)*EXPT/DOWN
            CC=(VS/(V*V))*(CK+1.5*ALOG(T)+ALOG(V))
            PPVT=AA+BB+CC+(V-VS)/(V*V)
            P=2.0*T*PPVT
            F11=(1.0-EXPST**XL)/(1.0-EXPST)
            E=BO*VS/VSO
            F12=(EXPST**XL)*(CKK**0.333)*(VS**0.333-(B/4.0)**0.333)*(T**0.5)
            F1=F11+F12
            P1=-(6.0*VS*T/(V*V))*ALOG(F1*(1.0-EXPST))
            P=P+P1
            IF(ABS(P-POLC).LT.1.0)       GO   TO    901
            POLD=P
            M=M+1
            IF(M.GT.50)    GO   TO     101
      C     START ON THE ITERATIVE CALCULATIONS
            VS=VSO*EXP(-BETA*P)
            IF(V.LE.VS)   GO   TO   99
         98 CONTINUE
            ES=ESO*(VSO/VS)**0.333
            CALL  TVSET(V,T)
            GO  TO     100
         99 N=N+1
            VS=V/2.0
            IF(N.GT.2)   GO   TO    101
            GO   TO   98
        101 CONTINUE
        901 CONTINUE
            RETURN
            END
```

```
:V C LEVEL 0, MOD 0            MAIN            DATE = 67264        14/50/12

      C
      C     CALCULATE THE ISOTHERMS
      C    SUB   PLOT1
            SUBROUTINE  PLOT1(V,T)
            COMMON/DATAM/M
            COMMON/BCC/BLANK,DOT,C(13)
            COMMON/YSET/Y,UVOO
            WRITE(6,450)
          450 FORMAT('C',2X,'ISOTHERMS')
            VIN=V
            TIN=T
            IF(M.LE.2)   GO  TO   300
            DT=50.0
            GO  TO  301
          300 DT=100.0
          301 CONTINUE
            T=T-DT
            DO  10 K=1,5
      C     ASSIGN A CHARACTER FOR PLOTTING
            Y=C(K)
            T=T+DT
            WRITE(6,451) K,T
          451 FORMAT('C',2X,'ISOTHERM ',I2,5X,'TEMPERATURE ',F10.4,'(K)')
            WRITE(6,201)
          201 FORMAT('C',16X,'V(CC/GM)',13X,'T(K)',15X,'P(BAR)',12X,
           1'E(CAL/GM)',13X,'S(CAL/GM-K)',10X,'V/VO')
            V=VIN+VIN/10.0
            DO  10  N=1,10
            V=V-VIN/10.0
      C     CALCULATE P
            CALL WRITE1(V,T)
           10 CONTINUE
            V=VIN
            T=TIN
            RETURN
            END
```

```
V G LEVEL 0, MOD 0            MAIN              DATE = 67264          14/50/12
      C
            SUBROUTINE  WRITE1(V,T)
            COMMON/DATAM/M
            COMMON/APLOT/AP(101,101)
            COMMON/YSET/Y,UVOO
            COMMON/CLOSET/A,ES,VS,SN,SS,CK,EEO,PPO,VO,TO,CKK ,VSO
            VOO=VO/39.944
            TIN=T
            VIN=V
      C     CALCULATE P,E,AND S
            PP=P(V,T)
            EE=E(V,T)
            S1=S(V,T)
      C     CHANGE UNITS
            V=V/39.944
            PP=PP*1000.0/(24.21*0.987)
            EE=EE/39.944
            S1=S1/39.944
            VR=V/VOO
      C     WRITE V,T,P,E,S AND V/V0
            WRITE(6,202)V,T,PP,EE,S1,VR
        202 FORMAT(' ',7X,6E20.6)
      C     LOCATE THE POINT(P,V)
            UVOO=VOO/100.0
            N=1.5+V/UVOO
            IF(M.EQ.1)     GO     TO       300
            K=(10000.0-PP)/100.0+1.5
            GO   TO   111
        300 K=(20.0-PP)/0.2+1.5
        111 CONTINUE
      C     GET RID OF THOSE POINTS OUTSIDE THE REGION(101*101)
            IF(K.GT.101)   GO   TO   400
            IF(K.LT.1)  GO  TO  400
            IF(N.GT.101)   GO   TO   400
            IF(N.LT.1)   GO   TO   400
            AP(K,N)=Y
        400 CONTINUE
            V=VIN
            T=TIN
            RETURN
            END
```

PART B

ACOUSTIC WAVES FOLLOWING STRONG SHOCK WAVES

G. R. Fowles

I. Introduction

Conventional dynamic equation of state experiments, in which the wave and particle velocities of plane shock waves are measured in a sample, yield only partial information about the state of the shocked material. This information comprises the stress component normal to the wave front, the density, and the internal energy. In particular, the normal stresses across a plane perpendicular to the shock front are not determined. Knowledge of these stress components in addition to the stress normal to the front is tantamount to knowing the shear modulus and the yield strength of the material under shock conditions.

In an elastic-plastic solid the shear modulus and yield strength must be known in order to treat problems involving interactions of shock and rarefaction waves; a simple example is that of a decaying shock. Shock attenuation experiments on aluminum and other materials have shown that material rigidity, characterized by the yield stress and shear modulus, has a significant effect on shock attenuation at pressures up to at least 200 Kbar. Moreover, the values of these parameters are not simply predictable from known zero-pressure values.[1,2,3]

Attempts to determine the shear modulus and yield strength by means of one-dimensional shock attenuation experiments have been only partially successful. Spallation of the

free surface on which measurements are made severely limits the information obtainable.

In this paper I report preliminary results of a study of small amplitude wave propagation in an elastic-perfectly plastic solid considered to be previously stressed to the yield point in uniaxial strain--as, for example, by a uniform plane shock. By relaxing the restriction that the flow be strictly one-dimensional, i.e., by allowing the (plane) acoustic waves behind the shock to propagate at arbitrary angles with respect to the direction of propagation of the shock one finds that four distinct acoustic waves are possible, compared with two for the one-dimensional case. Their velocities depend in general on the shear modulus, and their amplitudes on the yield strength. Thus, there are a greater variety of measurements possible in the two-dimensional case than in the one-dimensional case. This result is promising; however, it is not yet clear how best to make use of these waves experimentally. They can be generated by such means as reflection at interfaces oriented obliquely to the direction of shock propagation.

Another application of the theory is to problems such as oblique reflection of shocks at interfaces. These problems have not yet been investigated, but their solution is a natural extension of the results reported.

II. Fundamental Relations and Initial Conditions

As the starting point for the problem we assume a plane shock propagating in the x_1 direction in an isotropic elastic-

perfectly plastic solid satisfying the V. Mises yield criterion. The amplitude of the shock is arbitrary except that it must be large enough to bring the material to the yield point. Certain fundamental relations to which we will make reference are listed below.

We assume Cartesian coordinates $x_i (i = 1,2,3)$ and let u_i be the velocity of the material at point x_i. Strains are assumed small and the strain rate is therefore given by:

$$\dot{n}_{ij} = \tfrac{1}{2}\left(\frac{\partial u_i}{\partial x_j} + \frac{\partial u_j}{\partial x_i}\right) .$$

For elastic strains, Hooke's law yields,

$$E\dot{e}_{ij} = (1 + \nu)\, \dot{\sigma}'_{ij} - \nu\, \dot{\sigma}_{kk}\, \delta_{ij} \tag{1}$$

where σ_{ij} is the stress tensor, E and ν are Young's modulus and Poisson's ratio, and e_{ij} are elastic strains.
The plastic strain rate tensor is

$$\dot{e}_{ij} = \dot{n}_{ij} - \dot{e}_{ij}$$

and the deviatoric stress tensor is

$$\sigma'_{ij} = \sigma_{ij} - \sigma_{kk}\, \delta_{ij} . \tag{2}$$

The second invariant of the deviatoric stress tensor s, is given by,

$$2s^2 = \sigma'_{ij}\, \sigma'_{ij} . \tag{3}$$

For a V. Mises solid, $s \leq k$ where k is the yield stress in simple shear--assumed constant. Plastic deformation occurs only when

$$s = k \ , \quad \dot{s} > 0 \ . \tag{4}$$

Otherwise the deformation is elastic and $n_{ij} = e_{ij}$. When yielding occurs the flow rule is

$$\dot{\epsilon}_{ij} = K \sigma'_{ij} \tag{5}$$

where K is an undetermined constant. The equation of motion (for small amplitude waves) is:

$$\frac{\partial}{\partial x_i} (\sigma_{ij}) = \rho \dot{u} \ , \tag{6}$$

where ρ is assumed constant.

The stress matrix of the original state is diagonal, of the form:

$$A = \begin{bmatrix} a_{11} & 0 & 0 \\ 0 & a_{22} & 0 \\ 0 & 0 & a_{33} \end{bmatrix}$$

with $a_{22} = a_{33}$ from symmetry. Moreover, the yield criterion (Eq. 4), written in terms of principal stresses is:

$$(\sigma_1 - \sigma_2)^2 + (\sigma_2 - \sigma_3)^2 + (\sigma_3 - \sigma_1)^2 = 6k^2 = 2Y^2 \tag{7}$$

where Y is the yield stress in simple tension.

For matrix A this implies

$$a_1 - a_2 = \sqrt{3}\, k = Y . \tag{8}$$

III. Elastic (Unloading) Waves

A. Shear Waves

An unloading wave by definition does not produce plastic flow. That is, $\dot{s} < 0$. For these waves, Hooke's law expresses the relation between stress and strain rate tensors, and the velocities are those of elastic longitudinal or shear waves, i.e., $\rho c_1^2 = \lambda + 2\mu$ or $\rho c_2^2 = \mu$ where λ and μ are the Lame constants.

We assume an unloading shear wave whose wave front is parallel to the X_3 axis and is inclined to the X_1 axis. Its velocity is $c_2 = \sqrt{\mu/\rho}$; we wish to find its amplitude such that superposition of the stress matrix associated with the wave and the initial stress matrix just maintains the material at the yield point. That is, we wish to find the maximum amplitude of an unloading elastic shear wave whose wave front is inclined at angle α with respect to the original shock (Fig. 18).

The stress matrix associated with the shear wave alone is

$$B = \begin{bmatrix} b_{11} & b_{12} & 0 \\ b_{21} & b_{22} & 0 \\ 0 & 0 & 0 \end{bmatrix} = \begin{bmatrix} b_{11} & b_{12} \\ b_{21} & b_{22} \end{bmatrix} .$$

It is subject to the restriction

$$b_{kk} = b_{11} + b_{22} = 0$$

and $$b_{12} = b_{21} \ .$$

We wish to find the values of the components of B such that the eigenvalues of the matrix [A + B] just satisfy the yield criterion (Eq. 7). Adding A and B ,

$$A' = A + B = \begin{bmatrix} a_{11} + b_{11} & b_{12} & 0 \\ b_{21} & a_{22} + b_{22} & 0 \\ 0 & 0 & a_{22} \end{bmatrix}$$

$$= \begin{bmatrix} a_{11} + b_{11} & b_{12} & 0 \\ b_{12} & a_{22} - b_{11} & 0 \\ 0 & 0 & a_{22} \end{bmatrix} \ .$$

The characteristic equation of this matrix is

$$\begin{vmatrix} a_{11} + b_{11} - \lambda' & b_{12} & 0 \\ b_{12} & a_{22} - b_{11} - \lambda' & 0 \\ 0 & 0 & a_{22} - \lambda' \end{vmatrix} = 0 \ .$$

Expanding the determinant:

$$(a_{11} + b_{11} - \lambda')(a_{22} - b_{11} - \lambda')(a_{22} - \lambda') - b_{12}^2(a_{22} - \lambda') = 0$$

one root is therefore $\lambda'_3 = a_{22}$. The other roots are

solutions of

$$(a_{11}+b_{11}-\lambda)(a_{22}-b_{11}-\lambda') - b_{12}^2 = 0$$

or

$$\lambda'_{1,2} = \tfrac{1}{2}(a_{11}+a_{22}) \pm \tfrac{1}{2}\sqrt{(a_{11}+a_{22})^2 - 4(a_{11}a_{22}+b_{11}a_{22}-a_{11}b_{11}-b_{11}^2-b_{12}^2)}.$$

If the yield criterion is to be satisfied we must have:

$$(\lambda'_1-\lambda'_2)^2 + (\lambda'_2-\lambda'_3)^2 + (\lambda'_3-\lambda'_1)^2 = 2Y^2$$

After some reduction this relation is

$$(a_{11}-a_{22})^2 - 3\left[b_{11}a_{22} - a_{11}b_{11} - b_{11}^2 - b_{12}^2\right] = Y^2$$

But, from (8), $a_{11}-a_{22} = Y$, so that,

$$b_{11}(Y) + b_{11}^2 + b_{12}^2 = 0$$

or

$$b_{11} = -\tfrac{1}{2}Y \pm \tfrac{1}{2}\sqrt{Y^2-4b_{12}^2} \qquad (9)$$

We can more easily describe the shear wave in terms of its principal stresses, or eigenvalues, λ. Hence, we solve the characteristic equation

$$\begin{vmatrix} b_{11}-\lambda & b_{12} \\ b_{12} & -b_{11}-\lambda \end{vmatrix} = 0$$

Thus, $\lambda = \pm\sqrt{b_{11}^2 + b_{12}^2}$.

But, from (9) $b_{11}^2+b_{12}^2 = -Y\,b_{11}$.

Therefore $\lambda = \pm \sqrt{-Y\, b_{11}}$. (10)

The eigenvectors associated with the shear wave can now be found from

$$\begin{bmatrix} b_{11} & b_{12} \\ b_{12} & -b_{11} \end{bmatrix} \begin{bmatrix} x_1 \\ x_2 \end{bmatrix} = \lambda \begin{bmatrix} x_1 \\ x_2 \end{bmatrix}$$

Expanding,

$$b_{11}\, x_1 + b_{12} x_2 = \lambda\, x_1$$

$$b_{12}\, x_1 - b_{11} x_2 = \lambda\, x_2 \ .$$

Eliminating b_{12} :

$$\frac{\lambda\, x_1 - b_{11} x_1}{x_2} = \frac{\lambda\, x_2 + b_{11} x_2}{x_1}$$

$$\left(\frac{x_1}{x_2}\right)^2 = \frac{\lambda + b_{11}}{\lambda - b_{11}}$$

Substituting from (10) for $b_{11} = \frac{\lambda^2}{Y}$

$$\left(\frac{x_1}{x_2}\right)^2 = \pm \sqrt{\frac{1 - \lambda/Y}{1 + \lambda/Y}} \qquad (11)$$

Equation 11 gives the principal stresses associated with the shear waves as a function of the tangent of the angle between the principal axes of the original stress matrix and the

principal axes of the shear wave. Figure 19 shows a plot of this relation. The ordinate is the principal stress of the shear wave; the abscissa is the angle between principal axes (θ), or the angle between wave fronts (α). (Note that the principal axes of a shear wave are inclined 45° with respect to the wave front.)

B. Longitudinal Waves

We adopt the same approach as for shear waves, except that the matrix B is now:

$$B = \begin{bmatrix} b_{11} & b_{12} & 0 \\ b_{21} & b_{22} & 0 \\ 0 & 0 & b_{33} \end{bmatrix} .$$

Elastic longitudinal waves are characterized by the relations between principal stresses:

$$\lambda_2 = \lambda_3 = \frac{\nu}{1-\nu} \lambda_1 .$$

The invariants of the B matrix are then:

$$I_1 = b_{11} + b_{22} + b_{33} = \left(\frac{1+\nu}{1-\nu}\right) \lambda_1 \qquad (12)$$

$$I_2 = - (b_{11}b_{22} + b_{22}b_{33} + b_{11}b_{33}) + b_{12}^2 = - \frac{\nu(2-\nu)}{(1-\nu)^2} \lambda_1^2 \qquad (13)$$

$$I_3 = b_{11}b_{22}b_{33} - b_{33}b_{12}^2 = \left(\frac{\nu}{1-\nu}\right)^2 \lambda_1^3 . \qquad (14)$$

The matrix of superposed stresses is

$$A' = A+B = \begin{bmatrix} a_{11}+b_{11} & b_{12} & 0 \\ b_{12} & a_{22}+b_{22} & 0 \\ 0 & 0 & a_{22}+b_{33} \end{bmatrix}$$

with secular equation:

$$(a_{11}+b_{11} - \lambda')(a_{22}+b_{22} - \lambda')(a_{22}+b_{33} - \lambda') - (a_{22}+b_{33} - \lambda')b_{12}^2 = 0.$$

The roots of this equation are:

$$\lambda_3' = a_{22}+b_{33} \tag{15}$$

$$\text{and } \lambda_{1,2}' = \tfrac{1}{2}(a_{11}+b_{11}+a_{22}+b_{22}) \pm \tfrac{1}{2}\sqrt{(a_{11}+b_{11}+a_{22}+b_{22})^2 + 4[b_{12}^2-(a_{11}+b_{11})(a_{22}+b_{22})]}. \tag{16}$$

These roots must satisfy the yield criterion:

$$(\lambda_1'-\lambda_2')^2 + (\lambda_2'-\lambda_3')^2 + (\lambda_3'-\lambda_1')^2 = 2Y^2 \quad . \tag{17}$$

Inserting the values for λ_i' from (15) and (16) into (17); we get after simplification:

$$(a_{11}+b_{11})^2 - (a_{11}+b_{11})(a_{22}+b_{22}) + (a_{22}+b_{22})^2 -(a_{22}+b_{33})(a_{11}+b_{11}+a_{22}+b_{22}) + (a_{22}+b_{33})^2 + 3b_{12}^2 = Y^2 \; . \tag{18}$$

This equation is to be solved simultaneously with Eqs. 12, 13, 14 to establish maximum longitudinal wave amplitudes.

Recalling that $a_{11}-a_{22} = Y$ we can rewrite (18) as:

$$b_{11}^2+b_{22}^2+b_{33}^2 + Y(2b_{11}-b_{22}-b_{33}) - b_{11}b_{22} - b_{11}b_{33}$$

$$-b_{22}b_{33} = -3b_{12}^2$$

But from (13)

$$b_{11}b_{22} + b_{11}b_{33}+b_{22}b_{33} = b_{12}^2 + \frac{\nu(2-\nu)}{(1-\nu)^2}\lambda_1^2 \quad .$$

Eliminating b_{12} between these equations and employing Eq. 12 to eliminate b_{33} yields:

$$3\, b_{11}\, Y - \frac{1+\nu}{1-\nu}\lambda_1\, Y + \left[\frac{4\nu^2 - 4\nu+1}{(1-\nu)^2}\right]\lambda_1^2 = 0 \quad . \qquad (19)$$

We now note that x_3 is a principal direction of both matrices A and $A' = A+B$. (Eq. 15.) Hence b_{33} must be an eigenvalue of the B matrix, i.e.,

$$b_{33} = \lambda_3 = \frac{\nu}{1-\nu}\lambda_1$$

Hence, from (12) again

$$b_{22} = \left(\frac{1+\nu}{1-\nu}\right)\lambda_1 - b_{11} - b_{33} \qquad (20)$$

$$= \frac{\lambda_1}{1-\nu} - b_{11} \quad .$$

Equations 19 and 20 give b_{11} and b_{22} in terms of the principal stress of the longitudinal wave, parallel to the direction of propagation, λ_1 .

If we now solve for the eigenvectors of B, we get

$$(b_{11}-\lambda)x_1 + b_{12}x_2 = 0$$

$$b_{12}x_1 + (b_{22}-\lambda)x_2 = 0$$

$$(b_{33}-\lambda)x_3 = 0$$

$$\left(\frac{x_1}{x_2}\right)^2 = \frac{\lambda - b_{22}}{\lambda - b_{11}} = \frac{\lambda_1 - \frac{\lambda_1}{1-\nu} + b_{11}}{\lambda_1 - b_{11}} \qquad (\lambda = \lambda_1)$$

and, substituting for b_{11} from (19),

$$\left(\frac{x_1}{x_2}\right)^2 = \frac{2\nu^2 - 3\nu+1 - (4\nu^2-4\nu+1)\frac{\lambda_1}{Y}}{4\nu^2 - 6\nu+2 + (4\nu^2-4\nu+1)\frac{\lambda_1}{Y}}$$

This expression gives the amplitude of a longitudinal wave whose wave front is inclined at an angle $\tan^{-1}\left(\frac{x_1}{x_2}\right)$ with respect to the original shock front and which just maintains the material at the yield point. It is of the form

$$\left(\frac{x_1}{x_2}\right)^2 = \frac{a - b\frac{\lambda_1}{Y}}{2a + b\frac{\lambda_1}{Y}}$$

where a and b are functions of Poisson's ratio, ν.

Figure 20 shows a plot of λ_1/Y as a function of the angle $\alpha = \cot^{-1}\left(\frac{x_1}{x_2}\right)$ for several values of ν_1. Note that the wave is compressive for angles greater than about 55° $\left(\frac{x_1}{x_2} = \frac{1}{\sqrt{2}}\right)$. For shallower angles the wave is a rarefaction wave and can be quite large for large values of Poisson's ratio.

IV. Plastic (Loading) Waves

Loading waves occur whenever Eq. 4 is satisfied. The flow rule relating the strain rate tensor to the stress rate tensor is then modified by the addition of a term given by Eq. 5. Thus,

$$\dot{n}_{ij} = \left(\frac{1+\nu}{E}\right) \dot{\sigma}_{ij} - \frac{\nu}{E} \dot{\sigma}_{kk} \delta_{ij} + K\sigma'_{ij} .$$

We take the direction of propagation of a plastic wave behind the shock as the x_i' direction and assume the other axes are oriented so that the shear stresses σ_{13}, and σ_{23} ahead of the wave are zero. That is, the prime set of axes is rotated about x_3 with respect to the unprimed set (which are principal directions of the initially stressed material). The wave is also assumed to have infinitesimal amplitude. We wish to find the velocity of the wave as a function of the angular difference between the plastic wave and the initial shock.

Craggs (5) has shown that an infinitesimal discontinuity in stress and strain propagates under these conditions with a velocity that is one of the roots of the quadratic

$$A\rho C_p^4 - B\rho\mu C_p^2 + C\mu^2 = 0 \qquad (21)$$

where C_p is the plastic wave velocity, μ the shear modulus, ρ the density, and A, B, and C are given by,

$$A = (1 - 2\nu)k^2$$

$$B = (3 - 4\nu)k^2 - (1 - 2\nu)(\sigma_{11}'^2 + \sigma_{12}^2)$$

$$C = 2(1 - \nu)k^2 - (1 - 2\nu)\,\sigma_{11}'^2 - 2(1 - \nu)\sigma_{12}^2$$

This can be written alternatively in terms of the two elastic velocities C_1 and C_2 and the bulk, or hydrodynamic sound speed, CH , where

$$C_1^2 = \frac{\lambda + 2\mu}{\rho}$$

$$C_2^2 = \frac{\mu}{\rho}$$

$$C_h^2 = \frac{K}{\rho} \qquad (K = \text{incompressibility})$$

In terms of these quantities, Eq. 21 becomes,

$$\left(\frac{C_p}{CH}\right)^4 - \left(\frac{C_p}{CH}\right)^2 \left[\left(\frac{C_1}{CH}\right)^2 + \frac{3}{4}\left(\frac{C_1^2}{CH^2} - 1\right)\left(1 - \frac{\sigma_{12}^2}{k^2} - \frac{\sigma_{11}'^2}{k^2}\right)\right] \qquad (22)$$

$$+ \frac{3}{4}\frac{C_1^2}{CH^2}\left(\frac{C_1^2}{CH^2} - 1\right)\left(1 - \frac{\sigma_{12}^2}{k^2}\right) - \frac{9}{16}\left(\frac{C_1^2}{CH^2} - 1\right)^2 \frac{\sigma_{11}'^2}{k^2} = 0$$

where $\frac{C_1^2}{CH^2} = \frac{3(1-\nu)}{1+\nu}$.

In order to find the velocity in a given direction we need to know the stresses ahead of the wave, σ_{12} and σ_{11}' . Taking a_1 and a_2 as the principal stresses behind the initial shock, and α as the angle of rotation of the prime coordinate system about the x_3 axis (i.e. α is the angle between the wave fronts), we have

$$\sigma_{11} = a_1 \cos^2\alpha + a_2 \sin^2\alpha$$

$$\sigma_{12} = (-a_1+a_2) \sin\alpha \cos\alpha \quad .$$

Moreover,

$$a_1 - a_2 = Y .$$

Hence,

$$\sigma_{11} = a_1 - Y \sin^2\alpha$$

$$\sigma_{12} = -Y \sin\alpha\cos\alpha$$

and

$$\sigma_{11}' = \sigma_{11} - p = Y(2/3 - \sin^2\alpha)$$

Inserting these values into Eq. 22 yields two velocities for each value of Poisson's ratio and for each angle, α . A representative case is plotted in Fig. 21.

Several features of these curves are noteworthy. For zero angle of inclination the plastic waves travel with the velocities of hydrodynamic and elastic shear waves respectively. For other angles one plastic wave speed falls between C_1 and CH, and the other is less than C_2. The faster wave speed increases to C_1 at just that angle for which a longitudinal elastic unloading wave can have only zero amplitude (Fig. 3). These waves are in general mixed waves that produce changes both in the stress normal to the front and in the shear stress tangential to the front. Thus, they tend to rotate the principal axes. The stress discontinuities as given by Craggs, are:

$$\text{(a)} \quad \sigma_{11}' \Delta\sigma_{33} = \left\{\sigma_{33}' - \frac{2\mu(\sigma_{33}' + \nu\sigma_{22}')}{(1-2\nu)\rho C_p^2}\right\} \Delta\sigma_{11} \qquad (23)$$

$$(b)\quad \sigma_{11}' \Delta \sigma_{22} = \left\{\sigma_{22}' - \frac{2\mu(\sigma_{22}' + \nu \sigma_{33}')}{(1-2\nu)\ \rho C_p^{\,2}}\right\} \Delta \sigma_{11}$$

$$(c)\quad \Delta \sigma_{12} = \frac{\sigma_{12}}{\sigma_{11}'} \left(\frac{C_p^{\,2} C_1^{\,2}}{C_p^{\,2} - C_2^{\,2}}\right) \Delta \sigma_{11}$$

It is easily shown that for any plastic wave $\frac{\Delta \sigma_{11}}{\sigma_{11}'} > 0$, and , moreover, the two plastic velocities are bounded by the elastic velocities

$$C_2 < Cp_1 < C_1 \; ; \quad Cp_2 < C_2$$

Hence, from the equation for $\Delta \sigma_{12}$ above (23c), we see that the faster wave tends to decrease the shear stress, σ_{12} , while the slower wave tends to increase it.

Some appreciation for the structure of a finite amplitude plastic wave can be gained by numerical integration of the above equations. Each infinitesimal wave front alters the stress state behind it and since the wave velocity depends on the stress state ahead, finite amplitude waves will generally show amplitude dispersion.

Fig. 22 shows a plot of the stress normal to the (fast) plastic wave as a function of the wave velocity for particular values of Poisson's ratio and the angular difference between the

plastic wave and the initial shock. The angular difference in this case is such that the head of the plastic wave travels with velocity C_1. In general it is slower than C_1 so that there is a region of uniform stress between elastic and plastic wave fronts. As the wave speed approaches hydrodynamic wave speed, increasingly large increments in the stress normal to the front are required for a given increment in wave speed. Thus, the shear stress only asymptotically tends to zero and the wave speed asymptotically approaches hydrodynamic speed.

This model does not permit the formation of a shock front as a true discontinuity in stress although the stress gradient becomes larger with increasing stress. However, we recall that the equations are based on the assumption of small amplitudes and the equation of motion therefore has no convective term. It would be of interest to extend the theory to include finite amplitudes.

REFERENCES

1. Donald R. Curran, "Nonhydrodynamic Attenuation of Shock Waves in Aluminum," J. Appl. Phys. 34, 2677-2685 (September, 1963).
2. John O. Erkman and George E. Duvall, "Elastoplasticity and the Attenuation of Shock Waves," Paper presented at the Ninth Midwestern Mechanics Conference, University of Wisconsin, Madison, August 16-18, 1965.
3. P. J. A. Fuller and J. H. Price, "The Elasto-Plastic Release Behavior of Magnesium at 80 Kb," Fourth Symposium (International) on Detonation, U.S. Naval Ordnance Laboratory, White Oak, Maryland, October 12-15, 1965. (U.S. Government Printing Office, Wash. D.C.)
4. J. W. Craggs, "The Propagation of Infinitesimal Plane Waves in Elastic-Plastic Materials," J. Mech. and Phys. Solids 5, 115-124 (1957). Pergamon Press Ltd., London.

FIGURE CAPTIONS

Fig. 18. Wave front configuration.

Fig. 19. Maximum shear wave amplitudes as function of angle of inclination of wave fronts.

Fig. 20. Maximum dilatational wave amplitudes as function of angle of inclination of wave fronts.

Fig. 21. Plastic wave velocities as function of angle of inclination of wave fronts. Poisson's ratio, $\nu = 0.25$.

Fig. 22. Normal stress, σ_{11}, of plastic wave as function of velocity. Poisson's ratio, $\nu = 0.30$, inclination of wave fronts, $\alpha = 51.6^{\circ} = 0.9$ radian.

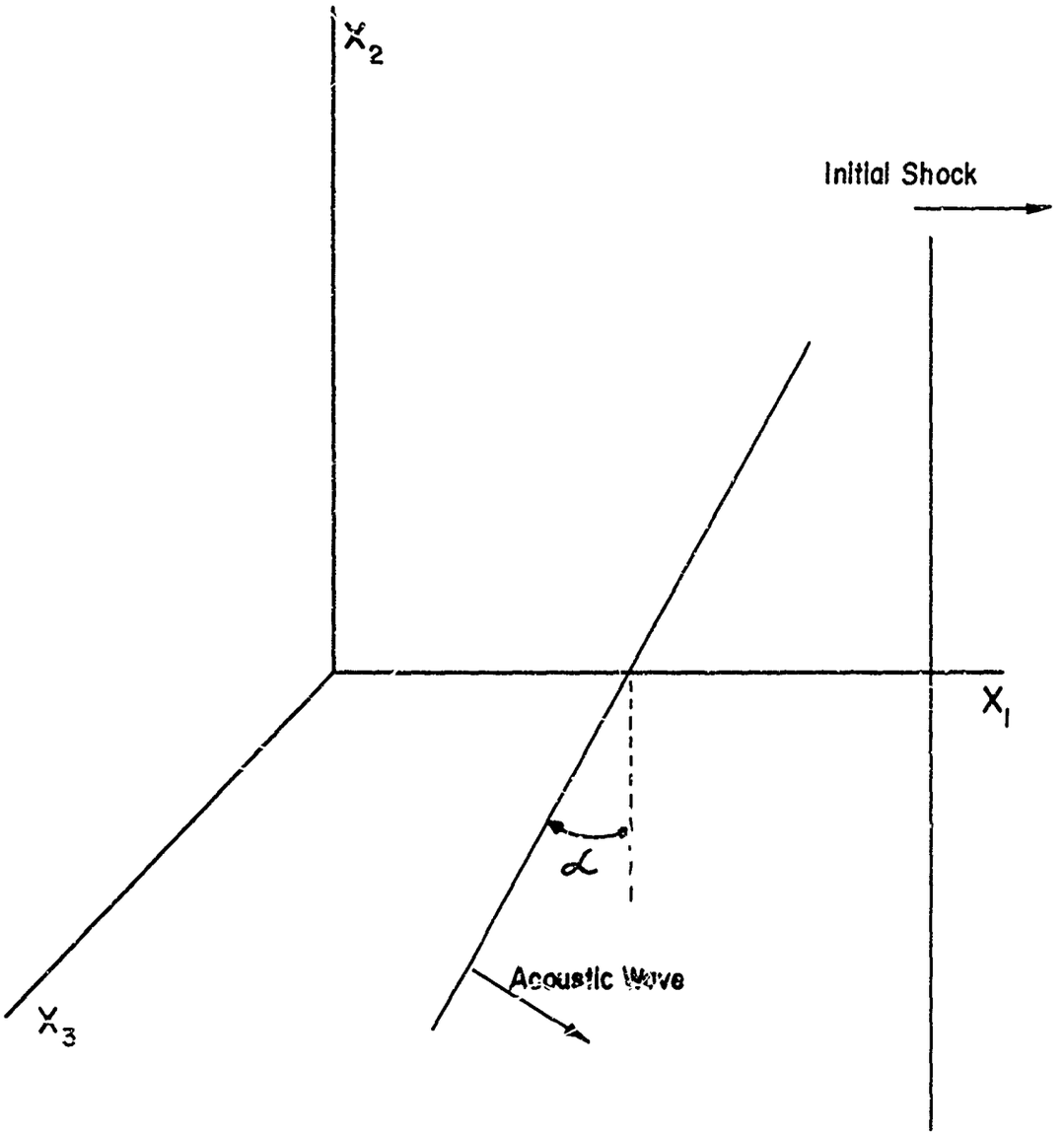

Fig. 18

Wave Front Configuration

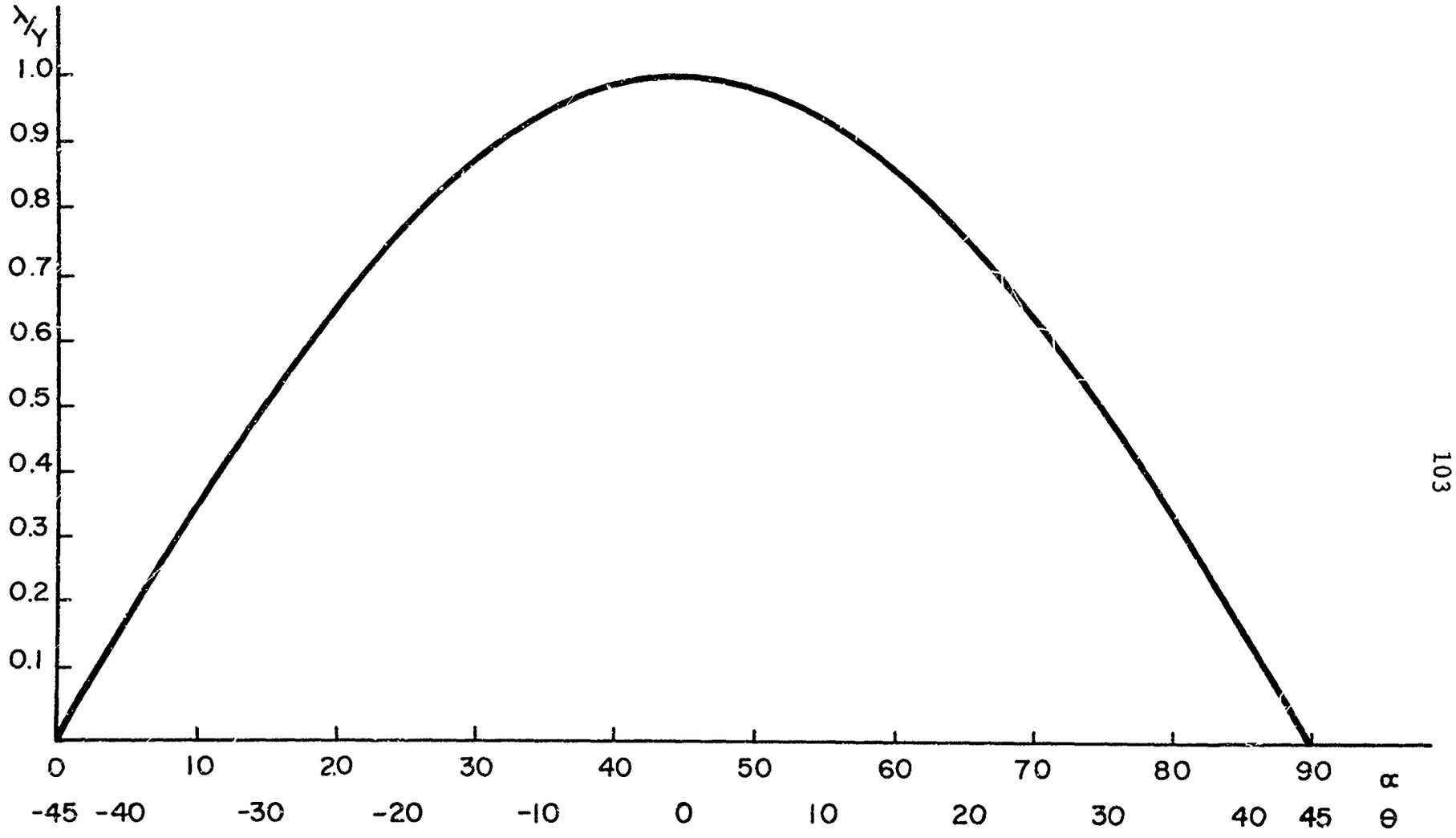

Fig. 19

Maximum Shear Wave Amplitudes as Function of Angle of Inclination of Wave Fronts

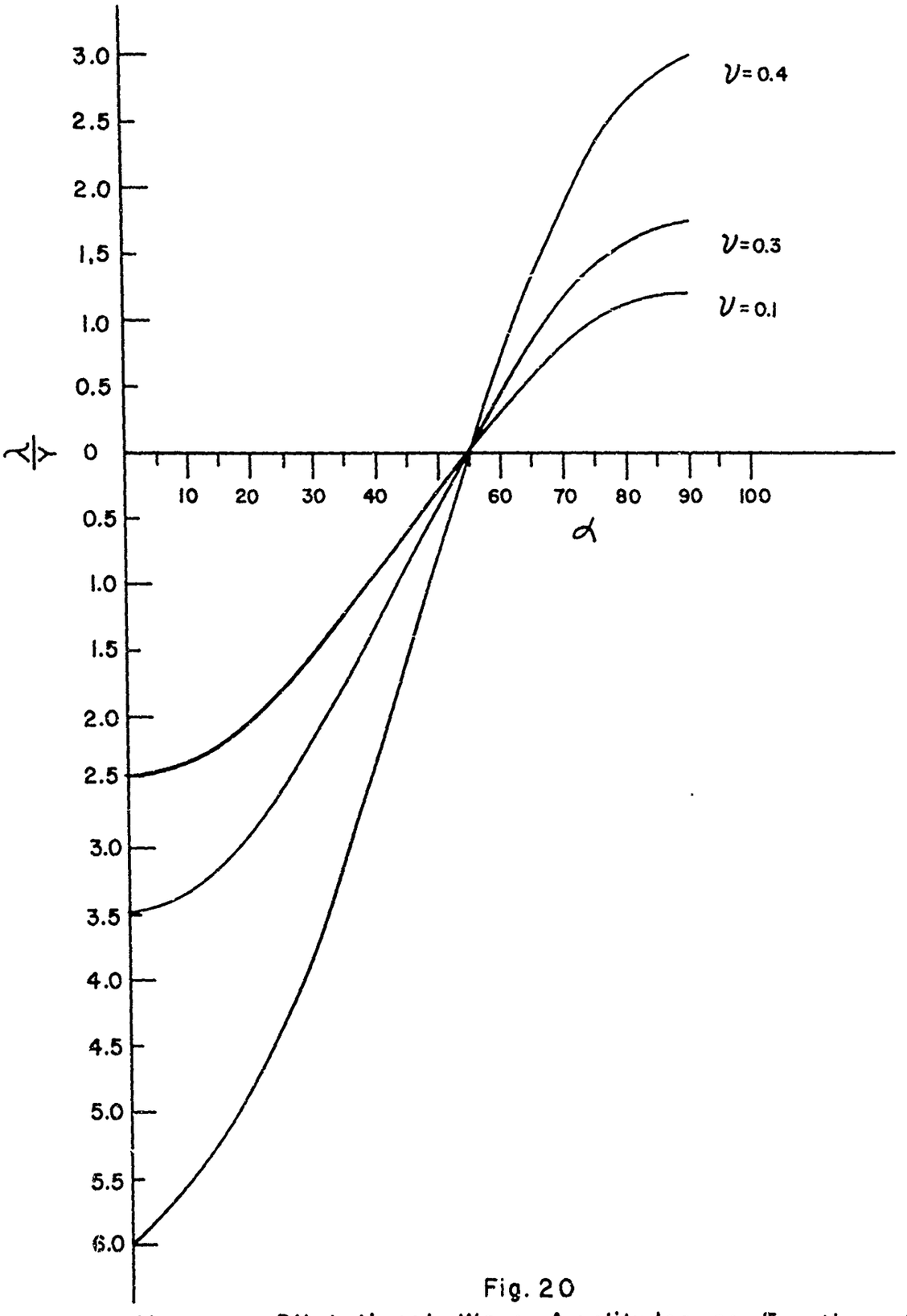

Fig. 20
Maximum Dilatational Wave Amplitudes as Function of Angle of Inclination of Wave Fronts

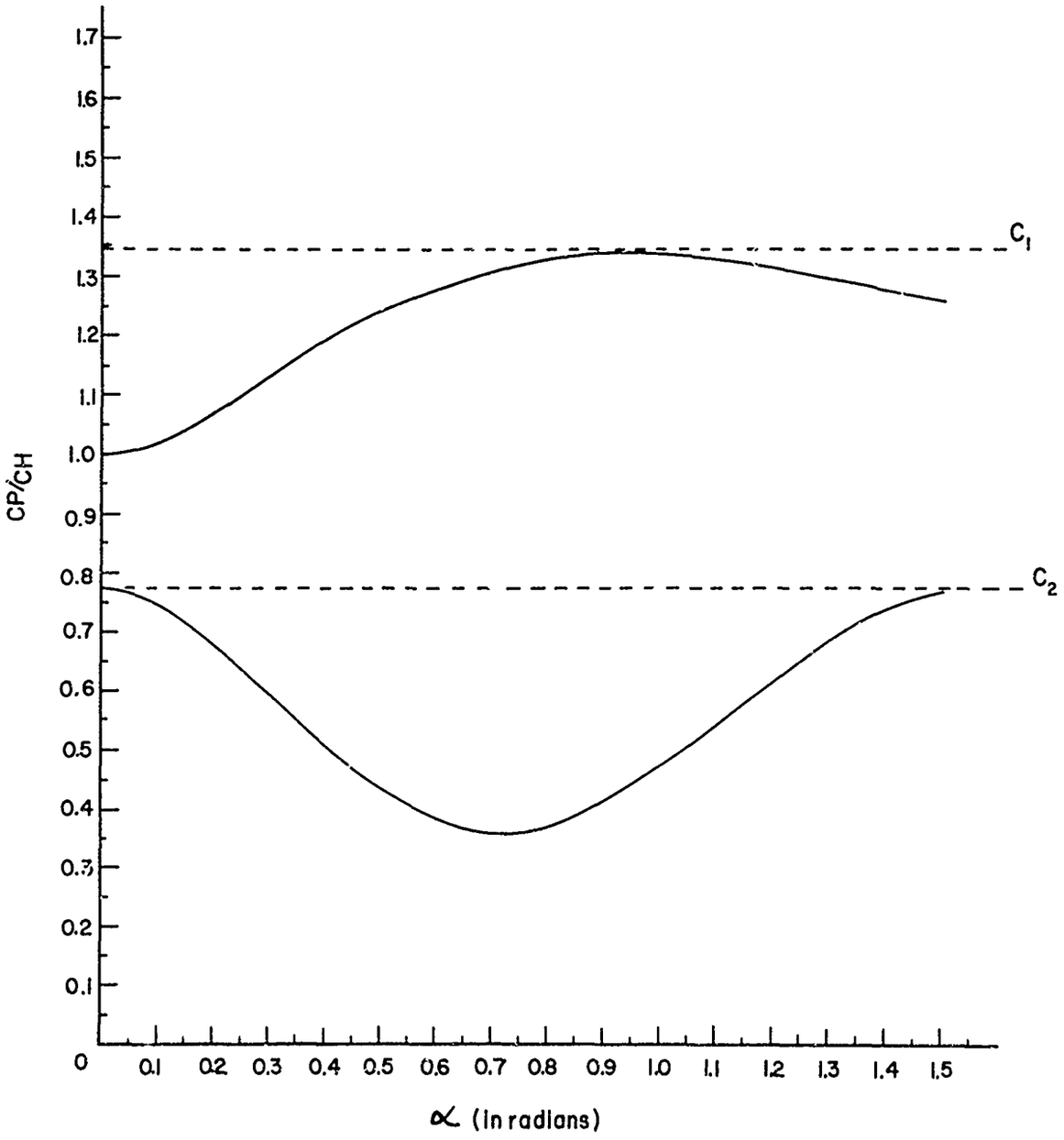

Fig. 21

Plastic Wave Velocities as Function of Angle of Inclination of Wave Fronts

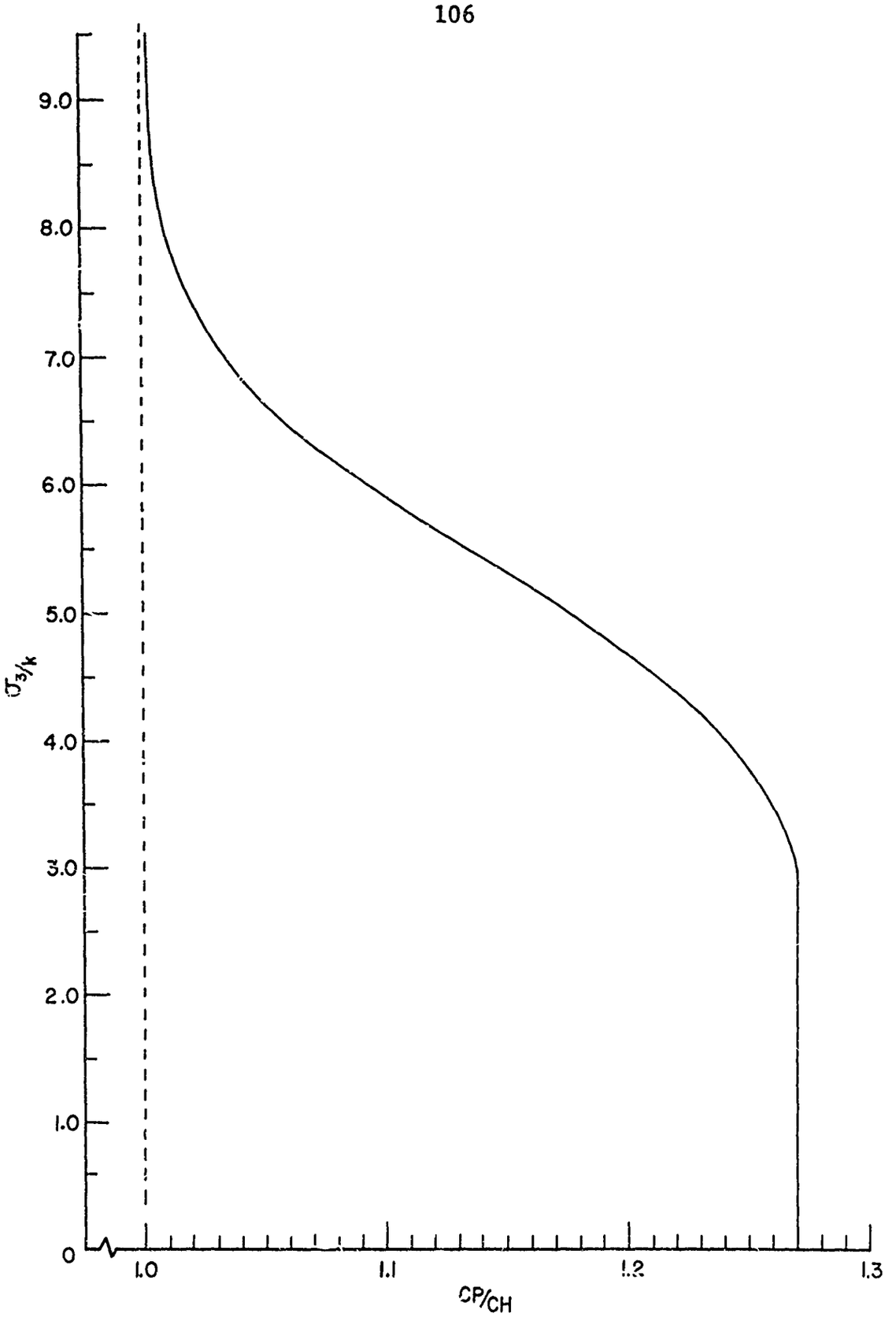

Fig. 22

Normal Stress, σ_{11}, of Plastic Wave as Function of Velocity

PART C

PHASE TRANSITIONS UNDER DYNAMIC CONDITIONS

M. H. Miles

I. Physical Considerations

The purpose of this paper is to survey our present understanding of shock induced phase transformations in solids. It is commonly observed that a stable crystal structure at a given temperature and pressure becomes unstable upon change of temperature or pressure. In general we expect an increase in pressure to favor rearrangement of the atoms into a crystal structure that minimizes the volume while an increase in temperature favors an arrangement of atoms that maximizes entropy.

From the most fundamental viewpoint we would desire to be able to predict in advance the equilibrium structure from the known properties of isolated atoms. This would entail the many-bodied quantum mechanical calculations of the cohesive energy for the various likely crystal structures as functions of pressure and temperature. Unfortunately the cohesive energy for the different crystal structures even far removed in temperature or pressure from a phase boundary are not too different. The difference is often of the order of a percent of the cohesive energy and this is within the accuracy of the quantum mechanical calculation. It is doubtful if the fundamental approach is capable of reliably predicting in advance the phase boundaries on a PVT diagram.

Another less fundamental approach is to avoid the quantum mechanics by using a model calculation based on an assumed atomic interaction. Again the details of the calculation are complicated and only approximate solutions to the model are obtainable. Even if the model seems to favor a given crystal structure it is always somewhat uncertain if this is due to the mathematical approximations or to the model itself. Since effective forces between atoms extend beyond nearest neighbor as evidenced by differences in cohesive energy between hexagonal close packed and face centered cubic structures, the more tractable models are expected to be poor approximations to the real binding forces.

A third approach is an engineering one based upon some thermodynamical model for the phase transformation. Often this approach is a combination of empirical and semi-empirical correlations largely based upon experimental observations of a particular system. A phase transition is feasible if the Gibbs free energy for the rival structures are equal. We may indicate this situation by showing the Gibbs free energy and enthalpy for two polymorphs as functions of temperature at constant pressure and by showing the Gibbs and Helmholtz free energies of the two polymorphs as functions of pressure at constant temperature. Confidence in this approach necessitates accurate calculations of the required thermodynamic quantities or at least a useful representation of the necessary thermodynamic quantities empirically from experimental observations. A partial solution

or at least a useful classification of phase transformation is obtained with the aid of the Clapeyron equation. The Clausius-Clapeyron equation gives the variation of the transition pressure with temperature. This requires accurate calculation of the volume change and entropy change but useful information is obtained if merely the sign of the entropy and volume changes can be obtained.

In attempting to understand shock-induced phase transformations one would like answers to such basic questions as (1) why does the transformation occur, (2) what is the mechanism for the transformation, and (3) what differences exist in static versus shock induced transformations. We have touched upon some of the difficulties pertinent to the first question. In dynamic shock the shifting of atoms to a new structure must occur in times of the order of the transient pressure duration. This time is short, being of the order of microseconds. The situation under dynamic shock may well be influenced more by the kinetics than by the equilibrium thermodynamics of the transformation.

Since our present fundamental understanding of the stability of solids is in a rudimentary state, it seems advisable to carefully review the present experimental knowledge concerning pressure induced phase transformations. The "130-kbar" polymorphic transition in iron has attracted considerable static and dynamic experimentation. The first observation of this polymorph was reported in 1956 in the shock-wave investigation of Bancroft, Peterson, and Minshall.[1] For some time the nature of the

transformation was considered to be the bcc to fcc (α to γ) transformation of iron such as occurs at 910°C and atmospheric pressure. Several investigators[2,3,4] investigated the α to γ phase boundary out to pressures of about 90 kbar. The temperature dependence of the phase line around room temperature was investigated by Minshall[5] under dynamic conditions which seemed inconsistent with any reasonable extension of the α to γ phase line. This led Fowler, Zukas, and Minshall[6] to question the alpha to gamma transition supposition. Johnson, Stein, and Davis[7] reported in 1962 shock compression results on specimens in the temperature range of 70°K to 1158°K. For temperatures up to about 500°C results similar to Bancroft's were obtained while above 500°C a transition that was much more pressure dependent was indicated in fair agreement with the low pressure α to γ statically determined phase boundary. Johnson's et al. temperature-pressure data together with microstructual observations suggested a triple point at about 110 kbar and 500°C. They concluded that the low pressure, high temperature phase line was the alpha to gamma transition while below 500°C the transformation was from α to an "x" phase different from γ, being most likely hcp.

Balchan and Drickamer[8] obtained the phase change statically, observing a sharp change of resistance at 133 kb and 20°C. The first high pressure X-ray investigation was performed by Jamieson and Lawson.[9] In the high pressure phase region at room temperature they observed an extra X-ray line that agreed with

known volumes significantly better if it were assigned to an intense hcp line rather than to a corresponding fcc line. Later improved X-ray work by Clendenen and Drickamer[10] and by Takahashi and Bassett[11] established that the high-pressure phase at room temperature was indeed a hexagonal structure. More recently Bundy[12] has confirmed the pressure-temperature phase diagram for iron placing the triple point at 110 ± 3 kbar and 490 ± 10°C. Bundy calibrated his data by assuming that the 110 kbar assignment by Johnson et al. for the triple point was correct. The justification being that their room temperature data correlated well with the 130 kbar α, ϵ shock transition of Bancroft.

Loree et al.[13] has recently studied the dynamic transformation for pure iron obtaining for the best value for the onset of the dynamic transition 129 ± 1 kbar at room temperature. Earlier transformation pressures appear to be too high for two reasons: (1) the possibility of overdriving the transformation with excessively high input pressures, and (2) the samples were not annealed. It is expected that annealed samples would have the lowest elastic wave and therefore the lowest transition pressure. This seems to be indicated by the work of Loree et al. It is interesting that Bundy[14] has presented evidence that dynamic and static pressures for initiation of transformations are identical for pure iron but the static pressures for iron alloys of V and Co show much larger increases compared to the dynamic pressures as the percentage of V or Co is increased. The difference at 20 wt % Co is huge, being about 288 kb statically

compared to 136 kb for shock.

Another transformation with considerable static and dynamic experimentation occurs in bismuth. Duff and Minshall[15] were the first to observe shock induced phase change in bismuth. Their shock data for specimen temperatures of -27°, 42°, 87°, and 236°C indicated a transition about 3.5 kbars higher than the statically determined phase diagram of Bridgman. The slope of the shock data was -50.8 bars/°C compared to the statically determined slope for the BiI to Bi II phase line of -50 bars/°C. On this basis it was assumed that the high pressure phase was Bi II even though the samples were subjected to shock pressures far into the Bi III static equilibrium region. The 236°C shocked crystal was driven into the liquid bismuth region of the equilibrium phase diagram. Since melting is considered to be a slow process compared to shock pressure durations and there apparently was no evidence for melting, it appears that this is a clear example of a shock-induced transition to a thermodynamically unstable crystal lattice instead of to the stable liquid phase. Larson[16] has repeated room temperature shock investigation of bismuth. Larson measured the sample pressure using quartz pressure gauges whose readings were calibrated assuming linear Hugoniots for bismuth and quartz. After adjusting the observed dynamic transition pressure to an effective hydrostatic pressure Larson achieved a transition pressure of 25.4 kbars for isotropic bismuth and 25.9 kbars for large grain cast bismuth. There was no overdriving of the transition pressure even for samples down to 1.5 mm in thickness. Since the transit time of the shock

wave through such a thin sample is less than a microsecond, the characteristic time for the transformation is much less than a microsecond, being perhaps of the order of a few nanoseconds. The static transformation pressure at room temperature has been determined to excellent precision by Kennedy and La Mori[17] to be 25.4 ± 0.1 kbar. It appears that bismuth and, perhaps also pure iron, cannot be overdriven even for very thin specimens. The importance of sizeable shear stress in reducing the nucleation and growth times is suggested by comparing the shock results with the pure hydrostatic pressure results of Davidson and Lee.[18] Delay times for initiation of the high pressure phase of the order of several minutes were observed for both poly and single crystal bismuth followed by slow growth of the high pressure phase. The transition pressure and transformation rate were found to be independent of the presence of grain boundaries. It seems that for very low shear stresses and pressures only slightly above the transition pressure that the transformation favors thermally activated nucleation and growth processes. However in the shock data for bismuth the new phase must nucleate extremely fast and the new phase must propagate in the shocked sample with a velocity close to the sound velocity.

Other materials such as antimony relax into a new structure much more slowly than iron or bismuth. Minshall's work on antimony referred to by McQueen[19] showed overdriving of the transition pressure for samples thicker than 20 mm. Warnes[20] has recently confirmed and extended Minshall's earlier

work. Apparently the overdriving is due to delay in nucleation or an initial slow growth process. It is reported by the data of Breed and Venable[21] from the PHERMEX facility that X-ray photographs show that the plastic-two wave forms at the sample interface and accelerates rather slowly to its characteristic velocity. This gives a time dependent phase transition with the plastic 2 wave being delayed about 0.6 microseconds.

It is obvious that the short duration of the transient pressure pulse places severe limitation on any mechanism of transformation that requires appreciable time. This suggests that shock-induced transformation should be considered to be classified as Martensitic among the vast literature of solid transformations. Certainly any growth by diffusion of atom by atom across the interface simply requires orders of magnitude too much time. The individual atoms must undergo a correlated relative movement of somewhat less than one interatomic distance. This correlated atomic shuffles or movements are similar to what occurs for example during mechanical turning. There are many examples of temperature induced Martensitic transformations that are fast enough to suggest that similar atomic shuffles are initiated by pressure pulses. It is felt that a study of the Martensitic transformations will shed light upon the transformation process and that shock studies may well prove a useful approach in understanding the martensitic transformations.

The most obvious characteristic of the martensitic transformation is the so-called shape deformation. This reveals itself in rather well-defined surface distortions. These surface

relief effects usually indicate that straight lines in the crystal are transformed into straight lines and planes are transformed into planes. It is also known that the martensitic phase even though it has a different crystal structure has a definite lattice orientation relationship to the parent phase. The particular plane of the parent structure called the habit plane separates the two phases. For convenience we will make two classifications of martensite transformations. The most common is perhaps the platelike martensite which forms from numerous nuclei in a crystal with each plate apparently growing independently into a distinct plate. There is also a "single-interface type" martensite which occurs in some materials such as Au-Cd alloys. In a single crystal the parent-product interface extends completely across the crystal so that the interface plane does not experience the volume constraints present for platelike martensite formation. The boundary between the parent phase and the region of product phase is planar for a single crystal. Included regions of platelike martensite are usually lenticular in shape. The shape deformation of martensitic plates constrained by the parent matrix gives rise to strain energy that may be very large so that further growth is stopped. Additional growth upon cooling does not begin until the chemical driving force can overcome this strain energy. There may be competing nucleation and growth processes which begin at smaller driving forces giving rise to the oft observed martensite appearing only during rapid cooling from above the transformation

temperature. The reaction starts at a characteristic temperature (M_s) which depends upon previous mechanical and thermal history and on grain size. For martensite in steels, the chemical driving force is about 300 cal/mole but for other solids with smaller shape change the driving force may be smaller. In general a large driving force implies a large temperature hysteresis between M_s for the cooling transformation and M_d for the reverse transformation upon heating.

If the chemical driving force is not large enough for spontaneous transformation or even of the wrong sign, martensite may sometimes be produced by externally applied stress. The lattice transformation may be viewed as a mode of mechanical deformation comparable with mechanical twinning. The shape of the mechanical twins are often very similar to the shape of martensitic plates.

The crystallographic theory of martensitic transformations as developed by Wechsler, Lieberman, and Read[22] and a fundamentally equivalent theory by Bowles and Mackenzie[23] is essentially phenomenological, concerned only with the crystallographic features. The problem of nucleation and kinetics remains essentially unsolved. The central aspect of the crystallographic theory is to describe the proper initial and final atom positions and to satisfy experimentally observed shape deformations with an undistorted, unrotated habit plane. Using methods of matrix algebra it is possible to transform one crystal structure into another but an additional matrix is generally needed to give the correct shape deformation and the invariant habit plane. Physically the

additional matrix represents twinning or dislocation slip. As far as the theory is concerned there is no preference given to the order of events between the lattice deformation and the crystal deformation or between the choice of slip or twinning.

Under shock conditions it is not known if the phenomenological theory applies. Both elements of a crystal deformation and lattice deformation are expected to exist under shock conditions since the solid has been driven into a region of plastic relaxation prior to relaxation into the high pressure crystal structure. The restrictions of a specific shape deformation and an undistorted, unrotated habit plane may or may not remain for shock conditions.

In discussing the kinetics of martensitic transformations it is often the nucleation rather than growth that is rate determining. The work of Bunshah and Mehl[24] on an iron-nickel-carbon alloy indicates that the linear growth of individual plates is about one-third the velocity of sound in the alloy. The velocity was observed to be independent of temperature in the range -20° to -200°C indicating that the growth was not thermally activated. This interpretation does help in understanding athermal martensite where the nucleation rate is a function of temperature independent of time and the understanding of isothermal martensite where the nucleation rate for a particular temperature is time dependent. In shock, if there is a delay in nucleation of the high pressure phase we should expect a high pressure precursor to the relaxation, due to phase change, which decays at a rate depending upon the nucleation delay time.

Warnes[20] has suggested that as some of the material behind the shock begins to relax into its higher-density form, rarefaction waves are emitted. The forward rarefaction overtakes the overdriven shock thus attenuating it. The progress of the plastic 2 wave is being delayed by the relaxing material ahead of it. When the nucleated region relaxes to a state on the Hugoniot near the transition pressure, emission of further rarefaction is no longer possible. The plastic 2 wave is presumed to now proceed with its characteristic velocity.

At present we have little or no understanding why a given phase transformation behaves as observed. What seems totally lacking is any detailed plausible models for initiation of a new phase and the subsequent kinetics of growth yielding the plastic 2 wavefront. The role of crystal defects in nucleation of the new phase seems so far essentially unexplored. There is need of further data especially on the simpler solid state systems. For example the simplest martensitic transformation is from a high temperature fcc phase to a low temperature hcp phase as found in cobalt. An evaluation of plausible mechanisms for phase transformations seems in order. Useful theoretical proposals should be amenable to experimental evaluation and sufficiently realistic to be taken seriously by shock wave experimenters.

II. A Simple Martensitic Model

Suppose that each grain of mean diameter d has N_o nucleation sites distributed around its boundary and that $N(P)$ of these are activated at pressures less than P. Suppose

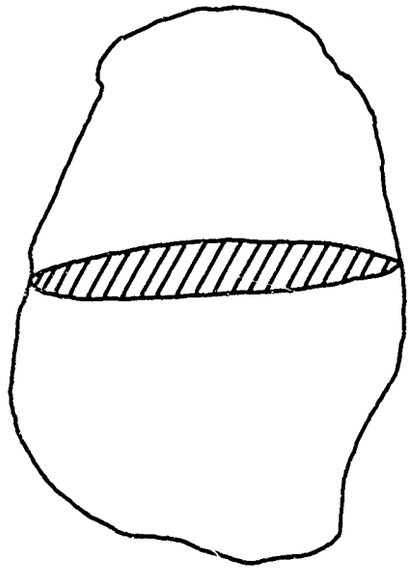

Fig. 23

Platelet of Phase 2 in a Grain of Phase I

further that once a site is activated, it generates a platelet of volume αd which runs across the grain in time d/c, where c is sound velocity in the original material, Fig. 23.

For simplicity take the densities of old and new phases to be the same. Then when the first platelet runs across the grain it transforms a mass fraction $\alpha d/d^3$ to the new phase. As transformation proceeds, the amount of mass transformed by activation of each new site is reduced. Assume that when a fraction λ has been transformed, activation of a new site increases λ by an amount $(1-\lambda)\,\alpha/d^2$. Then for very slow increase in pressure, λ can be assumed to equal its equilibrium value, λeq. Then

$$\frac{d\lambda eq}{dP} = \frac{dN}{dP}\frac{(1-\lambda eq)\alpha}{d^2}$$

or

$$\lambda eq = 1 - \exp(-\alpha N/d^2) \qquad (2.1)$$

A graph of λeq vs P might have the general features shown in Fig. 24. At some pressure P_1 one would say the transformation started. At P_2 it would be effectively completed.

If we now forego the earlier assumption that the two phases have equal densities, the curve of Fig. 24 can be converted to a P-V curve, as in Fig. 25. Here OAC and QBD are compression curves of phases 1 and 2, respectively. OAB is the curve obtained by plotting the average specific volume, v, against P, where

$$v = (1 - \lambda)v_1 + \lambda v_2 \qquad (2.2)$$

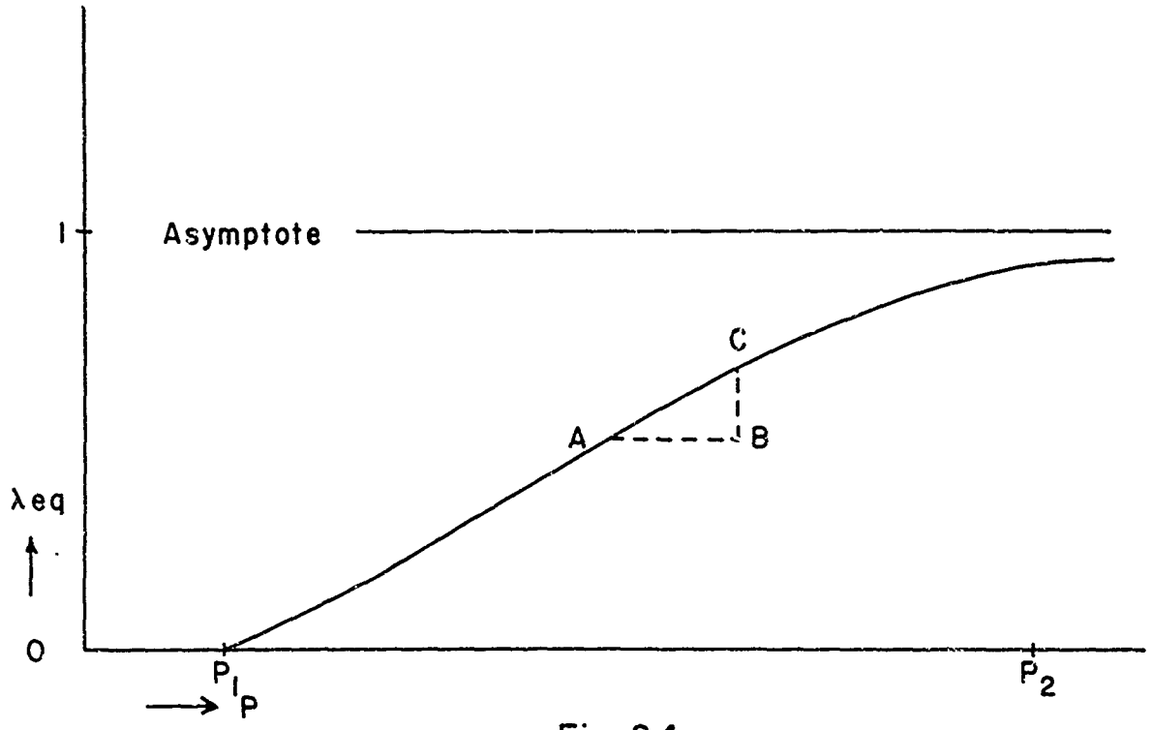

Fig. 24

Schematic Diagram of
Transformation Parameter vs Pressure

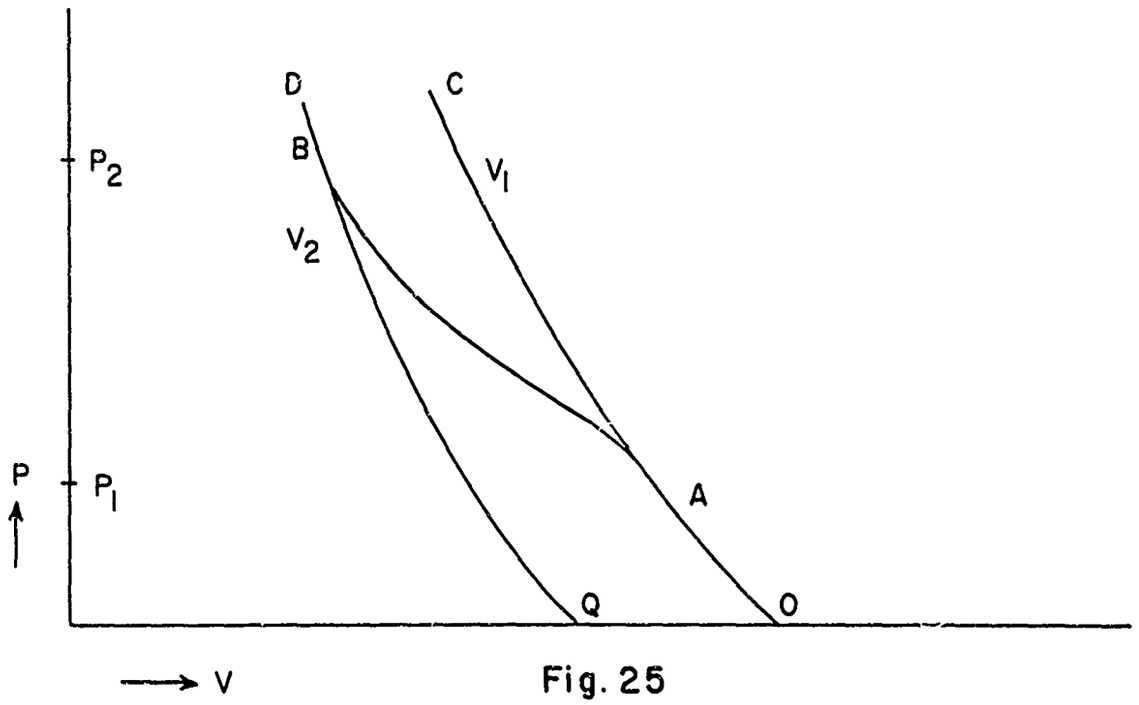

Fig. 25

Compression Curve Corresponding to Fig. 24 & Eq. (22)

and λ is taken to be λ_{eq} of Eq. (2.1) and Fig. 24. The slope of OAB at any point can be determined by differentiating Eq. (2.2) and combining with Eq. (2.1):

$$\frac{dv}{dP} = (1 - \lambda_{eq})\frac{dv_1}{dP} + \lambda_{eq}\frac{dv_2}{dP} + (v_2 - v_1)\frac{\alpha}{d^2}\frac{dN}{dP}(1 - \lambda_{eq}) \qquad (2.3)$$

If $dv_1/dP = dv_2/dP$ and $v_2 - v_1 = Dv$ = constant, this reduces to

$$dv/dP = (dv_1/dP) + Dv\,\alpha(1 - \lambda_{eq})(dN/dP)/d^2 \qquad (2.4)$$

In its integrated form, Eq. (2.2) is

$$v = v_2 + (v_1 - v_2)\,e^{-\alpha N/d^2}\,. \qquad (2.5)$$

If pressure increases very rapidly the growth of platelets may fall behind the pressure increase, so λ may have other than its equilibrium value. Suppose, in Fig 25, that the system is at some point A and that P is suddenly increased to $P + \delta P$ at B. Then the number of activated sites is increased to $N + (dN/dP)\delta P$ and λ starts to increase toward point C at the rate

$$\frac{d\lambda}{dt} = \frac{dN}{dP}\,\delta P\,(1-\lambda)\frac{\alpha C}{d^3} = \delta\lambda_{eq}\,c/d \qquad (2.6)$$

$$= (\lambda - \lambda_{eq})c/d \qquad (2.7)$$

by Eq. (2.1).

Eqs. (2.1), (2.2), (2.5) and (2.7) compose a phenomenologically completedescription of the transition process for

incorporation into the flow equations. In order to illustrate some of their features, note first that d/c in Eq. (2.7) plays the role of a relaxation time. For $d = 0.1$ mm and $c = 5$ mm/μsec, this becomes $\tau = d/c = .02$ μsecs, a much shorter relaxation time than was reported by Novikov et al.[25] and one which would play little role in shock observations.

The equilibrium curve, Eq. (2.5), can be illustrated as follows for iron: Take

$$N = (N_o/2)\left[1 + \tanh\left((P-P_m)/\Delta P\right)\right] \tag{2.8}$$

$$\mu_1 = (v_o/v_1) - 1$$

$$P(v_1) = 1.667\,\mu_1 + 3.4\,\mu_1^2$$

$$\Delta v = v_1 - v_2 = .00596 \text{ cc/g}$$

$$v_o = .1275 \text{ cc/g}$$

$$P_m = .175 \text{ megabars}$$

N_o , α/d^2 and ΔP to be varied

The results of these computations are shown in Fig. 26. The parameters for each curve are given in Table 2.1. It is apparent that the equilibrium curve can be shifted quite arbitrarily in the transition region with even such a simple model as this. Since thermodynamic calculations give almost horizontal adiabat and Hugoniot curves in the mixed phase region, it is conceivable that careful shock measurements in the mixed

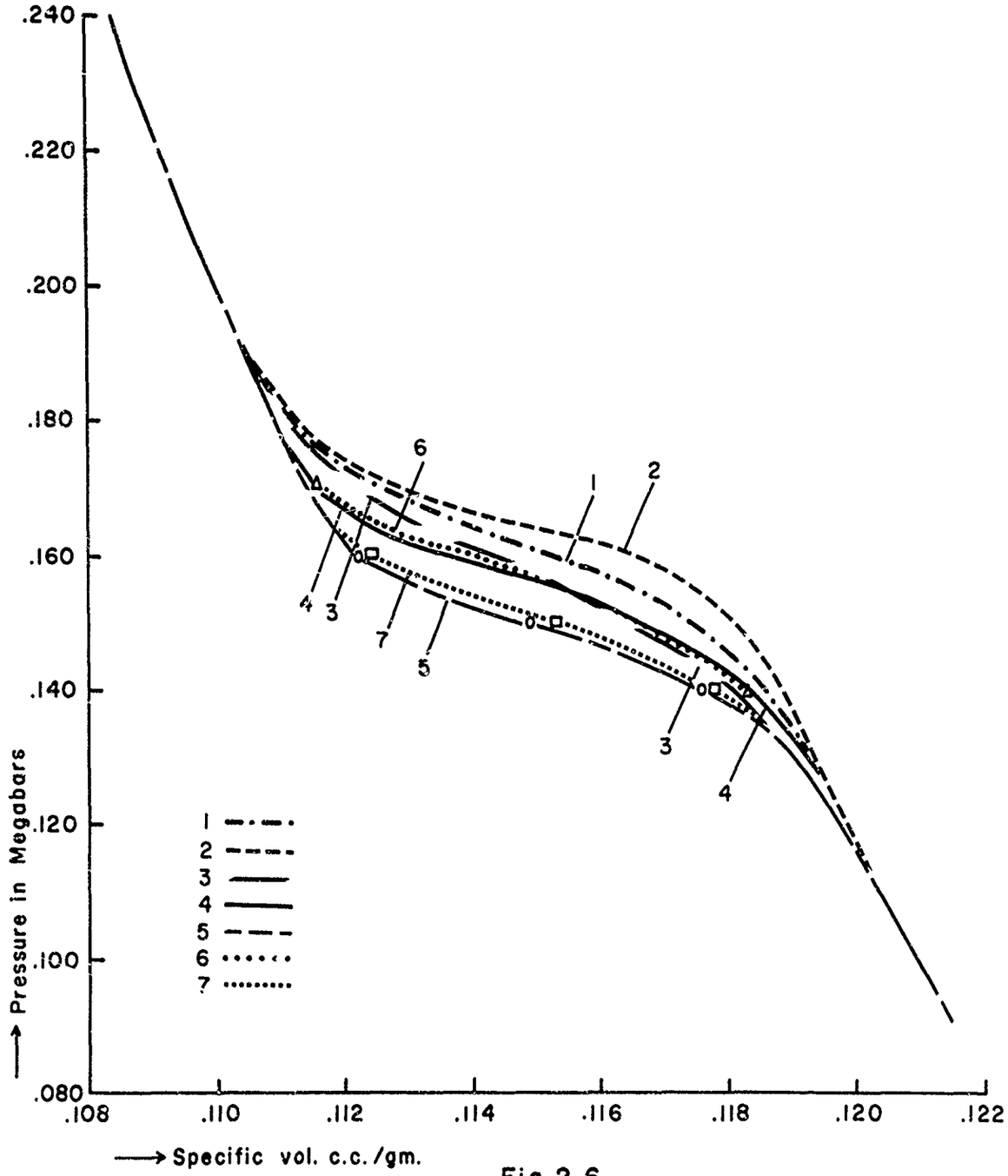

Fig. 2 6

P-V Curves Obtained by Varying Parameters of Martensitic Model

(See Table 2.1)

Table 2.1

Parameters for Fig. 2.1

Curve Number	ΔP Megabars	N_o	α/d^2
1	.015	100	.05
2	.01	100	.05
3	.02	100	.05
4	.015	200	.05
5	.015	500	.05
6	.015	100	.1
7	.015	100	.2

phase region can be used to shed light on deviations from thermodynamic equilibrium.

REFERENCES

1. D. Bancroft, E. L. Peterson, and S. Minshall, J. Appl. Phys. 27, 291 (1956).
2. H. M. Strong, J. Geophys. Res. 64, 653 (1959).
3. W. F. Claussen, Rev. Sci. Instr. 31, 878 (1960).
4. L. Kaufman, E. V. Clougherty, and R. S. Weiss, Acta Met. 11, 323 (1963).
5. F. S. Minshall, "Response of Metals to High Velocity Deformation," AIME Conf. 9, 249 (Interscience Publishers, New York, 1960).
6. C. M. Fowler, F. S. Minshall, and E. G. Zukas, Discussion to paper by the same, "Response of Metals to High Velocity Deformation," AIME Conf. 9, 306 (Interscience Publishers, New York, 1960).
7. P. C. Johnson, B. A. Stein, and R. S. Davis, J. Appl. Phys. 33, 557 (1962).
8. A. I. Balchan and H. G. Drikamer, Rev. Sci. Instr. 32, 308 (1961).
9. J. C. Jamieson and A. W. Lawson, J. Appl. Phys 33, 776 (1962).
10. R. L. Clendenen and H. G. Drickamer, J. Phys. Chem Solids 25, 865 (1964).
11. T. Takahashi and W. A. Bassett, Science 145, 483 (1964).
12. F. P. Bundy, J. Appl. Phys. 36, 616 (1965).
13. T. R. Loree, C. M. Fowler, E. G. Zukas, and F. S. Minshall, J. Appl. Phys. 37, 1918 (1966).

14. F. P. Bundy, J. Appl. Phys. 38, 2446 (1967).

15. R. E. Duff and F. S. Minshall, Phys. Rev. 108, 1207 (1957).

16. D. B. Larson, J. Appl. Phys. 38, 1541 (1967).

17. G. C. Kennedy and P. N. La Mori, J. Geophys. Res. 67, 851 (1962).

18. T. E. Davidson and A. P. Lee, Trans. Met. Soc. AIME, 230, 1035 (1964).

19. R. G. McQueen, "Metallurgy at High Pressures and High Temperatures," K. A. Gschneidner, Jr., M. T. Hepworth, and N. A. D. Parlee, Eds. (Gordon and Breach Science Publishers. New York, 1964), p. 44.

20. R. H. Warnes, J. Appl. Phys. 38, 4629 (1967).

21. B. R. Breed and D. Venable (unpublished).

22. M. S. Wechsler, D. S. Lieberman, and T. A. Read, Trans. AIME 197, 1503 (1953).

23. J. S. Bowles and J. K. Mackenzie, Acta Met. 2, 129, 138, 224 (1954).

24. R. F. Bunshah and R. F. Mehl, Trans. AIME 197, 1251 (1953).

25. Novikov, S. A., Divnov, I. I., and A. G. Ivanov, "Investigation of the Structure of Compressive Shock Waves in Iron and Steel," Soviet Physics JETP 20, 3 (1965).

Unclassified
Security Classification

DOCUMENT CONTROL DATA - R & D
(Security classification of title, body of abstract and indexing annotation must be entered when the overall report is classified)

1 ORIGINATING ACTIVITY (Corporate author)
Washington State University
Dept. of Physics, Shock Dynamics Laboratory
Pullman, Washington 99163

2a. REPORT SECURITY CLASSIFICATION
UNCLASSIFIED

2b. GROUP

3 REPORT TITLE
EQUATIONS OF STATE IN SOLIDS (U)

4 DESCRIPTIVE NOTES (Type of report and inclusive dates)
Technical Summary Report No. 2 February 1968

5 AUTHOR(S) (First name, middle initial, last name)
G. E. Duvall, G. R. Fowles, M. H. Miles, and C. T. Tung

6 REPORT DATE	7a. TOTAL NO OF PAGES	7b. NO OF REFS
February 1968	130	A:13, B:4, C:25

8a CONTRACT OR GRANT NO	9a. ORIGINATOR'S REPORT NUMBER(S)
DA-04-200-AMC-1702(X)	SDL 68-01
b PROJECT NO	
c	9b. OTHER REPORT NO(S) (Any other numbers that may be assigned this report)
d	

10 DISTRIBUTION STATEMENT
Qualified requesters may obtain copies of this report from DDC.

11 SUPPLEMENTARY NOTES	12 SPONSORING MILITARY ACTIVITY
	U.S. Army Ballistics Research Laboratories Aberdeen Proving Ground, Maryland

13 ABSTRACT

An equation of state suitable for calculating the compression of a melting solid is described. Some elementary ideas about melting are reviewed and some standard relations between P and T in the melting region are described. The equation of state and melting law are combined in a program for calculating the Hugoniot through the mixed phase region. Results are described for lead, which melts at a shock pressure of about 400 kilobars with a Kennedy equation and 700 kilobars for a Simon equation.

The Eyring theory for equation of state of liquids is examined for argon, and Hugoniot curves are calculated. Calculations agree with the most dense case of van Thiel and Alder to 13 kilobars, then depart dramatically from measured values.

The theory of plastic wave propagation in two-dimensions is discussed and calculations of allowed directions are described. These will ultimately be of use in discussing the reflection of obliquely incident waves in an elastic-plastic medium.

Some of the basic physical mechanisms in solid-solid phase transitions are reviewed and the applicability of thermodynamics to such transitions is brought into question. An elementary model for a non-equilibrium transition in iron is suggested and p-v calculations are made for several values of the parameters. It is evident that no conclusions about the time dependence of the α-ϵ transition can be drawn from second state shock measurements, although it may be possible to infer useful information about metastable states.

DD FORM 1 NOV 1473

Unclassified
Security Classification

Unclassified
Security Classification

14 KEY WORDS	LINK A		LINK B		LINK C	
	ROLE	WT	ROLE	WT	ROLE	WT
Shock Waves Phase Transition Melting Plastic Waves Plasticity Lead						

Unclassified
Security Classification